# Construction and Characterisation of Heparan Sulphate Heptasaccharide Microarray

*Supplementary Information*

Jianhong Yang[†,‡], Po-Hung Hsieh[†], Xinyue Liu,[○] Wen Zhou[†,§], Xing Zhang,[○] Jing Zhao[○],

Yongmei Xu[†], Fuming Zhang,[○] Robert J. Linhardt,[○] and Jian Liu[†,*]

[†]Division of Chemical Biology and Medicinal Chemistry, Eshelman School of Pharmacy, University of North Carolina, Chapel Hill, NC 27599, USA.

[‡] College of Environmental & Safety Engineering, Changzhou University, Changzhou 213164, Jiangsu, China.

[○]Department of Chemistry and Chemical Biology, Centre for Biotechnology and Interdisciplinary Studies, Rensselaer Polytechnic Institute, Troy, New York 12180, USA.

[§] School of Chinese Medical Material, Guangzhou University of Chinese Medicine, Guangzhou city, Guangdong Province, 510006.

This work is supported in part by National Institutes of Health grants HL094463, GM102137, and HL62244 as well as UNC Eshelman Institute for Innovation Award. Jianhong Yang is supported by a fellowship of Jiangsu Overseas Research & Training Program.

Resubmission to *Chemical Communications*, December 2016

*To whom correspondence should be addressed: Rm 1044, Genetic Medicine Building, University of North Carolina, Chapel Hill, NC 27599. Tel.: 919-843-6511; E-mail: jian_liu@unc.edu

## Supplementary Experimental Procedures

*Immobilisation of oligosaccharide on the array slides.* HS oligosaccharides were dissolved in sodium phosphate buffer (pH 8.5, 50 mM) in concentrations of 5-1000 μM. The solution was spatially arrayed onto NHS-activated slides (Nexterion® Slide H from SCHOTT, Jena, Germany) under ~50% relative humidity at 20°C. The robotic arrayer S11 (from Scienion, Berlin, Germany) delivered 426 pL of the solution containing oligosaccharides to the array slide. The array spots had an average diameter of about 80 μm with a distance of 400 μm between the centres of adjacent spots. The slides were incubated overnight in a saturated $(NH_4)_2SO_4$ chamber (81% relative humidity). The slides were then washed with water to remove the unreacted oligosaccharides from the surface. The remaining *N*-hydroxysuccinimidyl groups were blocked by placing slides in a solution that contained 50 mM ethanolamine in PBST (137 mM NaCl, 13.2 mM $Na_2HPO_4$, 1.56 mM $NaH_2PO_4$, 2.68 mM KCl, 0.01% Tween 20) at 50°C for at least 1.5 h. Slides were rinsed several times with deionised water, and the residual liquid was dried by centrifugation.

*Hybridisation of array slides with fluorescently labeled 3-OST-1 and AT.* The hybridisation solution contained 10 μg $mL^{-1}$ of fluorescently labeled 3-OST-1 PBST (137mM NaCl, 2.7 mM KCl, 4.3 mM $Na_2HPO_4$, 1.4 mM $KH_2PO_4$, 0.05% Tween 20), 20 mM Tris (pH 7.5) and 10% bovine serum albumin (BSA). The solution was placed between array slide and cover slip and incubated for 1 h at room temperature in a saturated $(NH_4)_2SO_4$ chamber (81% relative humidity). The slide was then washed with 45 mL of PBST solution

containing BSA (1%) and Tris (20 mM) for 5 min in a clean 50 mL conical tube. The wash process was repeated twice before analyzing the slide with the array scanner. For the hybridisation with AT, the procedures were nearly identical with the exception that fluorescently labeled AT (10 μg $mL^{-1}$) was used to replace 3-OST-1 in the hybridisation step.

*Array data analysis.* The array slides were scanned by a GenePix 4300 scanner (Molecular Dynamics). Scanning wavelengths were 635, 594, 532 and 488 nm. Resolution was set at 10 μm. The array images were analyzed by GenePix Pro 7.2.29.002 software. Spots were automatically found and spot deviations were manually fit to correct. Mean median fluorescence intensities of arrays were obtained by Array Quality Control of software. Some thresholds were listed as follows: median signal-to-background, >10; mean of median background, < 500; median signal-to-noise, > 10; feature variation, 0.5; background variation, 0.5; features with saturated pixels, 0.1 %; not found features, 7 %; bad features, < 7 %.

*Synthesis of GlcA-pNA-$N_3$.* Pd/C (3.15 mg) was suspended in 20 mL of water, then 31.5 mg (0.1 mmol) of *p*-nitrophenyl-β-D-glucopyranosiduronic acid (PNP-GlcA, Chem-impex Int'l Inc.) was added. The reaction system was vacuumed and refilled with $H_2$ three times. After the reaction proceeded for 4 h under stirring, the solution was filtered. The filtrate was mixed with 5 mL of tetrahydrofuran (THF) and 0.8 mL of $KH_2PO_4$ (1 M). Succinimidyl 6-azidohexanoate (38.1 mg, 0.15 mmol) solution in 3 mL of THF was then added, and the reaction mixture was left overnight at room temperature. After THF was removed under reduced pressure, the reaction mixture was purified by using a $C_{18}$−column (1.5 × 70 cm,

Biotage) with gradient elution method (0‑100% methanol in $H_2O$, 0.1% trifluoroacetic acid, 2 mL $min^{-1}$) to obtain GlcA-pNA-$N_3$.

*Synthesis of succinimidyl 6-azidohexanoate*. 6-Azidohexanoic acid (1.5 g, 9.54 mmol, purchased from Fisher) was added to a solution of *N*-hydroxysuccinimide (1,206 mg, 10.5 mmol) in dichloromethane/DMF (12.5 mL/3.75 mL). The dicyclohexylcarbodiimide solution (2.16 g, 10.5 mmol) in dichloromethane (5 mL) was then added, and the reaction mixture was left overnight at room temperature. Dicyclohexylurea was removed by filtration and the filtrate was concentrated under reduced pressure to yield a crude product.

*Synthesis of compound **1** to **14***-The synthesis of **1** to **14** was completed according to the chemoenzymatic method published previously.[1,2] Briefly, heparosan synthase-2 (PmHS2) from *Pasteurella multocida* was used to elongate the monosaccharide, GlcA-pNA-$N_3$, to appropriate sized backbones. The backbone was then subjected to the modification of *N*-sulphotransferase, $C_5$-epimerase, 2-*O*-sulphotransferase, 6-*O*-sulphotransferase, and 3-*O*-sulphotransferase depending on the structures of products. There were five major steps involved in the overall synthesis, including Step a (elongation step), Step b (detrifluoroacetylation/N-sulphation step), Step c (6-*O*-sulphation step), step d (2-*O*-sulphation/epimerization) and step e (3-O-sulphation). Here is the brief description of each synthetic steps. Step a is to elongate the oligosaccharide backbone to the desired size, involving the addition of GlcNAc (or GlcNTFA) and GlcA residues. Briefly, GlcA-pNA-$N_3$ (1.67 mM) was dissolved in a buffer containing Tris (25 mM, pH 7.2), $MnCl_2$ (5 mM), pmHS2 (0.0525 mg $mL^{-1}$) and UDP-GlcNTFA (or UDP-GlcNAc, 2.5 mM), then incubated at 30°C overnight. For introduction of a GlcA residue, disaccharide (1 mM)

was dissolved in a buffer containing Tris (25 mM, pH 7.2), $MnCl_2$ (5 mM), pmHS2 ( 32 μg $mL^{-1}$) and UDP-GlcA (1.5 mM), then incubated at 30°C overnight. A $C_{18}$-column (1.5 × 70 cm, Biotage) was used for purification with gradient elution method (0–100% methanol in $H_2O$, 0.1% trifluoroacetic acid, 2 mL $min^{-1}$).

Step b was aimed to convert a GlcNTFA residue to a GlcNS residue, involving both detrifluoroacetylation and *N*-sulphation. The detrifluoroacetylation of oligosaccharide was conducted in 0.1 M LiOH under ice bath for 0.5 h. The products were monitored by electrospray ionization mass spectrometry (ESI-MS). After the reaction was completed, pH was immediately adjusted to 7.0 using hydrochloric acid (1 M). The detrifluoroacetylated oligosaccharide (0.45 mM) was *N*-sulphated in a solution containing 2-(*N*-morpholino) ethanesulphonic acid (MES, 50 mM) pH 7.0 and *N*-sulphotransferase (50 μg $mL^{-1}$) and PAPS (1.5 equiv. of free amino group amount) at 37°C overnight.

Step c was to introduce 6-*O*-sulphation using both 6-*O*-sulphotrasnferase isoform 1 and 3 (6-OST-1 and 6-OST-3). In this step, *N*-sulphated oligosaccharide (0.45 mM) was incubated in a buffer containing MES (50 mM, pH 7.0), 6-OST-1 (50 μg $mL^{-1}$), 6-OST-3 (50 μg $mL^{-1}$) and PAPS (1.5 equiv. of 6-hydroxyl group amount) at 37°C overnight. Step d was to convert a GlcA residue to an IdoA2S residue, involved using both $C_5$-epimerase and 2-*O*-sulphotransferase (2-OST). The oligosaccharide (0.45 mM) was incubated in a solution containing MES (50 mM) buffer (pH 7.0) and $C_5$-epimerase (50 μg $mL^{-1}$), 2-OST (50 μg $mL^{-1}$) and PAPS (0.675 mM or 1.35 mM) at 37°C overnight. Step e was to introduce 3-*O*-sulphation by 3-*O*-sulphotransferase 1 (3-OST-1). The oligosaccharides (0.45 mM) were incubated in a solution containing MES (50 mM) buffer (pH 7.0), 3-OST-1 (50 μg $mL^{-1}$) and PAPS (0.675 mM) at 37°C overnight.

The products from step b, c, d and e were purified using a same column, Toyopearl Giga Cap Q-650M column (15 × 30 cm, from Tosohaas) that was eluted with a linear gradient 0-100% 2 M NaCl in 20 mM NaOAc-HAc, pH 5.0 at a flow rate of 2 mL $min^{-1}$. The eluents were then dialyzed against deionised water to obtain pure oligosaccharides. At every synthesis step, the products were monitored by Shimadzu HPLC equipped with a polyamine II column (4.6 mm × 250 mm, from YMC), and the eluent was monitored at 245 nm. The structures of the intermediates from each step were characterised by electrospray ionisation mass spectrometry (ESI-MS).

The conversion of the azido group to amino group was achieved by catalytic hydrogenation to yield final products. Palladium and charcoal complex (2.5 mg, from Sigma Aldrich) was suspended in 2.5 mL of water, then 10 mg of azido oligosaccharide and 2.5 µL of acetic acid were added. The reaction system was vacuumed and refilled with $H_2$ three times. After the reaction was incubated at room temperature overnight, the reaction mixture solution was filtered. The product was purified by Toyopearl Giga Cap Q-650M column using the procedures as described above. The products were confirmed by the analysis of ESI-MS as well as high resolution MS.

*Expression of HS biosynthetic enzymes*. A total of seven enzymes were used for the synthesis, including NST, $C_5$-epi, 2-OST, 6-OST-1, 6-OST-3, 3-OST-1, and pmHS2. All enzymes were expressed in *E. coli* and purified by appropriate affinity chromatography as described previously [3,4].

*Preparation of fluorescently labeled oligosaccharides (compounds **15** to **21**)*- A GlcNTFA residue was introduced into azido heptasaccharide by step a as described above. The

detrifluoroacetylization was completed in 0.1 M LiOH under ice bath for 0.5 h to obtain octasaccharide with an *N*-unsubstituted glucosamine residue at the nonreducing end. The octasaccharide (2.5 μmol) was dissolved in 0.1 M sodium bicarbonate solution (1.5 mL), and 0.15 ml (5.1 μmol) Cy5 NHS ester (form Invitrogen) dissolved in DMSO (20 mg $mL^{-1}$) was added. The mixture was kept at room temperature overnight. Then Cy5 NHS ester DMSO solution (0.15 mL, 20 mg $mL^{-1}$, or 5.1 μmol) and sodium bicarbonate solution (0.15 mL, 0.1 M, or 15 μmol) were added twice at intervals of 12 h. After the reaction was continued for another 12 h, the mixture was dialyzed against deionised water and lyophilised. Cy5 labeled octasaccharide was dissolved in the mixed solvent of DMSO (0.7 mL) and THF (0.7 mL) containing 1.3 mg (5 μmol) $Ph_3P$. After the reaction was left for 24h at room temperature under $N_2$, 1 mL $H_2O$ and 10 μL of acetic acid were added. The mixture was continued to incubate at room temperature for 36 h and then isolated by Toyopearl Giga Cap Q-650M column as described above.

*Preparation for fluorescently labeled 3-OST-1 and AT*-Recombinant 3-OST-1 expressed in *E. coli* [5] was used to prepare fluorescently labeled 3-OST-1. The labeling of 3-OST-1 was completed by incubating recombinant 3-OST-1 (0.1 mg $mL^{-1}$) and heparin (0.1 mg $mL^{-1}$) with Alexa Fluo® 488 NHS ester (1 mg $mL^{-1}$, from Invitrogen) in a 25 mM phosphate buffer (pH 7.0) containing 500 mM NaCl in 3 mL. The reaction was incubated at room temperature for one hour. The reaction mixture was purified by Ni-agarose column (GE Health) to remove the unreacted Alexa Fluo 488 NHS ester. To prepare the fluorescently labeled AT, human AT (from Cutter Biologic) was used under identical condition to that for 3-OST-1, and the separation of fluorescently labeled AT and unreacted Alexa Fluo 488 NHS ester was achieved by heparin-agarose column (GE Health).

*Quantification of HS oligosaccharides on the array slide*- Compounds **1** and **4** (200 μM) in 50 mM sodium phosphate buffer (pH 8.5) were spotted onto the surface of Nexterion® Slide H MPX 16 (SCHOTT, Jena, Germany). An array of 25 x 25 spots was printed within each well, and the process was repeated on additional 15 wells for this slide. After immobilisation and blocking, 60 μL of heparin lyase solution (60 μg/ml of heparin lyase I, II and III) in 50 mM of sodium phosphate buffer (pH 7.0) was added into each well. Recombinant heparin lyase I, II and III from *Flavobacterium heparinum* were constructed in $(His)_6$-fusion proteins, expressed in *E. coli* and purified by Ni-Sepharose. The heparin lyase-containing solution was added to 15 wells, and one well was added to the buffer without heparin lyases to be used as a control. After being incubated at room temperature for 1.5 h, the hydrolysates were aspirated from the wells, and collected and analyzed via LC-MS/MS. The wells were immediately filled with 100 μL of sodium phosphate buffer (50 mM, pH 7.0). After 3 min incubation, aspirate the wash solution and fill with fresh sodium phosphate buffer. Repeat this procedure 3 times, then rinse once with $H_2O$. The slide spotted with compound **4** was then hybridised with 3-OST-1. Alexa-488 labeled 3-OST-1 solution (60 μL of 10 μg $mL^{-1}$) was added into every well and incubated at room temperature for 1 h. After washed and dried (the same way as mentioned earlier), the slide was scanned. The control well displayed the fluorescent signals due to the binding of compound **4,** but those signals were absent in those wells treated with heparin lyases.

For disaccharide analysis, 10 μL of compound **4** (7.7 μg) or compound **1** (6.5 μg) was digested by recombinant heparin lyase I, II, III (10 mU each) in 100 μL digestion buffer (50 mM $NH_4AcO$, 2 mM $CaCl_2$, pH 7.0) 37 °C water bath overnight. The reaction

was terminated by eliminating enzyme via passing through 3 KDa molecular weight cut-off spin columns. The filter unit was washed twice with 200 µL distilled water and the filtrate was finally lyophilised. Meanwhile, 400 µL of each component released from array-slide were lyophilised directly. The dried samples were 2-aminoacridone (AMAC)-labeled by adding 10 µL of 0.1 M AMAC in dimethylsulphoxide (DMSO)/acetic acid (17/3,V/V) incubating at room temperature for 10 min, followed by adding 10 µL of 1 M aqueous sodium cyanoborohydride and incubating for 1 h at 45 °C. The resulting samples were centrifuged at 13,200 rpm for 10 min. Finally, supernatant was collected and stored in a light resistant container at room temperature until analyzed via LC-MS/MS.

*LC-MS/MS analysis*. LC was performed on an Agilent 1200 LC system at 45 °C using an Agilent Poroshell 120 ECC18 (2.7 µm, 3.0 × 50 mm) column. Mobile phase A (MPA) was 50 mM ammonium acetate in aqueous solution, and the mobile phase B (MPB) was methanol. The mobile phase passed through the column at a flow rate of 300 µL $min^{-1}$. The gradient was 0-10 min, 5-45% B; 10-10.2 min, 45-100%B; 10.2-14 min, 100%B; 14-22 min, 100-5%B. Inject volume: 4 µL. A triple quadrupole mass spectrometry system equipped with an ESI source (Thermo Fisher Scientific, San Jose, CA) was used a detector. The online MS analysis was at the Multiple Reaction Monitoring (MRM) mode. MS parameters: negative ionization mode with a spray voltage of 3000 V, a vaporiser temperature of 300 ℃, and a capillary temperature of 270 ℃.

*Analysis of HS oligosaccharides by MS.* High resolution ESI-MS analysis was conducted on Thermo LTQ XL Orbitrap (Breman, Germany) under the following conditions. A Luna hydrophilic liquid interaction chromatography (HILIC) column (2.0 × 50 $mm^2$, 200 Å, Phenomenex, Torrance, CA) was used to separate the oligosaccharide mixture. Mobile

phase A was 5 mM ammonium acetate prepared with high performance liquid chromatography (HPLC) grade water. Mobile B was 5 mM ammonium acetate prepared in 98% HPLC grade acetonitrile with 2% of HPLC grade water. After injection of 5.0 µL oligosaccharide solution (1.0 µg $\mu L^{-1}$) through an Agilent 1200 autosampler. The gradient was used from 5% A to 70% A in 7 min then reset to 5% A at a flow rate of 250 µL $min^{-1}$. The LC column was directly connected online to the standard electrospray ionization source of LTQ-Orbitrap XL Fourier transform (FT) mass spectrometer (MS) (Thermo Fisher Scientific, San-Jose, CA). The source parameters for FT-MS detection were optimised using Arixtra® (purchased at a pharmacy) to minimise the insource fragmentation and sulphate loss and maximise the signal/ noise in the negative-ion mode. The optimised parameters, used to prevent in-source fragmentation, included a spray voltage of 4.2 kV, a capillary voltage of −40 V, a tube lens voltage of −50 V, a capillary temperature of 275° C, a sheath flow rate of 30, and an auxiliary gas flow rate of 6. External calibration of mass spectra routinely produced a mass accuracy of better than 3 ppm. All FT mass spectra were acquired at a resolution 60,000 with 200-1800 *m/z* mass range.

*NMR analysis*-The structure of synthetic compounds were analyzed by NMR experiments, including one dimensional- ("zg" pulse sequence $^{1}H$ and "zgdc30" pulse sequence $^{13}C$). NMR experiments were performed at 298 K on Bruker Avance 850 or 700 MHz spectrometer equipped with 5mm CryoProbe and processed by TopSpin 3.2 software. Samples (0.5 to 5.0 mg) were each dissolved in 0.5 mL $D_2O$ (99.994%, Sigma, Co.) and lyophilised three times to evaporate the exchangeable protons. The samples were re-dissolved in 0.5 mL $D_2O$ and transferred to NMR tubes (O.D. 5 mm, Norrell).

Compound **1** to **14** was dissolved in 0.5 mL $D_2O$. Chemical shifts are referenced to external 2,2-dimethyl-2-silapentane-5-sulphonate sodium salt (DSS, Sigma, Co.). 1D $^{1}$H-NMR experiments were performed with 32 scans and an acquisition time of 4.0 sec. 1D $^{13}$C-NMR experiments were performed with 5,000 scans and an acquisition time of 1.0 sec. Four dummy scans were used prior to the start of acquisition. $^{13}$C transmitter offset was set at 100.0 ppm. Anomeric proton and carbon signals were assigned based HSQC analysis and previously published assignments on structurally similar HS oligosaccharides [1,2,6].

**SPR analysis of protein binding to heparin**

*Preparation of heparin biochip.* Biotinylated heparin was prepared by conjugating its reducing end to amine-PEG3-Biotin (Pierce, Rockford, IL). In brief, heparin (2 mg) and amine-PEG3-Biotin (2 mg, Pierce, Rockford, IL) were dissolved in 200 μL $H_2O$, 10 mg $NaCNBH_3$ was added. The reaction mixture was heated at 70 °C for 24 h, after that a further 10 mg $NaCNBH_3$ was added and the reaction was heated at 70 °C for another 24 h. After cooling to room temperature, the mixture was desalted with the spin column (3,000 MWCO). Biotinylated heparin was collected, freeze-dried and used for streptavidin (SA) chip preparation.

The biotinylated heparin was immobilised to SA chip based on the manufacturer's protocol. The successful immobilisation of heparin was confirmed by the observation of a 200 resonance unit (RU) increase on the sensor chip. The control flow cell (FC1) was prepared by 1 min injection with saturated biotin.

*Kinetic measurement of interaction between heparin and proteins using BIAcore***.** The protein sample was diluted in HBS-EP buffer (0.01 M HEPES, 0.15 M NaCl, 3 mM EDTA,

0.005% surfactant P20, pH 7.4) (GE Healthcare, Uppsala, Sweden). Different dilutions of protein samples were injected at a flow rate of 30 µl/min. At the end of the sample injection, the same buffer flew over the sensor surface to facilitate dissociation. After a 2 min dissociation time, the sensor surface was regenerated by sequence injecting with 30 µL of 2 M NaCl to get fully regenerated surface. The response was monitored as a function of time (sensorgram) at 25 °C. The measured kinetic data for AT/heparin interaction are: association rate (ka) is $1.1 \pm 0.37 \times 10^5$ 1/MS (n = 5), disassociation rate (kd) is $2.1 \pm 0.75 \times 10^{-4}$ 1/S (n = 5), and the binding constant ($K_D$) is $1.9 \times 10^{-9}$ M. The measured kinetic data for 3-OST-1/heparin interaction are: association rate (ka) is $5.5 \pm 0.39 \times 10^4$ 1/MS (n = 5), disassociation rate (kd) is $4.1 \pm 0.9 \times 10^{-3}$ 1/S (n = 5), and the binding constant ($K_D$) is $7.5 \times 10^{-8}$ M.

*SPR solution competition study of HS oligosaccharides.* Solution competition study between surface heparin and soluble different HS oligosaccharides to measure $IC_{50}$ was performed using SPR [7]. In brief, AT (125 nM, from Cutter Laboratories) or 3-OST-1 (125 nM, prepared in-house) samples mixed with different concentrations of HS oligosaccharides in HBS-EP buffer were injected over heparin chip at a flow rate of 30 µL $min^{-1}$, respectively. After each run, the dissociation and the regeneration were performed as described above. For each set of competition experiments on SPR, a control experiment (only protein without HS oligosaccharide) was performed to make sure the surface is completely regenerated and that the results obtained between runs are comparable. Once the active binding sites on protein molecules are occupied by HS oligosaccharide in the solution, the binding of protein to the surface-immobilised heparin should decrease resulting in a reduction signal. The $IC_{50}$ values (concentration of

competing analyte resulting in a 50% decrease in response units (RU)) can be calculated from the plots (protein binding signal (normalised) versus HS oligosaccharide concentration in solution.

*Determination of the anti-FXa activity*. Assays were based on a previously published method [8,9]. Briefly, human factor Xa (FXa) (Enzyme Research Laboratories, South Bend, IN) was diluted to 50 $Uml^{-1}$ with PBS. The chromogenic substrates, S-2765 was from Diapharma (Westchester, OH) and made up at 1 $mgmL^{-1}$ in water. Compounds **1** to **14** was dissolved in PBS at the concentration of 0.1 mM (0.12 to 0.20 $mgmL^{-1}$, depending on the MW). Heparin (from US Pharmacopeia) 0.1 $mgmL^{-1}$ was used as a positive control in this experiment. The reaction mixture, which consisted of 60 μl of AT (0.03 $mgmL^{-1}$ with 1 $mgmL^{-1}$ BSA) and 5 μl of the solution containing the sample, was incubated at room temperature for 2 min. Factor Xa (100 μL) was then added. After incubating at room temperature for 4 min, 30 μl of S-2765 substrate was added. The absorbance of the reaction mixture was measured at 405 nm continuously for 2 min. The absorbance values were plotted against the reaction time (n=3). The initial reaction rates as a function of concentration were used to calculate the activity of FXa.

Supplementary Table 1. High resolution MS analysis of HS oligosaccharides synthesised in this study

| Compounds | Abbreviated sequence of oligosaccharides* | Theoretical molecular weight | Measured molecular weight |
|---|---|---|---|
| **1** | GlcA-GlcNAc-GlcA-GlcNS-GlcA-GlcNS-GlcA-pNA-$NH_2$ | 1611.3958 | 1611.3989 |
| **2** | GlcA-GlcNAc6S-GlcA-GlcNS6S-GlcA-GlcNS6S-GlcA-pNA-$NH_2$ | 1851.2663 | 1851.2683 |
| **3** | GlcA-GlcNAc-GlcA-GlcNS-IdoA2S-GlcNS-GlcA-pNA-$NH_2$ | 1691.3526 | 1691.3566 |
| **4** | GlcA-GlcNAc6S-GlcA-GlcNS6S-IdoA2S-GlcNS6S-GlcA-pNA-$NH_2$ | 1931.2231 | 1931.2239 |
| **5** | GlcA-GlcNAc6S-GlcA-GlcNS3S6S-IdoA2S-GlcNS6S-GlcA-pNA-$NH_2$ | 2011.1799 | 2011.1850 |
| **6** | GlcA-GlcNS-GlcA-GlcNS-GlcA-GlcNS-GlcA-pNA-$NH_2$ | 1649.3421 | 1649.3425 |
| **7** | GlcA-GlcNS6S-GlcA-GlcNS6S-GlcA-GlcNS6S-GlcA-pNA-$NH_2$ | 1889.2125 | 1889.2162 |
| **8** | GlcA-GlcNS-IdoA2S-GlcNS-IdoA2S-GlcNS-GlcA-pNA-$NH_2$ | 1809.2557 | 1809.2567 |
| **9** | GlcA-GlcNS6S-IdoA2S-GlcNS6S-IdoA2S-GlcNS6S-GlcA-pNA-$NH_2$ | 2049.1261 | 2049.1305 |
| **10** | GlcA-GlcNS-GlcA-GlcNS-IdoA2S-GlcNS-GlcA-pNA-$NH_2$ | 1729.2989 | 1729.3004 |
| **11** | GlcA-GlcNS6S-GlcA-GlcNS6S-IdoA2S-GlcNS6S-GlcA-pNA-$NH_2$ | 1969.1693 | 1969.1719 |
| **12** | GlcA-GlcNS6S-GlcA-GlcNS3S6S-IdoA2S-GlcNS6S-GlcA-pNA-$NH_2$ | 2049.1261 | 2049.1301 |
| **13** | GlcA-GlcNAc-GlcA-GlcNAc-GlcA-GlcNAc-GlcA-pNA-$NH_2$ | 1535.5033 | 1535.5022 |
| **14** | GlcA-GlcNS-GlcA-GlcNS-GlcA-pNA-$NH_2$ | 1232.2844 | 1232.2839 |
| **15** | (Cy5)GlcN-GlcA-GlcNS6S-GlcA-GlcNS6S-GlcA-GlcNS6S-GlcA-pNA-$NH_2$ | 2514.5486 | 2514.5452 |
| **16** | (Cy5)GlcN-GlcA-GlcNS-GlcA-GlcNS-IdoA2S-GlcNS-GlcA-pNA-$NH_2$ | 2354.6350 | 2354.6322 |
| **17** | (Cy5)GlcN-GlcA-GlcNS6S-GlcA-GlcNS6S-IdoA2S-GlcNS6S-GlcA-pNA-$NH_2$ | 2594.5048 | 2594.5048 |
| **18** | (Cy5)GlcN-GlcA-GlcNS-GlcA-GlcNS-GlcA-GlcNS-GlcA-pNA-$NH_2$ | 2274.6780 | 2274.6762 |
| **19** | (Cy5)GlcN-GlcA-GlcNAc-GlcA-GlcNAc-GlcA-GlcNAc-GlcA-pNA-$NH_2$ | 2160.8394 | 2160.8406 |
| **20** | (Cy5)GlcN-GlcA-GlcNAc6S-GlcA-GlcNS3S6S-IdoA2S-GlcNS6S-GlcA-pNA-$NH_2$ | 2636.5160 | 2636.5214 |
| **21**** | (Cy5)GlcN-GlcA-GlcNS-GlcA-GlcNS-IdoA2S-GlcNS-GlcA-pNA-$N_3$ | 2383.3021 | 2383.4 |

*Compounds **1**-**14** were fully characterised by MS and NMR. Fluorescent compounds **15**-**21** were characterised by MS as insufficient sample was prepared for NMR characterisation.

**Low resolution ESI-MS analysis was used to measure the molecular weight of Comp **21**.

Supplementary Table 2. Summary of $IC_{50}$ (μM) and solution based affinity ($K_i$) of HS oligosaccharides on inhibiting protein binding to heparin

| HS oligosaccharide | AT | | 3OST-1 | |
|---|---|---|---|---|
| | $IC_{50}$ (μM) | $K_i$ (μM)* | $IC_{50}$ (μM) | $K_i$ (μM)* |
| **1** | >250 | N.D.** | 75.4 | 27.9 |
| **2** | >250 | N.D. | 43.6 | 16.1 |
| **3** | >250 | N.D. | 99.3 | 36.8 |
| **4** | >250 | N.D. | 18.0 | 6.7 |
| **5** | 53.7 | 0.8 | 1.8 | 0.7 |
| **6** | >250 | N.D. | 56.6 | 20.9 |
| **7** | >250 | N.D. | 12.4 | 4.6 |
| **8** | >250 | N.D. | 22.3 | 8.3 |
| **9** | >250 | N.D. | 1.8 | 0.7 |
| **10** | >250 | N.D. | 72.0 | 26.7 |
| **11** | >250 | N.D. | 14.7 | 5.4 |
| **12** | 19.2 | 0.3 | 0.7 | 0.3 |
| **13** | >250 | N.D. | 104.8 | 38.8 |
| **14** | >250 | N.D. | 42.0 | 15.6 |

* Solution based affinities ($K_i$) were calculated from $IC_{50}$ measured from SPR competition experiments using the equation: $Ki = IC_{50}/1+[C]/K_D$, [C] is the concentration of protein used in the competition SPR, $K_D$ is the protein binding affinity to heparin.

**ND: not detected.

Conclusions:

1. Both compounds **5** and **12** bound to AT as determined by the inhibition constant ($K_i$) value of 0.7 μM and 0.3 μM, respectively.
2. Compounds **5**, **9**, and **12** bound to 3-OST-1 as determined by the inhibition constant ($K_i$) value of 0.7 μM, 0.7 μM and 0.3 μM, respectively.

## Reference


1 Hsieh, P.; Xu, Y.; Keire, D. A.; Liu, J. *Glycobiology*, 2014, **24**, 681.

2 Xu, Y.; Cai, C.; Chandarajoti, K.; Hsieh, P.; Lin, Y.; Pham, T. Q.; Sparkenbaugh, E. M.; Sheng, J.; Key, N. S.; Pawlinski, R. L.; Harris, E. N.; Linhardt , R. J.; Liu, J. *Nat Chem Biol*, 2014, **10**, 248.

3 Liu, R.; Xu, Y.; Chen, M.; Weïwer, M.; Zhou, X.; Bridges, A. S.; DeAngelis, P. L.; Zhang, Q.; Linhardt, R. J.; Liu, J. *J Biol Chem*, 2010, **285**, 34240.

4 Xu, D.; Moon, A.; Song, D.; Pedersen, L. C.; Liu, J. *Nat Chem Biol*, 2008, **4**, 200.

5 Edavettal, S. C.; Lee, K. A.; Negishi, M.; Linhardt, R. J.; Liu, J.; Pedersen, L. C. *J. Biol. Chem.*, 2004, **279**, 25789.

6 Hsieh, P.-H.; Thieker, D. F.; Guerrini, M.; Woods, R. J.; Liu, J. *Sci Rep*, 2016, **6**, 29602; doi: 10.1038/srep29602.

7 Beaudet, J. M.; Weyers, A.; Solakyildirim, K.; Yang, B.; Takieddin, M.; Mousa, S.; Zhang, F.; Linhardt, R. J. *J. Pharm. Sci.*, 2011, **100**, 3396.

8 Zhang, L.; Beeler, D. L.; Lawrence, R.; Lech, M.; Liu, J.; Davis, J. C.; Shriver, Z.; Sasisekharan, R.; Rosenberg, R. D. *J. Biol. Chem.*, 2001, **276**, 42311.

9 Duncan, M. B.; Chen, J.; Krise, J. P.; Liu, J. *Biochim Biophys Acta*, 2004, **1671**, 34.

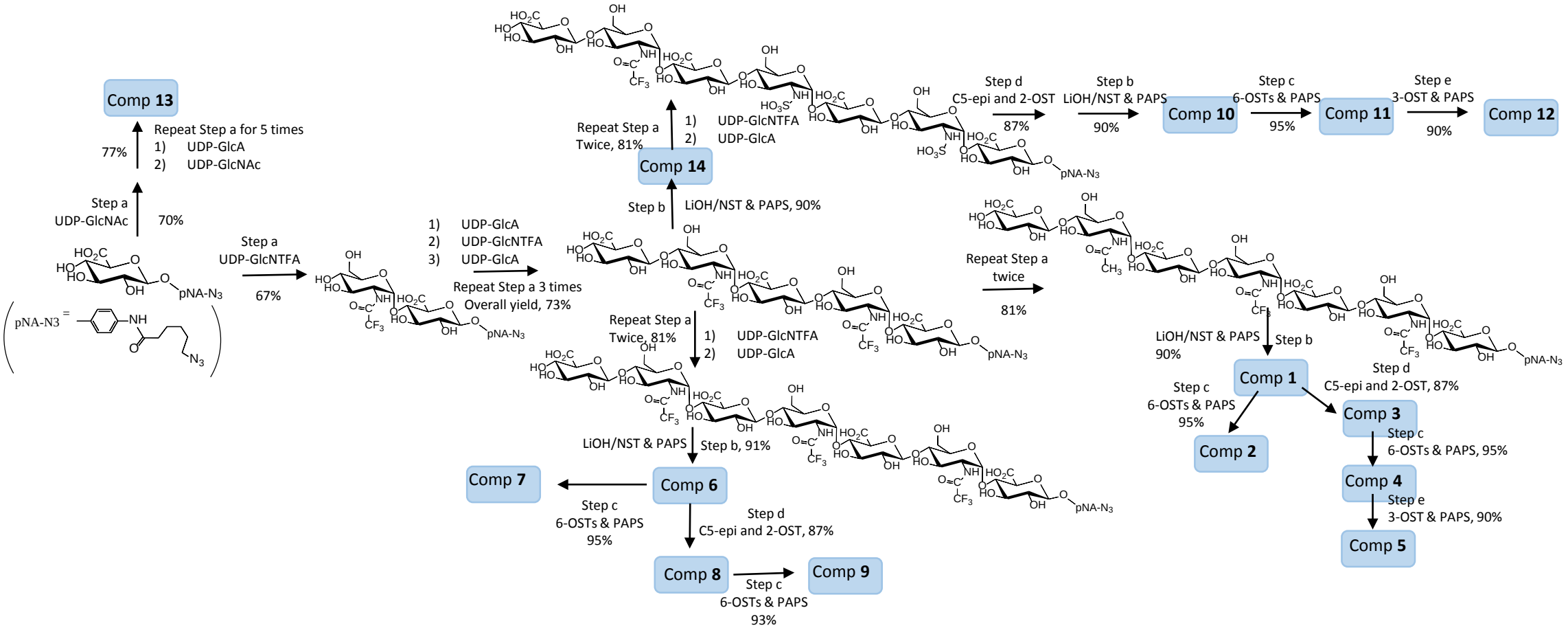


**Supplementary Fig 1**. Synthetic scheme for compounds **1** to **14**. The synthesis was initiated from monosaccharide, GlcA-pNA-$N_3$, to generate a series of oligosaccharides that had an azido group at the reducing end. These oligosaccharides were then subjected to catalytic hydrogenation to convert the azido group to an amino group to form the final compounds. For clarity, the catalytic hydrogenation step was omitted from the scheme. The recovery yield is indicated at each reaction step.

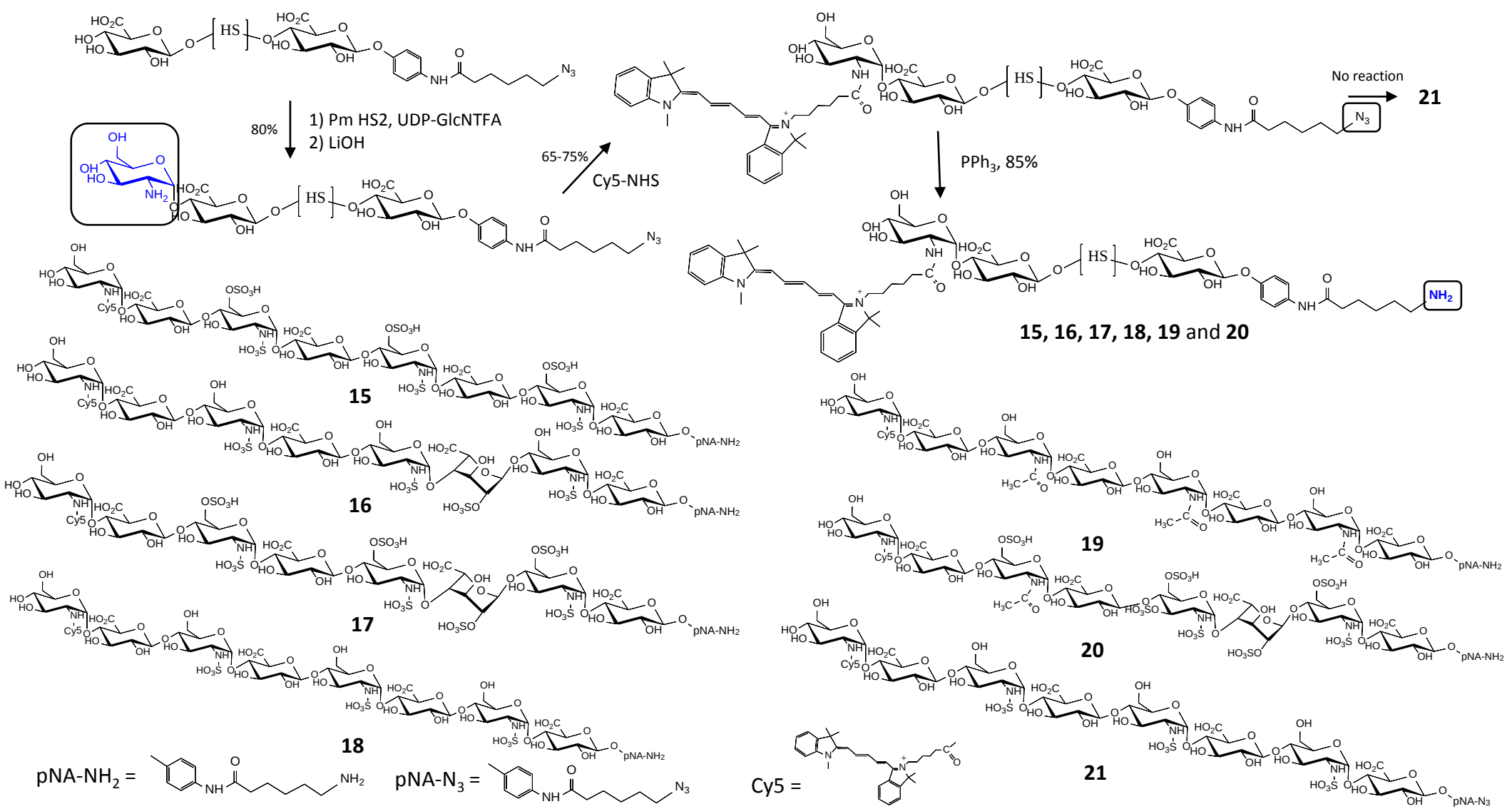


**Supplementary Figure 2**. Synthetic schemes for compounds **15** to **21**. This group of compounds were synthesised using the precursor compound **5**, **6**, **7**, **10**, **11** and **13,** all have an azido group at the reducing end. These precursor compounds were elongated to an octasaccharide followed by incorporation of the Cy5 fluorescent tag at the nonreducing end. The azido group in each compound was reduced to an amino group to form the final products. Compound **21** has an azido group at the reducing end. HS represents different sulfated carbohydrate sequences, which are shown at the bottom. The recovery yield is indicated at each reaction step.

# $^{1}$H-NMR of compound **1**

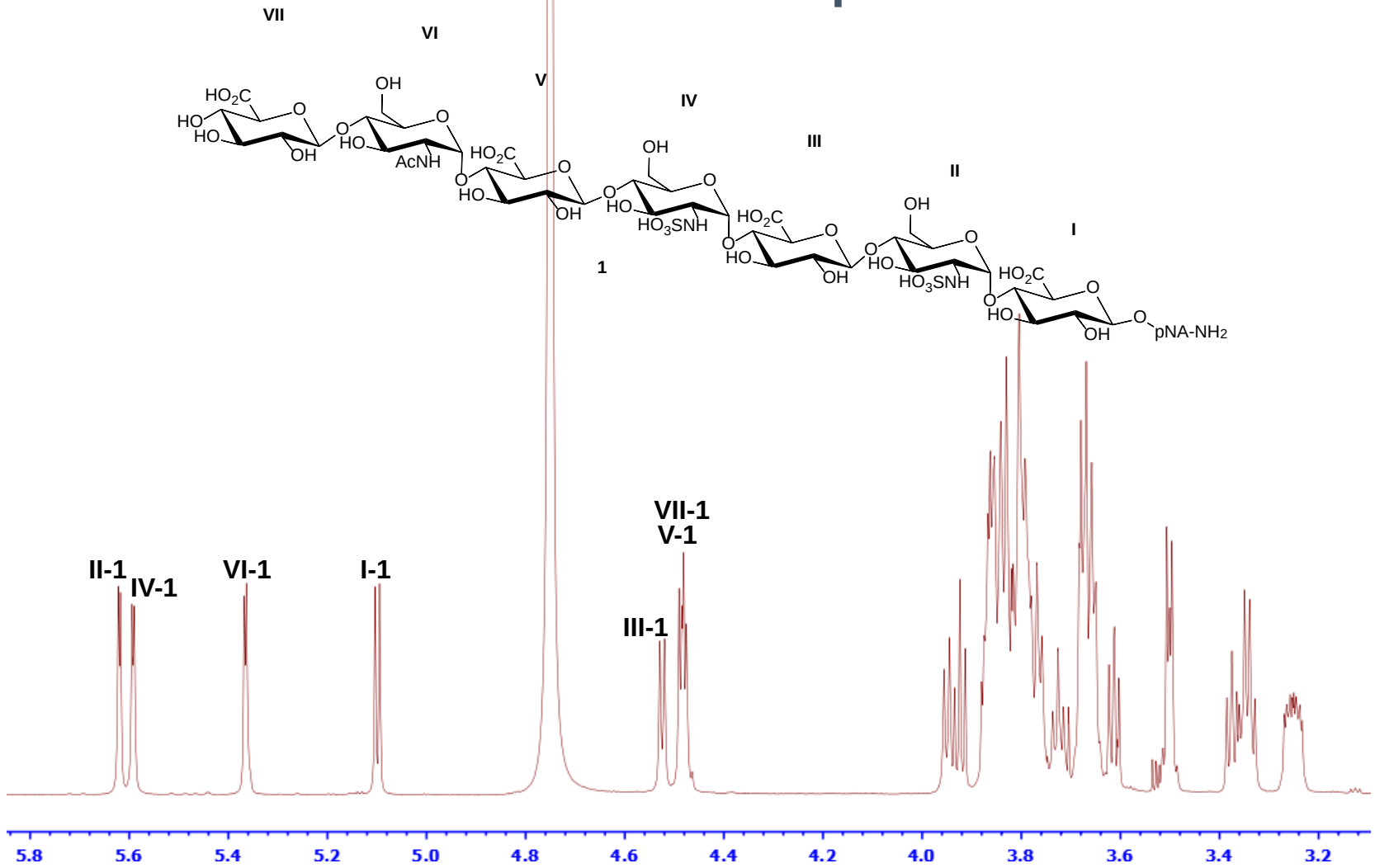


**Supplementary Fig 3**. $^{1}$H-NMR of compound **1** (850 MHz, $D_2O$). The signals of anomeric protons are indicated. The anomeric protons resonate as doublet at δ 5.62, 5.59, 5.37, 5.10, 4.53, 4.49, and 4.48 ppm. Chemical structure of compound **1** is shown on top of figure.

# $^{13}$C-NMR of compound **1**

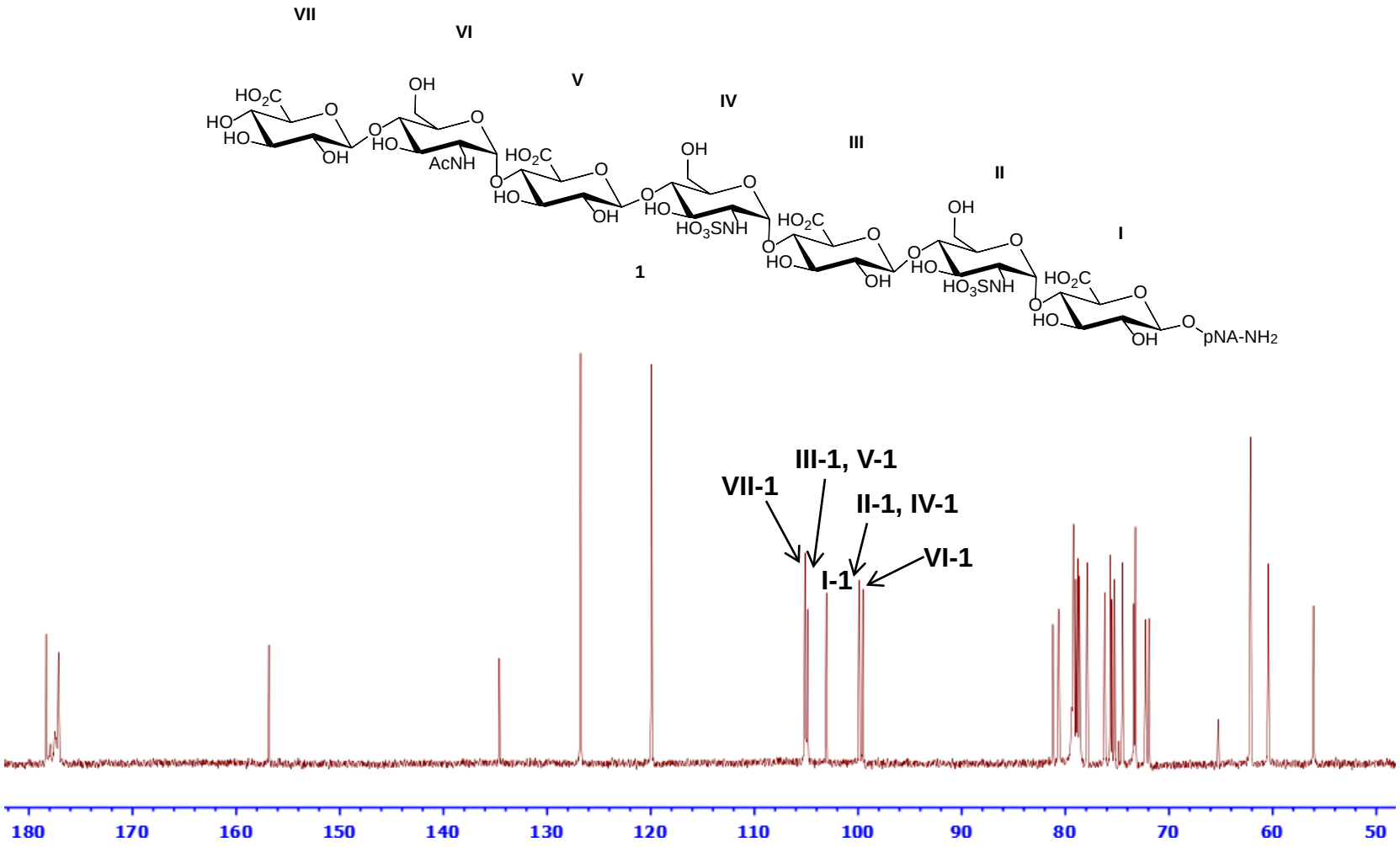


**Supplementary Fig 4**. $^{13}$C-NMR of compound **1** (212.5 MHz, $D_2O$). The signals of anomeric carbons are indicated. The anomeric carbons resonate at δ 105.1, 105.0, 104.9, 103.1, 99.9, 99.9, and 99.5 ppm. Chemical structure of compound **1** is shown on top of figure.

# $^{1}H$-$^{13}C$ HSQC spectrum of compound **1**

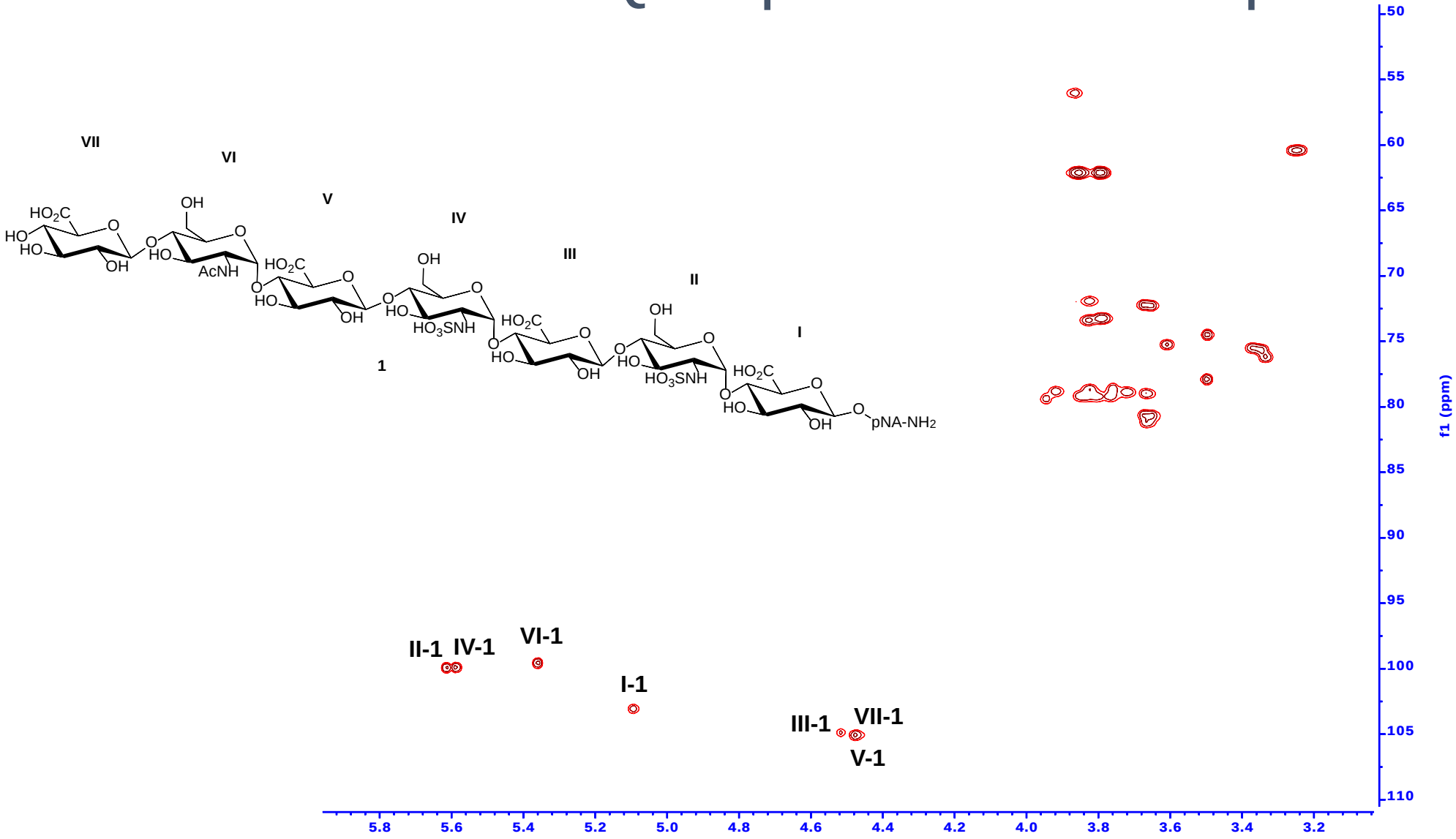


**Supplementary Fig 5**. $^{1}H$-$^{13}C$ HSQC spectrum of compound **1** (850 MHz, $D_2O$). The anomeric signals are indicated. Chemical structure of compound **1** is shown on top of figure.

# $^{1}$H-NMR of compound **2**

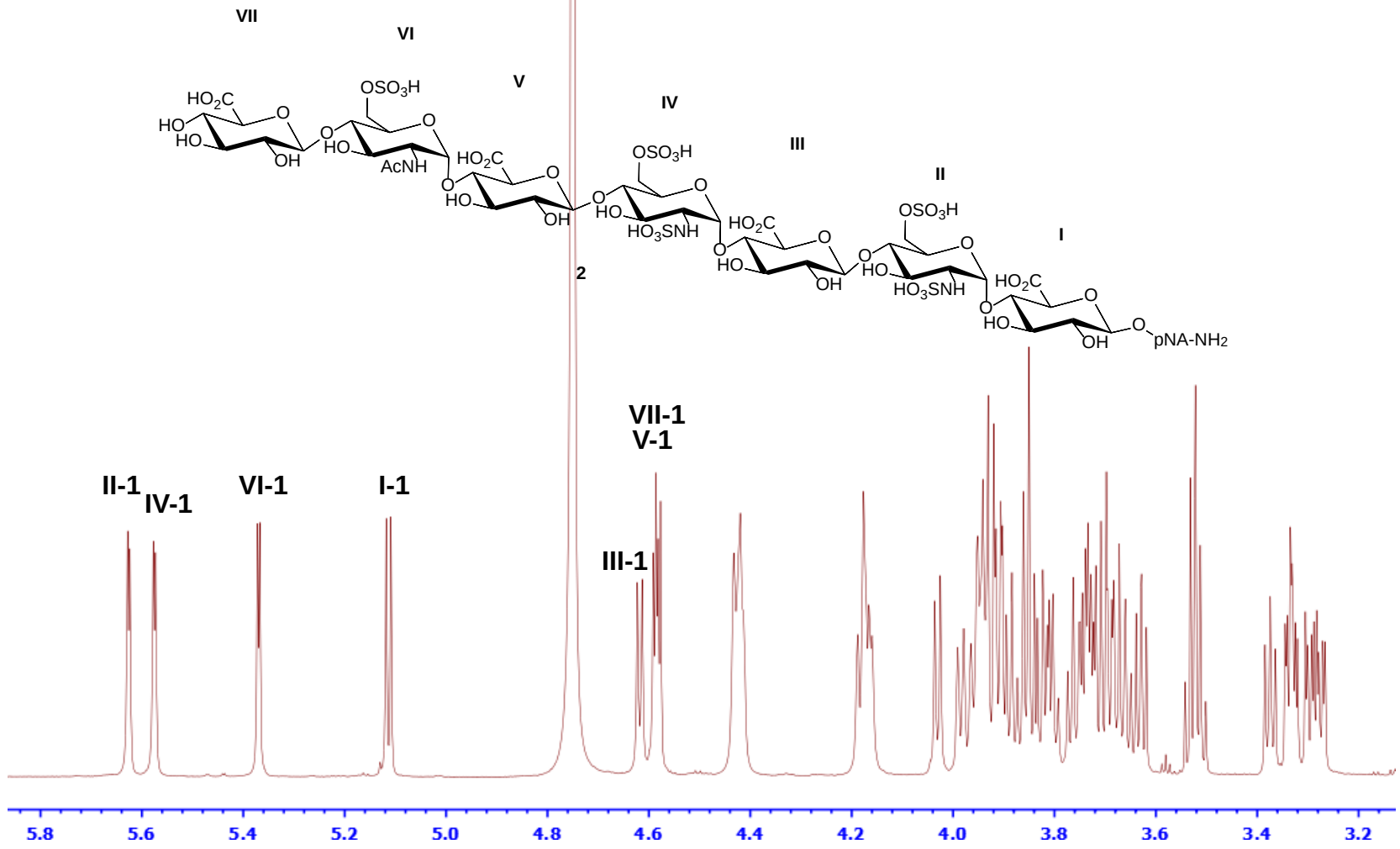


**Supplementary Fig 6**. $^{1}$H-NMR of compound **2** (850 MHz, $D_2O$). The signals of anomeric protons are indicated. The anomeric protons resonate as doublet at δ 5.63, 5.58, 5.37, 5.11, 4.62, 4.59, and 4.58 ppm. Chemical structure of compound **2** is shown on top of figure.

# $^{13}$C-NMR of compound **2**

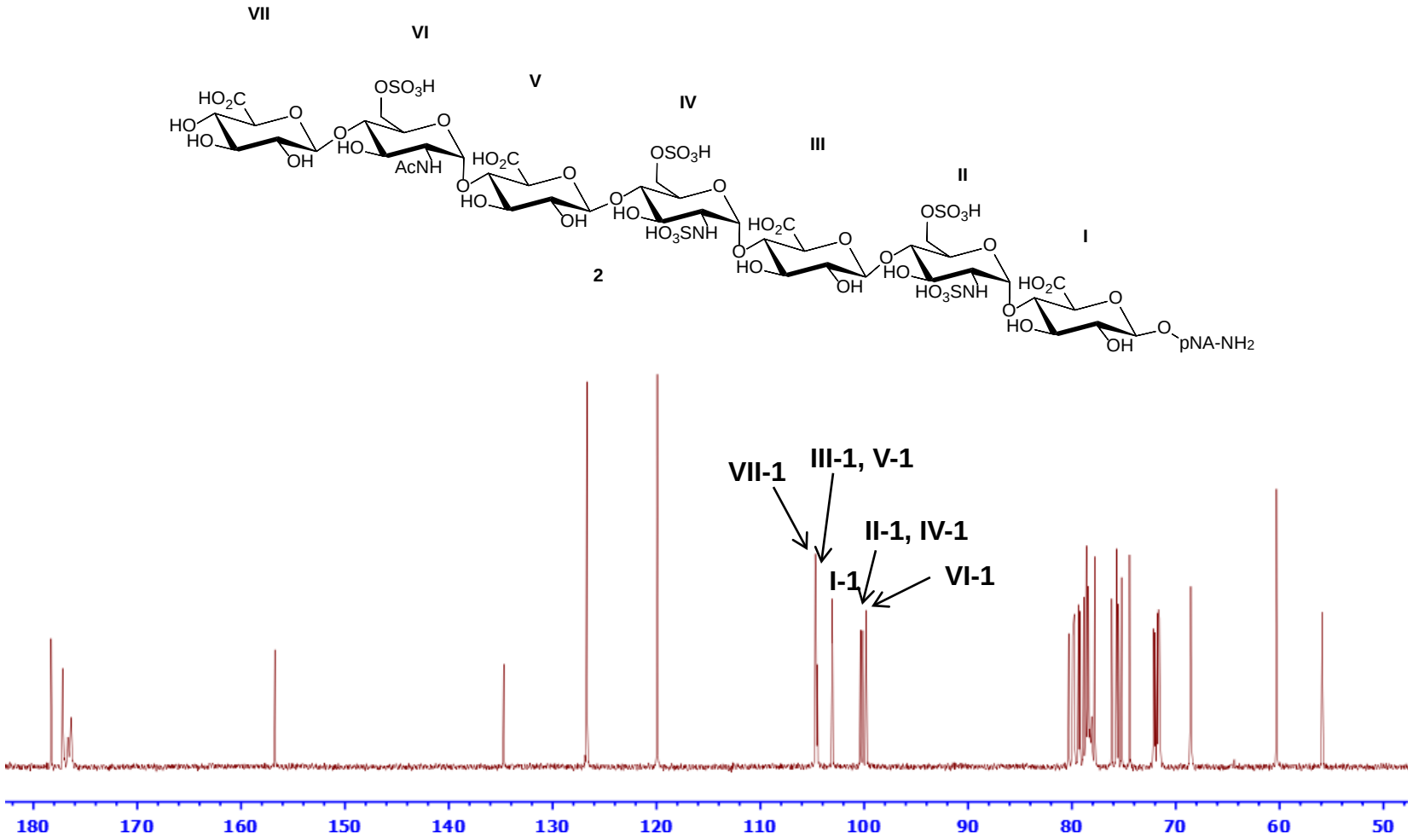


**Supplementary Fig 7**. $^{13}$C-NMR of compound **2** (212.5 MHz, $D_2O$). The signals of anomeric carbons are indicated. The anomeric carbons resonate at δ 104.7, 104.6, 104.5, 103.1, 100.4, 100.1, and 99.8 ppm. Chemical structure of compound **2** is shown on top of figure.

# $^{1}H$-$^{13}C$ HSQC spectrum of compound **2**

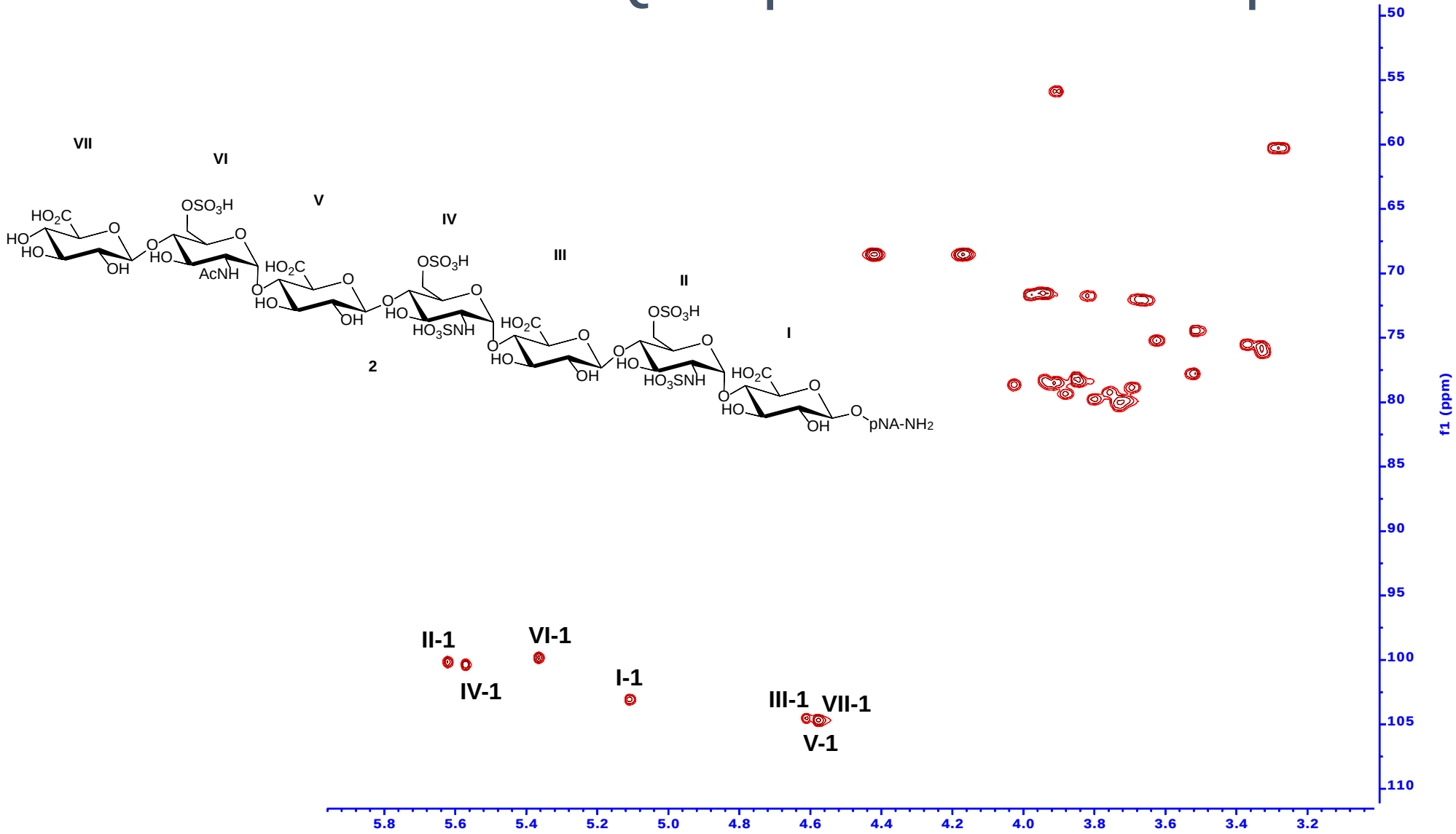


**Supplementary Fig 8**. $^{1}H$-$^{13}C$ HSQC spectrum of compound **2** (850 MHz, $D_2O$). The anomeric signals are indicated. Chemical structure of compound **2** is shown on top of figure.

# $^{1}$H-NMR of compound **3**

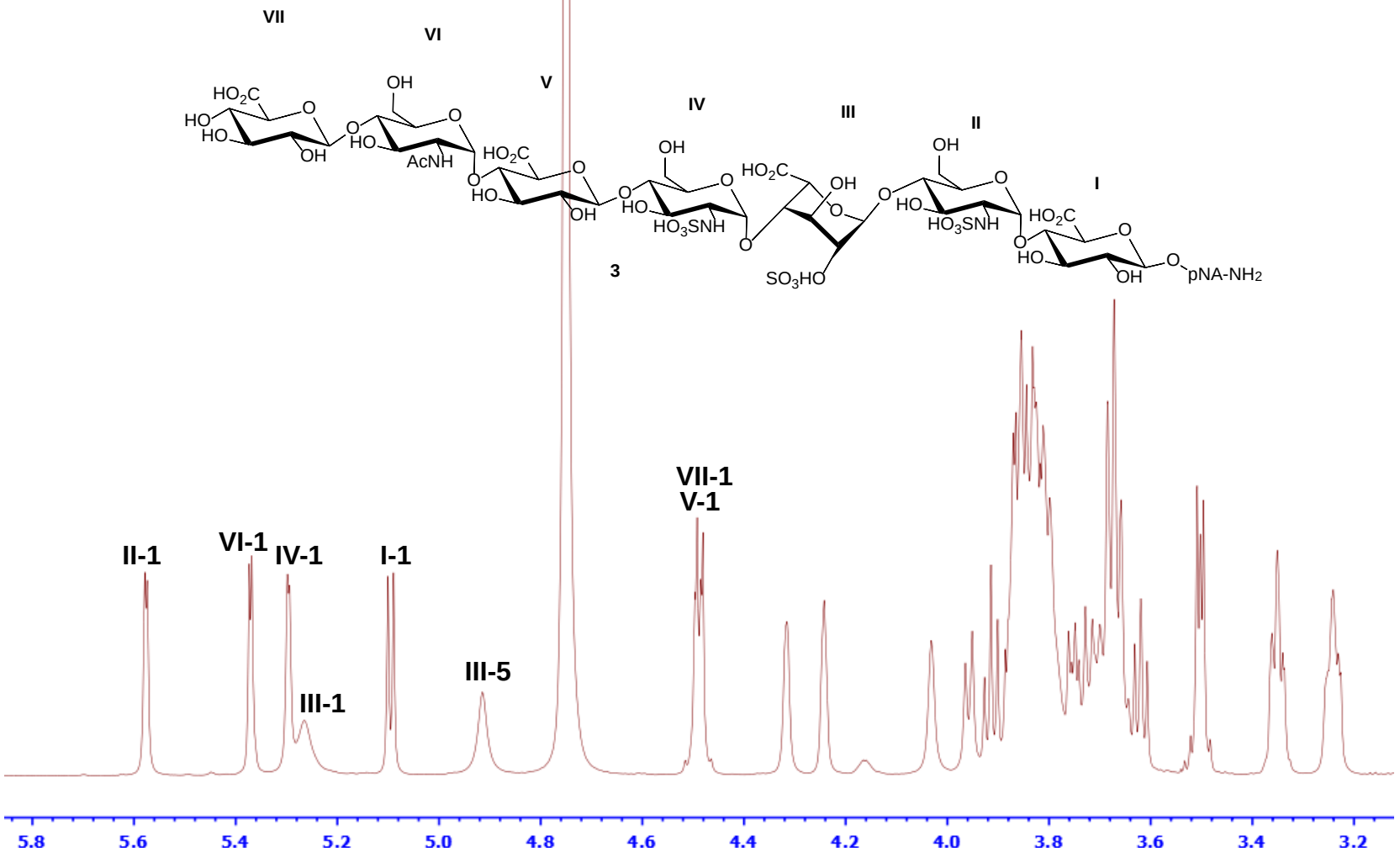


**Supplementary Fig 9**. $^{1}$H-NMR of compound **3** (700 MHz, $D_2O$). The signals of anomeric protons are indicated. The anomeric protons resonate as doublet at δ 5.58, 5.37, 5.30, 5.27, 5.10, 4.49, and 4.49 ppm. Chemical structure of compound **3** is shown on top of figure.

# $^{13}$C-NMR of compound **3**

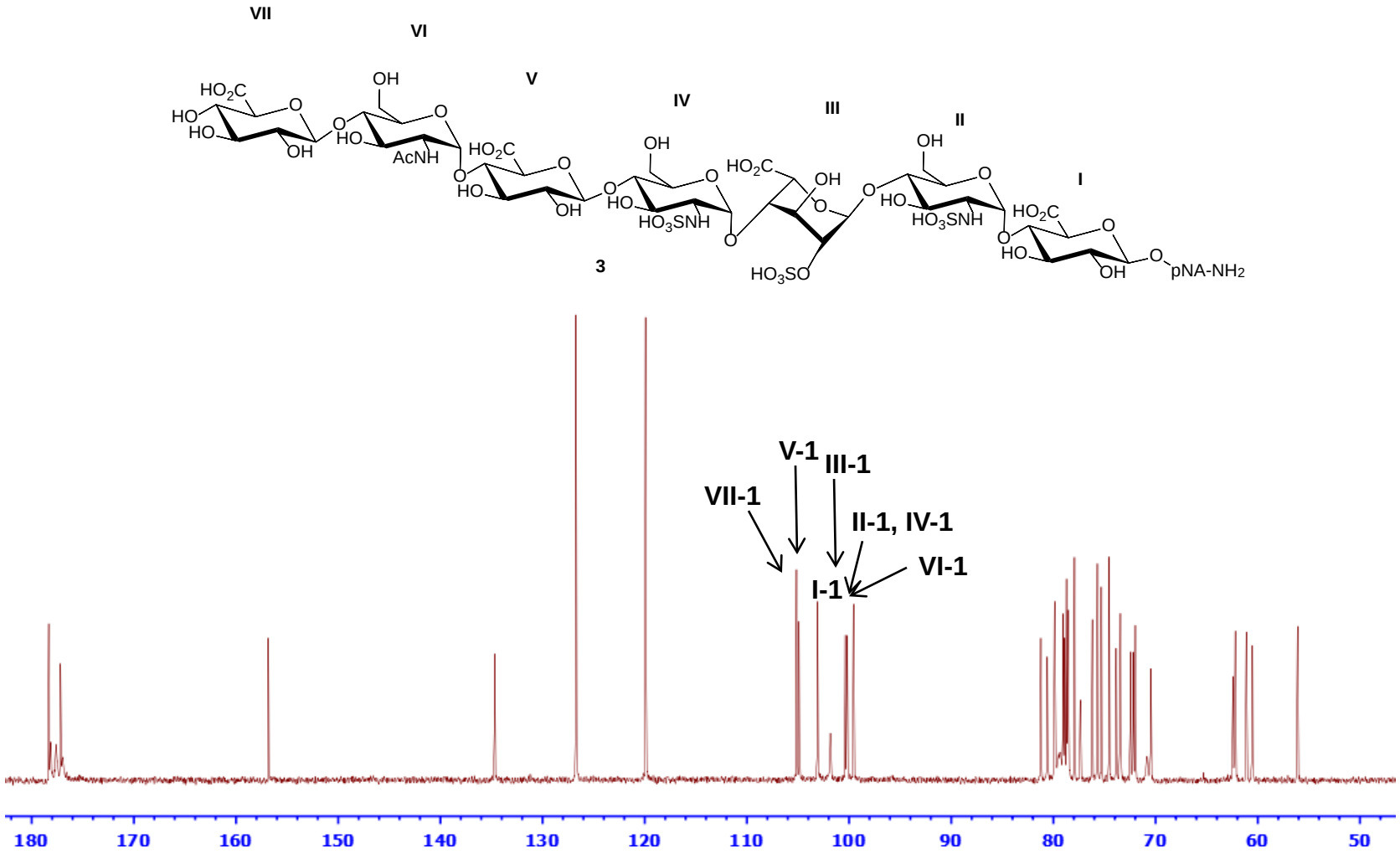


**Supplementary Fig 10**. $^{13}$C-NMR of compound **3** (175 MHz, $D_2O$). The signals of anomeric carbons are indicated. The anomeric carbons resonate at δ 105.1, 104.9, 103.1, 101.8, 100.4, 100.2, and 99.6 ppm. Chemical structure of compound **3** is shown on top of figure.

# $^{1}H$-$^{13}C$ HSQC spectrum of compound **3**

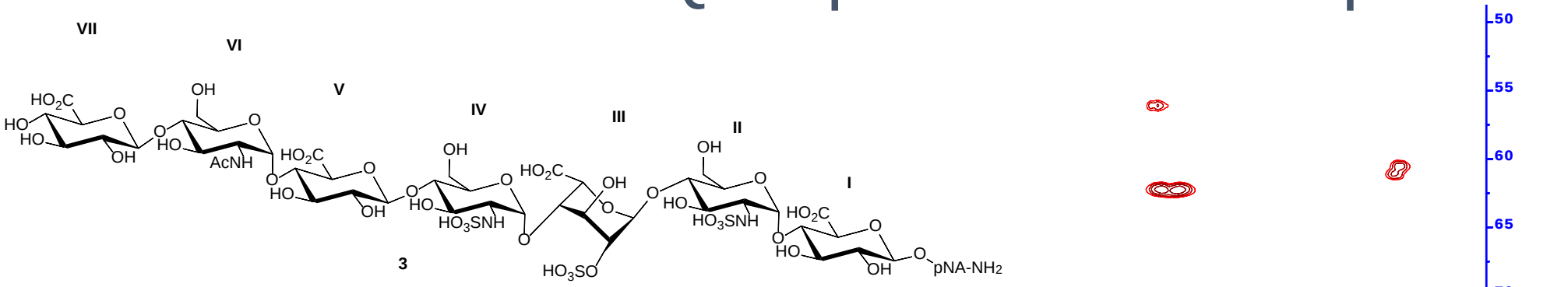





**Supplementary Fig 11**. $^{1}H$-$^{13}C$ HSQC spectrum of compound **3** (700 MHz, $D_2O$). The anomeric signals are indicated. Chemical structure of compound **3** is shown on top of figure.

# $^{1}$H-NMR of compound **4**

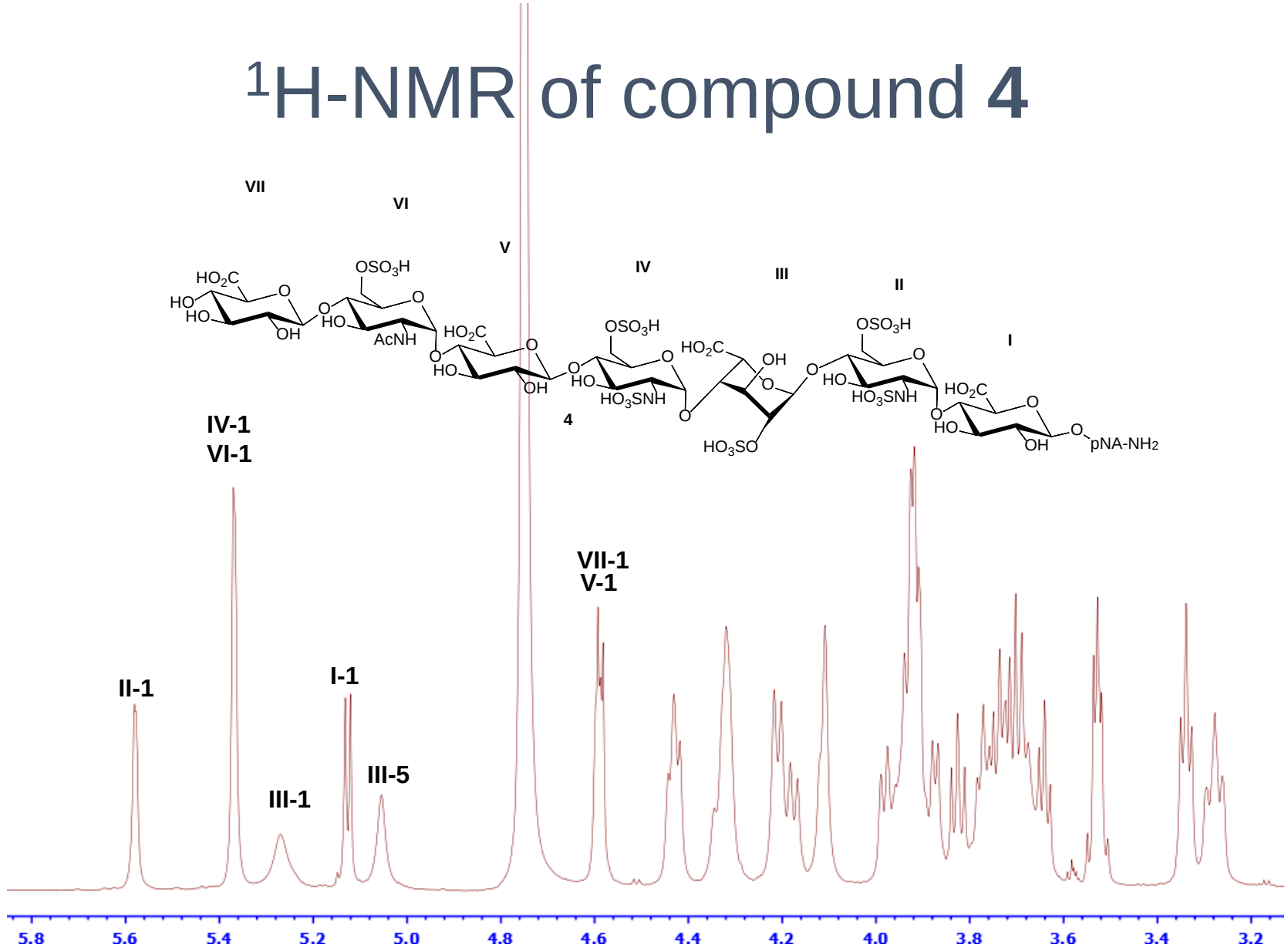


**Supplementary Fig 12**. $^{1}$H-NMR of compound **4** (700 MHz, $D_2O$). The signals of anomeric protons are indicated. The anomeric protons resonate as doublet at δ 5.58, 5.37, 5.37, 5.27, 5.13, 4.59, and 4.59 ppm. Chemical structure of compound **4** is shown on top of figure.

# $^{13}$C-NMR of compound **4**

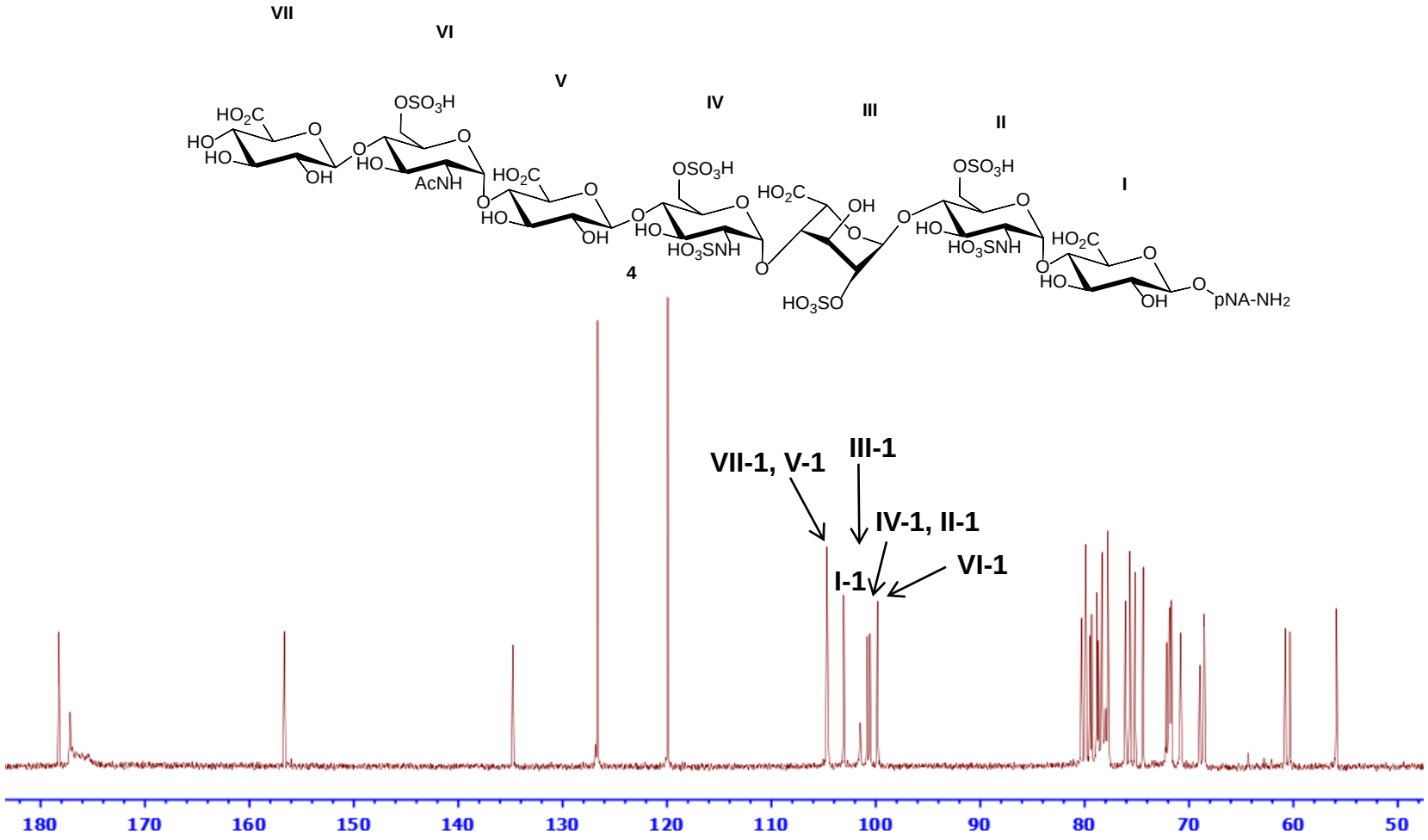


**Supplementary Fig 13**. $^{13}$C-NMR of compound **4** (175 MHz, $D_2O$). The signals of anomeric carbons are indicated. The anomeric carbons resonate at δ 104.7, 104.6, 103.1, 101.5, 100.8, 100.6, and 99.8 ppm. Chemical structure of compound **4** is shown on top of figure.

# $^{1}H$-$^{13}C$ HSQC spectrum of compound **4**

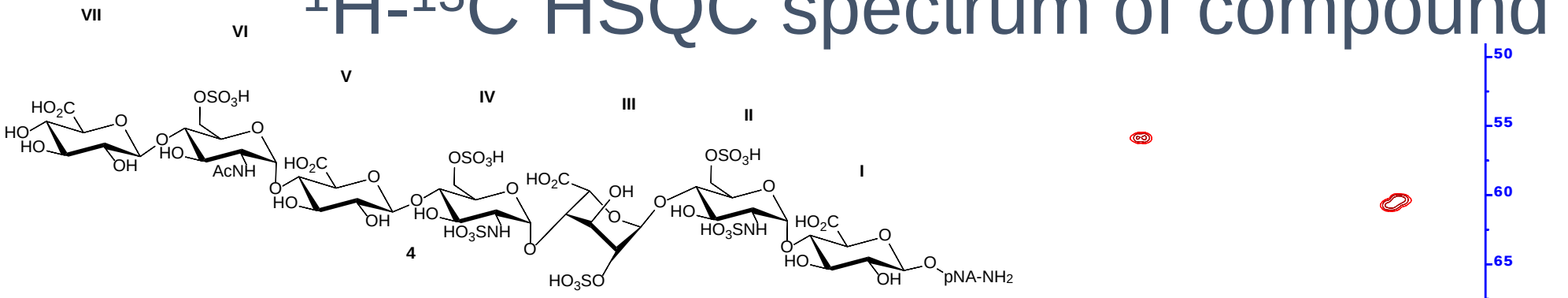





**Supplementary Fig 14**. $^{1}H$-$^{13}C$ HSQC spectrum of compound **4** (700 MHz, $D_2O$). The anomeric signals are indicated. Chemical structure of compound **4** is shown on top of figure.

# $^{1}$H-NMR of compound **5**

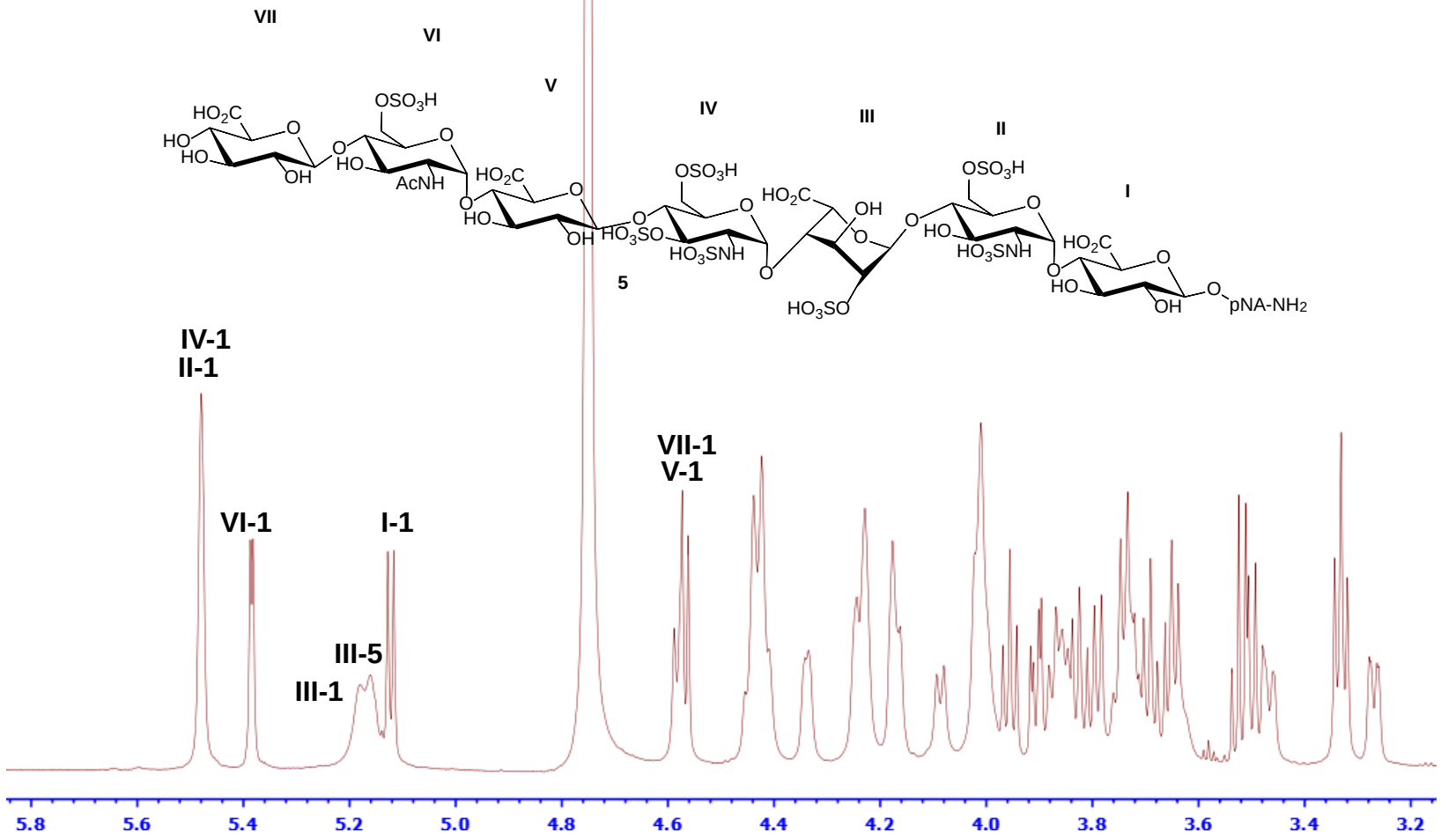


**Supplementary Fig 15**. $^{1}$H-NMR of compound **5** (700 MHz, $D_2O$). The signals of anomeric protons are indicated. The anomeric protons resonate as doublet at δ 5.48, 5.48, 5.39, 5.18, 5.12, 4.58, and 4.57 ppm. Chemical structure of compound **5** is shown on top of figure.

# $^{13}$C-NMR of compound **5**

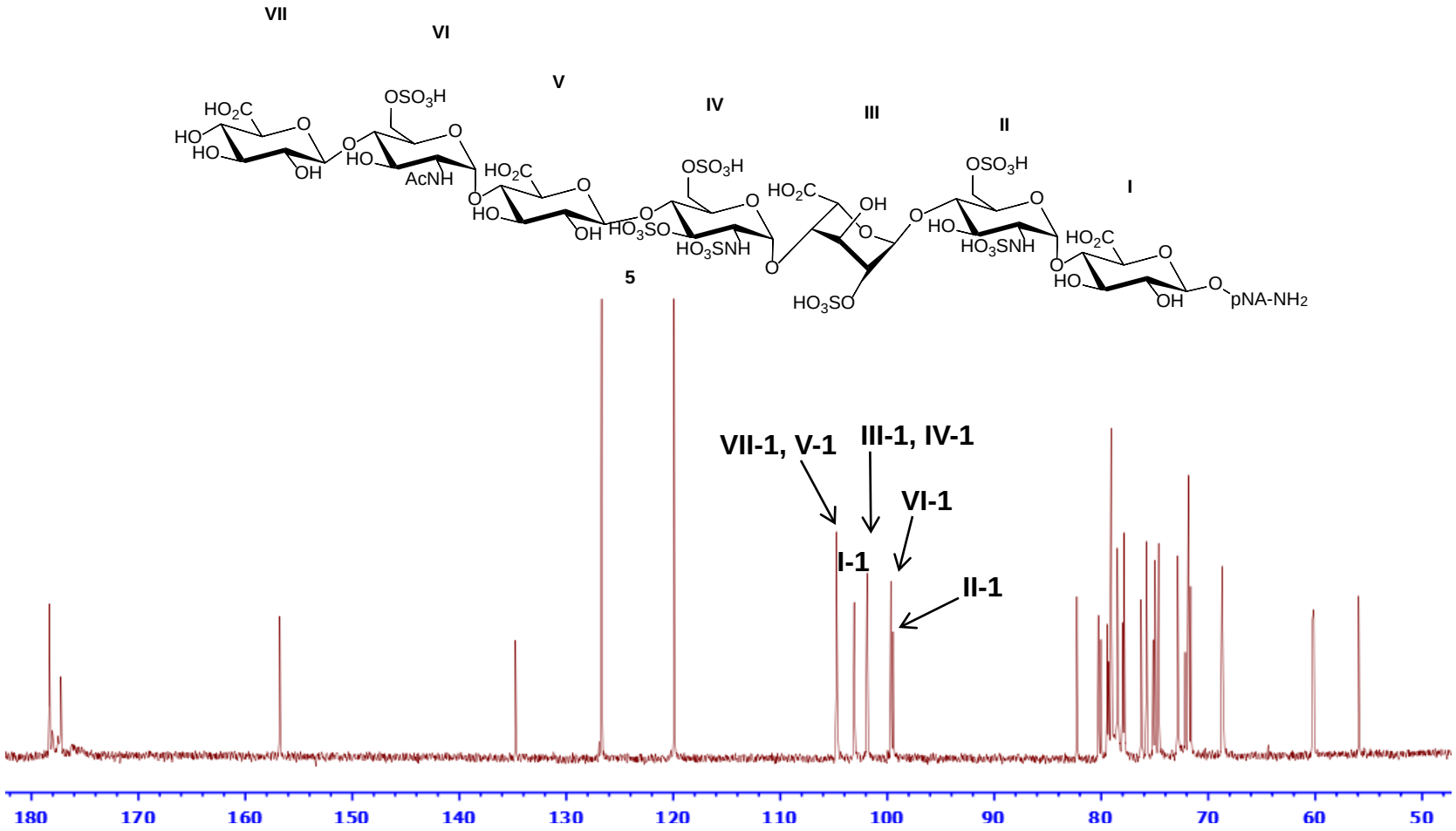


**Supplementary Fig 16**. $^{13}$C-NMR of compound **5** (175 MHz, $D_2O$). The signals of anomeric carbons are indicated. The anomeric carbons resonate at δ 104.8, 104.7, 103.1, 101.9, 101.9, 99.7, and 99.5 ppm. Chemical structure of compound **5** is shown on top of figure.

# $^{1}H$-$^{13}C$ HSQC spectrum of compound **5**

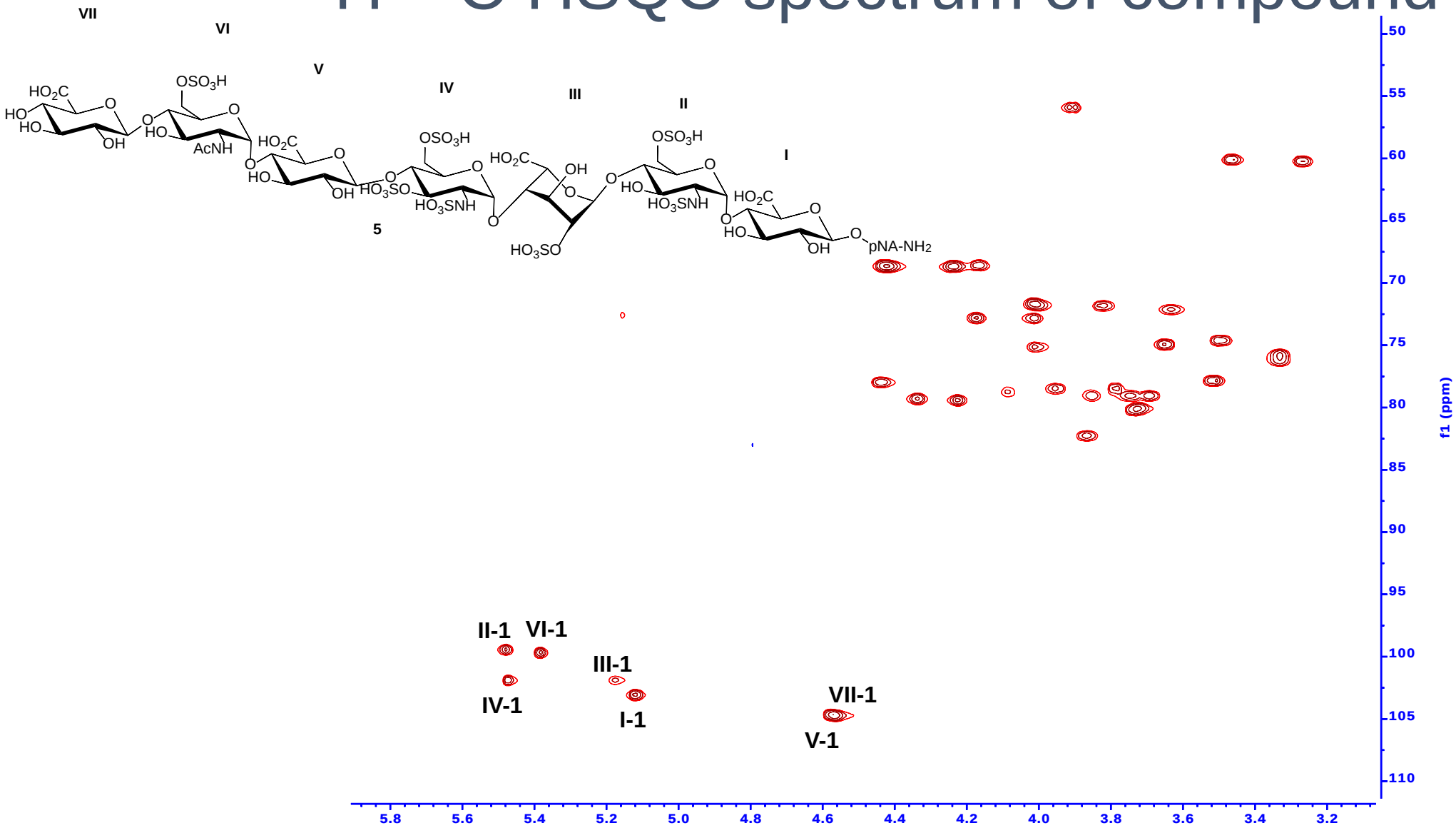


**Supplementary Fig 17**. $^{1}H$-$^{13}C$ HSQC spectrum of compound **5** (700 MHz, $D_2O$). The anomeric signals are indicated. Chemical structure of compound **5** is shown on top of figure.

# $^{1}$H-NMR of compound **6**

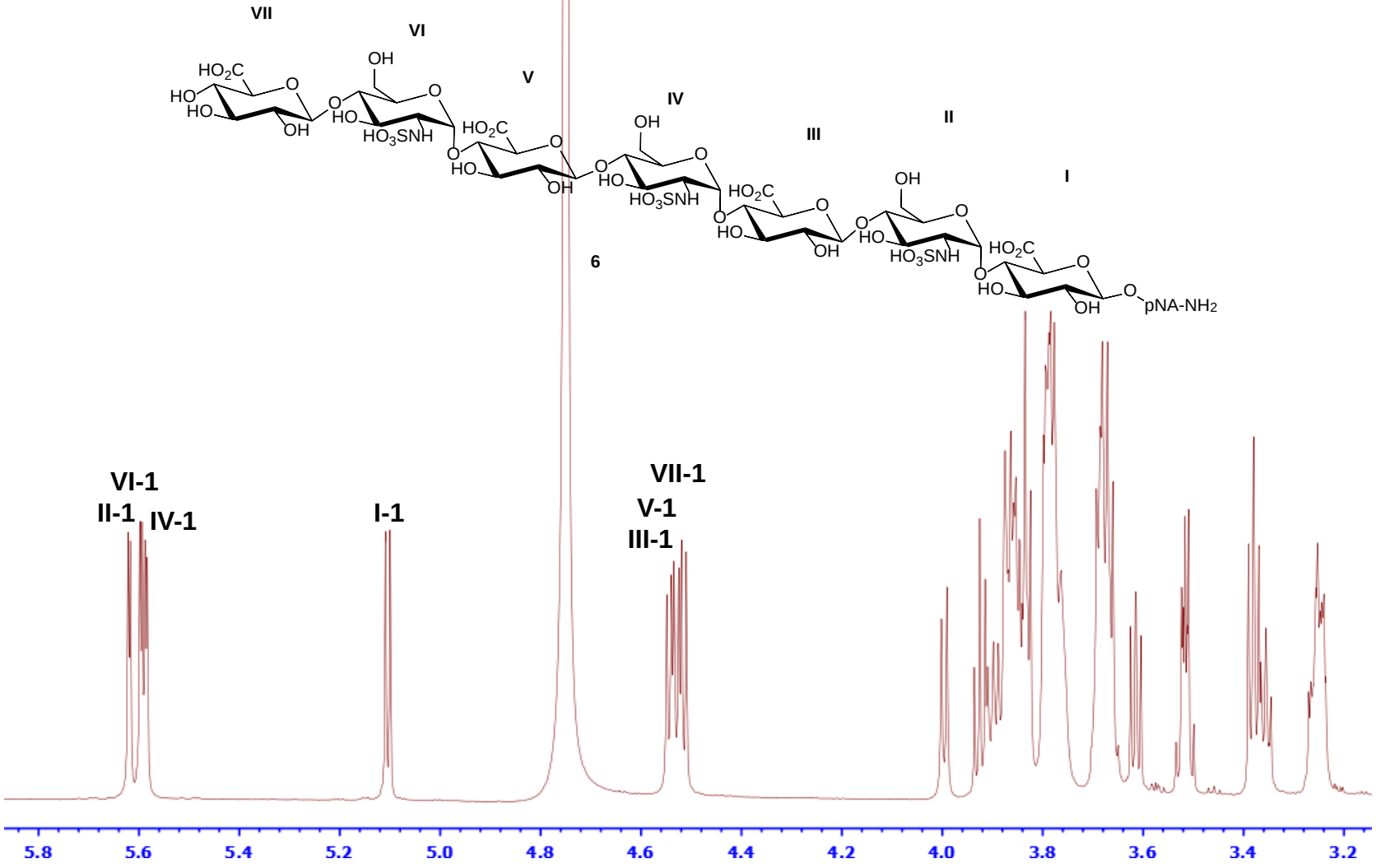


**Supplementary Fig 18**. $^{1}$H-NMR of compound **6** (850 MHz, $D_2O$). The signals of anomeric protons are indicated. The anomeric protons resonate as doublet at δ 5.62, 5.60, 5.59, 5.11, 4.54, 4.53, and 4.52 ppm. Chemical structure of compound **6** is shown on top of figure.

# $^{13}$C-NMR of compound **6**

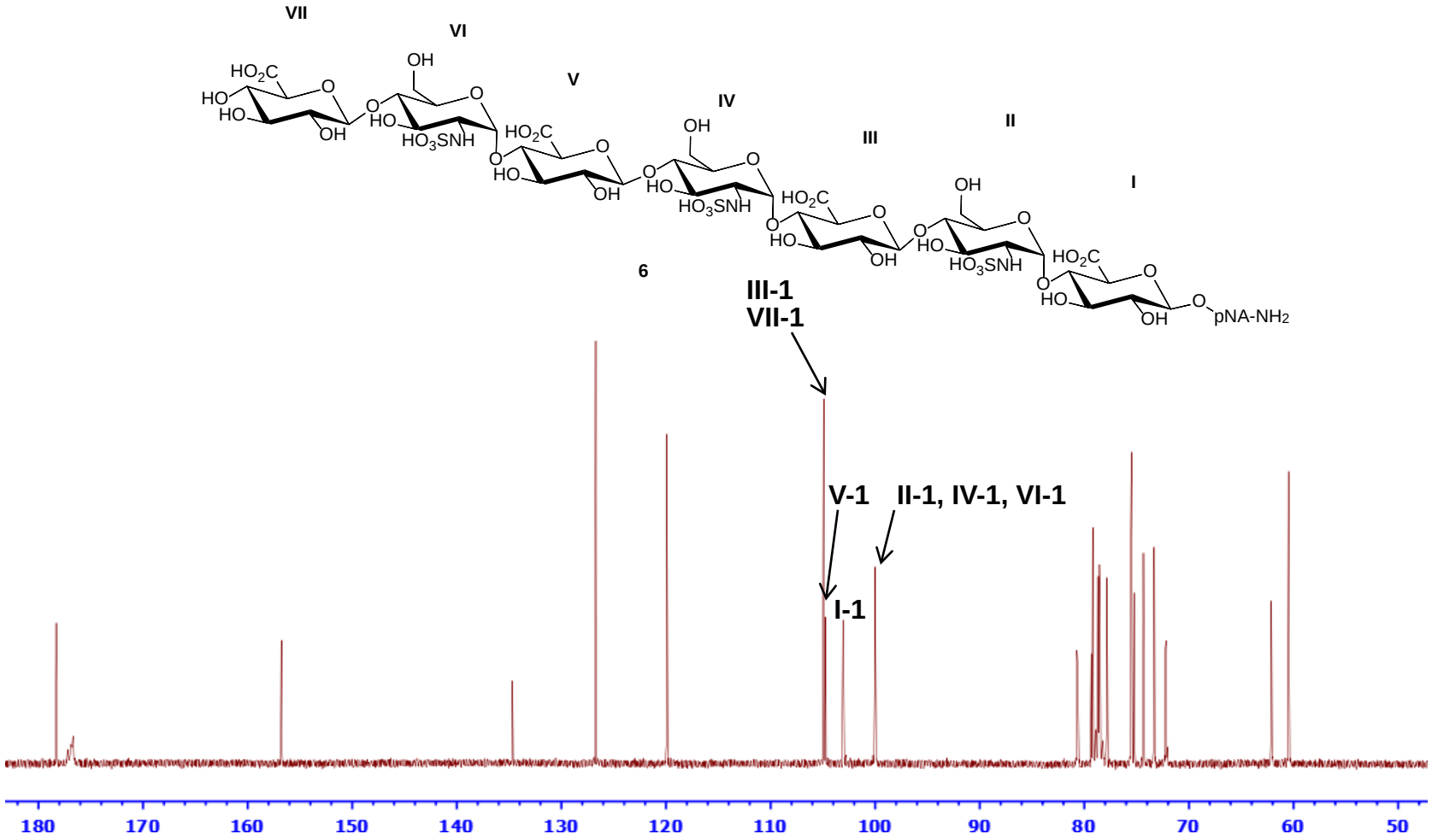


**Supplementary Fig 19**. $^{13}$C-NMR of compound **6** (212.5 MHz, $D_2O$). The signals of anomeric carbons are indicated. The anomeric carbons resonate at δ 104.9, 104.9, 104.7, 103.1, 100.0, 100.0, and 100.0 ppm. Chemical structure of compound **6** is shown on top of figure.

# $^{1}H$-$^{13}C$ HSQC spectrum of compound **6**

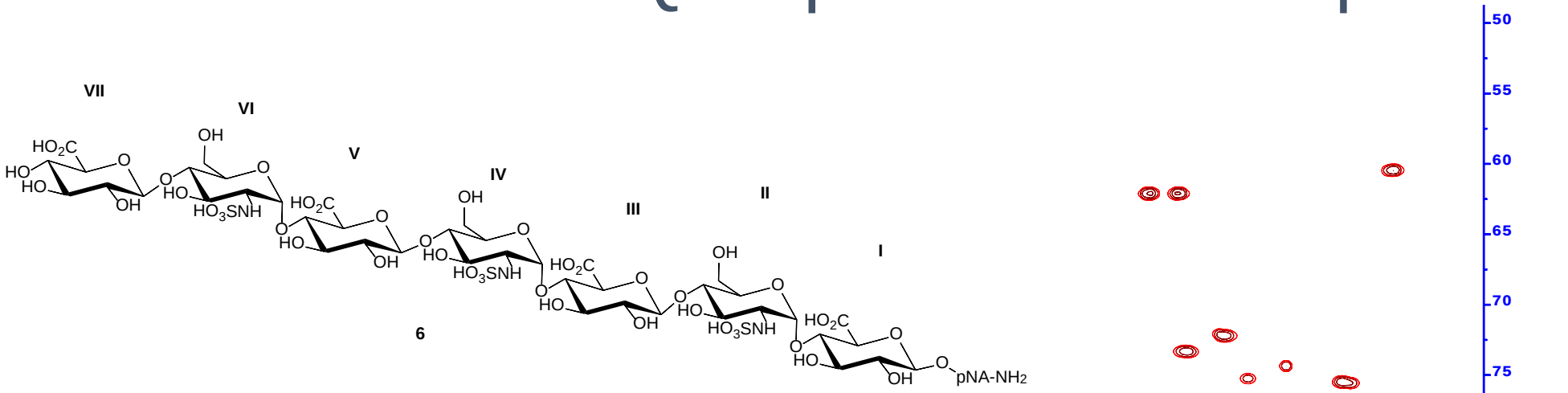





**Supplementary Fig 20**. $^{1}H$-$^{13}C$ HSQC spectrum of compound **6** (850 MHz, $D_2O$). The anomeric signals are indicated. Chemical structure of compound **6** is shown on top of figure.

# $^{1}$H-NMR of compound **7**

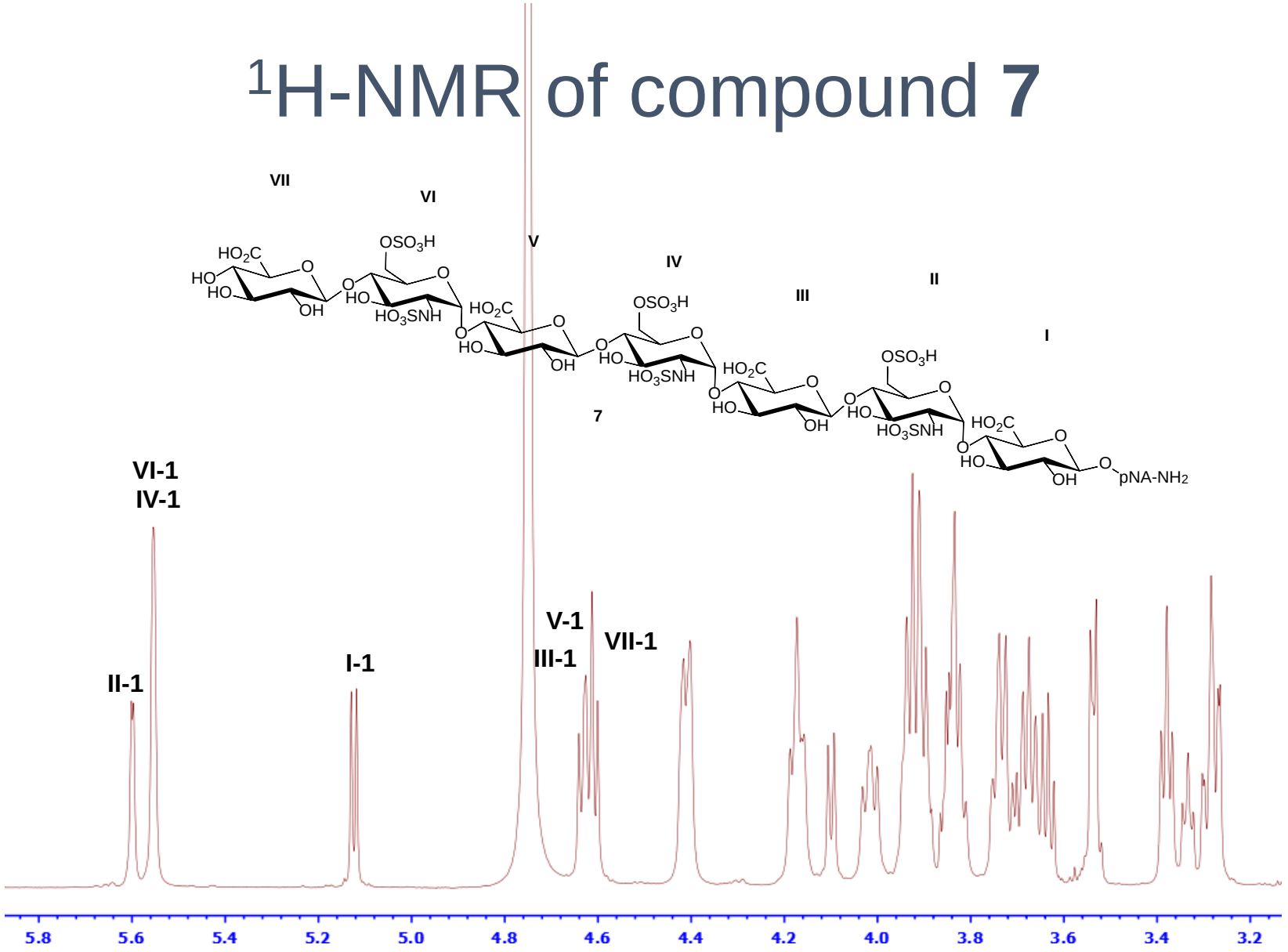


**Supplementary Fig 21**. $^{1}$H-NMR of compound **7** (700 MHz, $D_2O$). The signals of anomeric protons are indicated. The anomeric protons resonate as doublet at δ 5.60, 5.55, 5.55, 5.13, 4.64, 4.62, and 4.61 ppm. Chemical structure of compound **7** is shown on top of figure.

# $^{13}$C-NMR of compound **7**

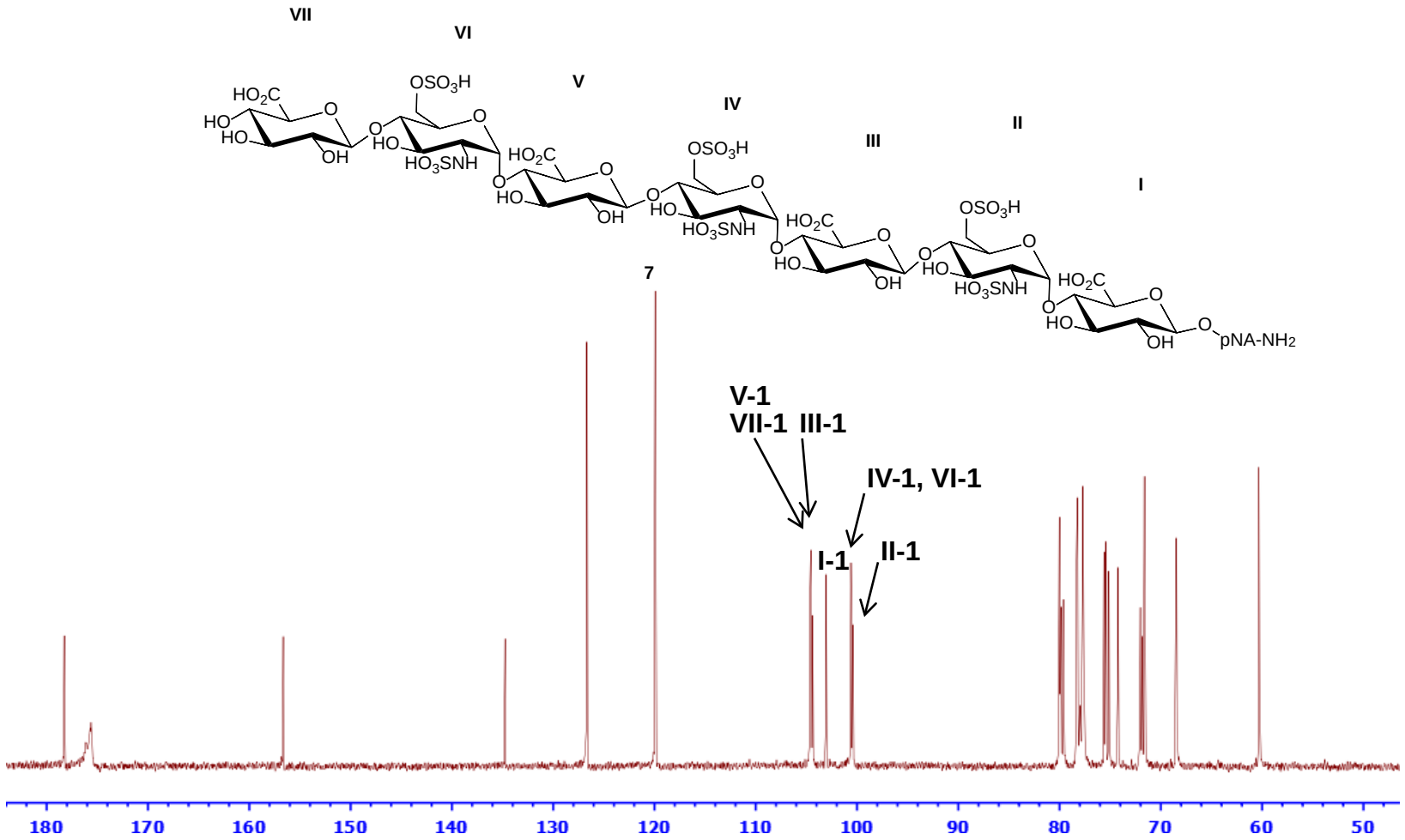


**Supplementary Fig 22**. $^{13}$C-NMR of compound **7** (175 MHz, $D_2O$). The signals of anomeric carbons are indicated. The anomeric carbons resonate at δ 104.6, 104.6, 104.4, 103.1, 100.6, 100.6, and 100.4 ppm. Chemical structure of compound **7** is shown on top of figure.

# $^{1}H$-$^{13}C$ HSQC spectrum of compound **7**

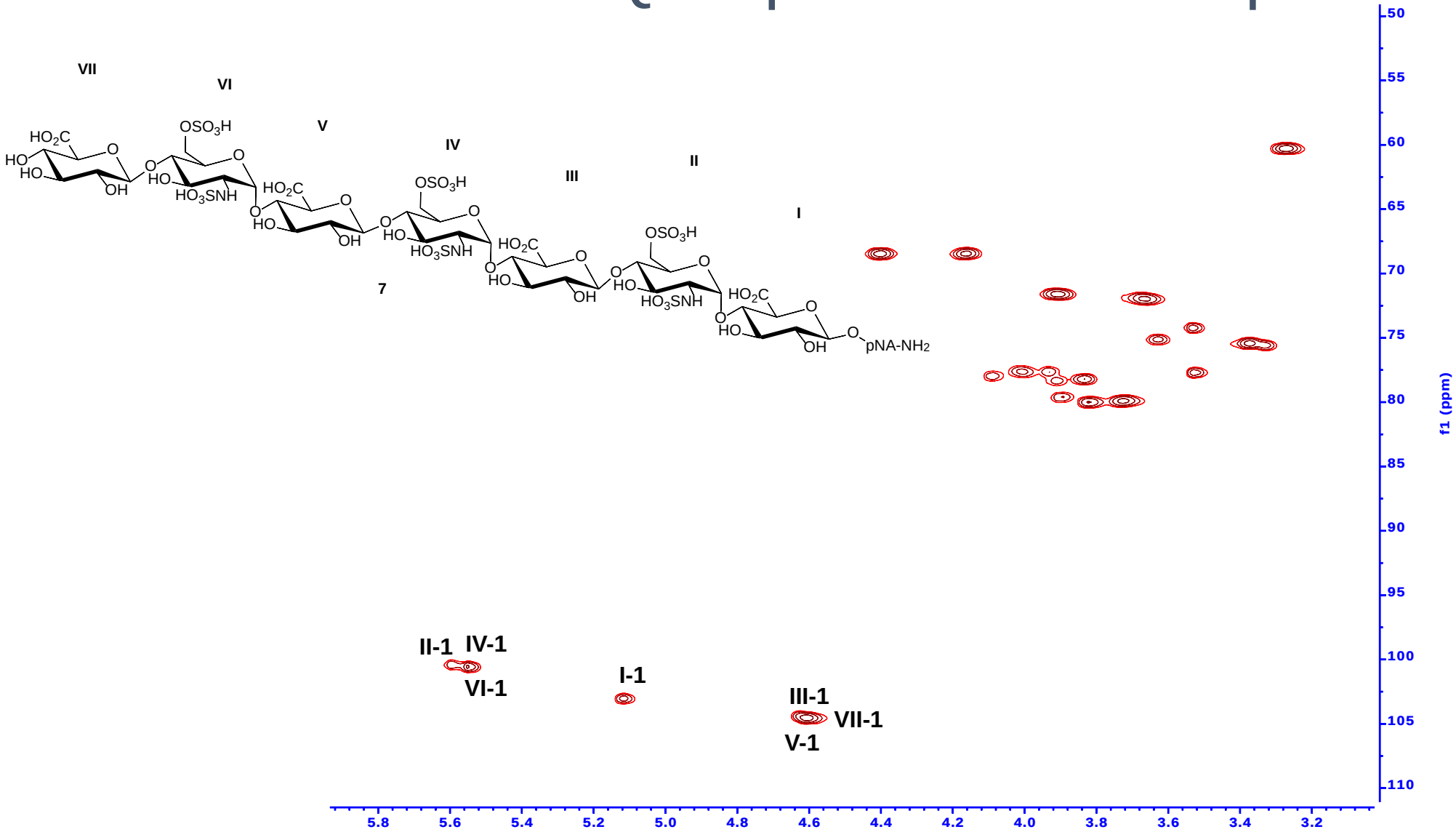


**Supplementary Fig 23**. $^{1}H$-$^{13}C$ HSQC spectrum of compound **7** (700 MHz, $D_2O$). The anomeric signals are indicated. Chemical structure of compound **7** is shown on top of figure.

# $^{1}$H-NMR of compound **8**

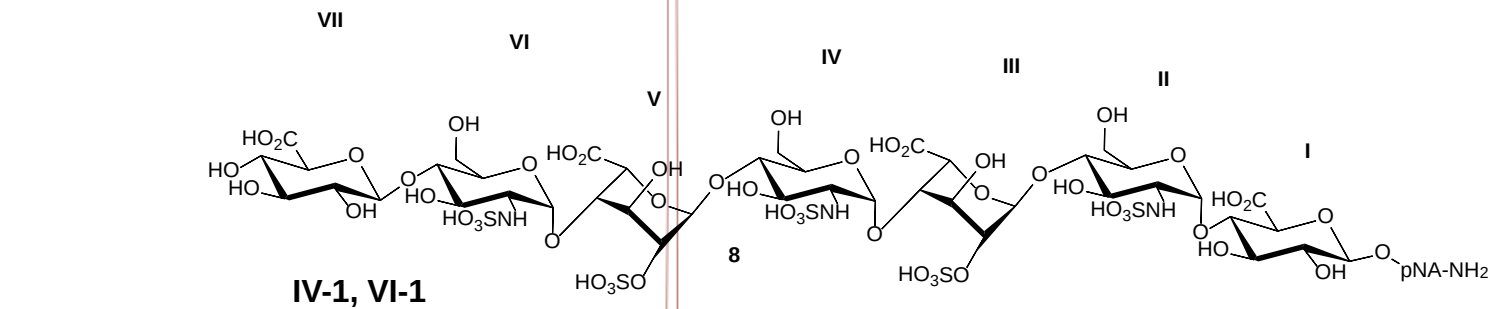


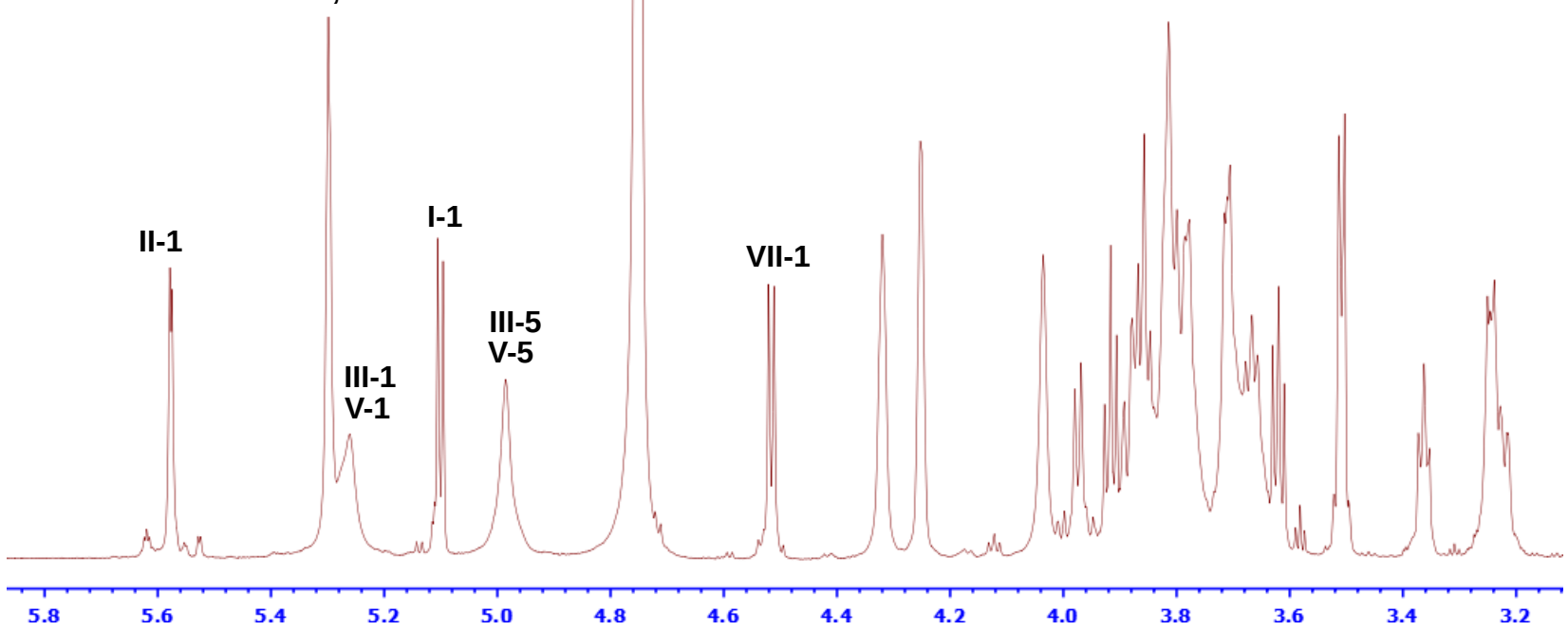


**Supplementary Fig 24**. $^{1}$H-NMR of compound **8** (850 MHz, $D_2O$). The signals of anomeric protons are indicated. The anomeric protons resonate as doublet at δ 5.58, 5.30, 5.30, 5.26, 5.26, 5.10, and 4.52 ppm. Chemical structure of compound **8** is shown on top of figure.

# $^{13}$C-NMR of compound **8**

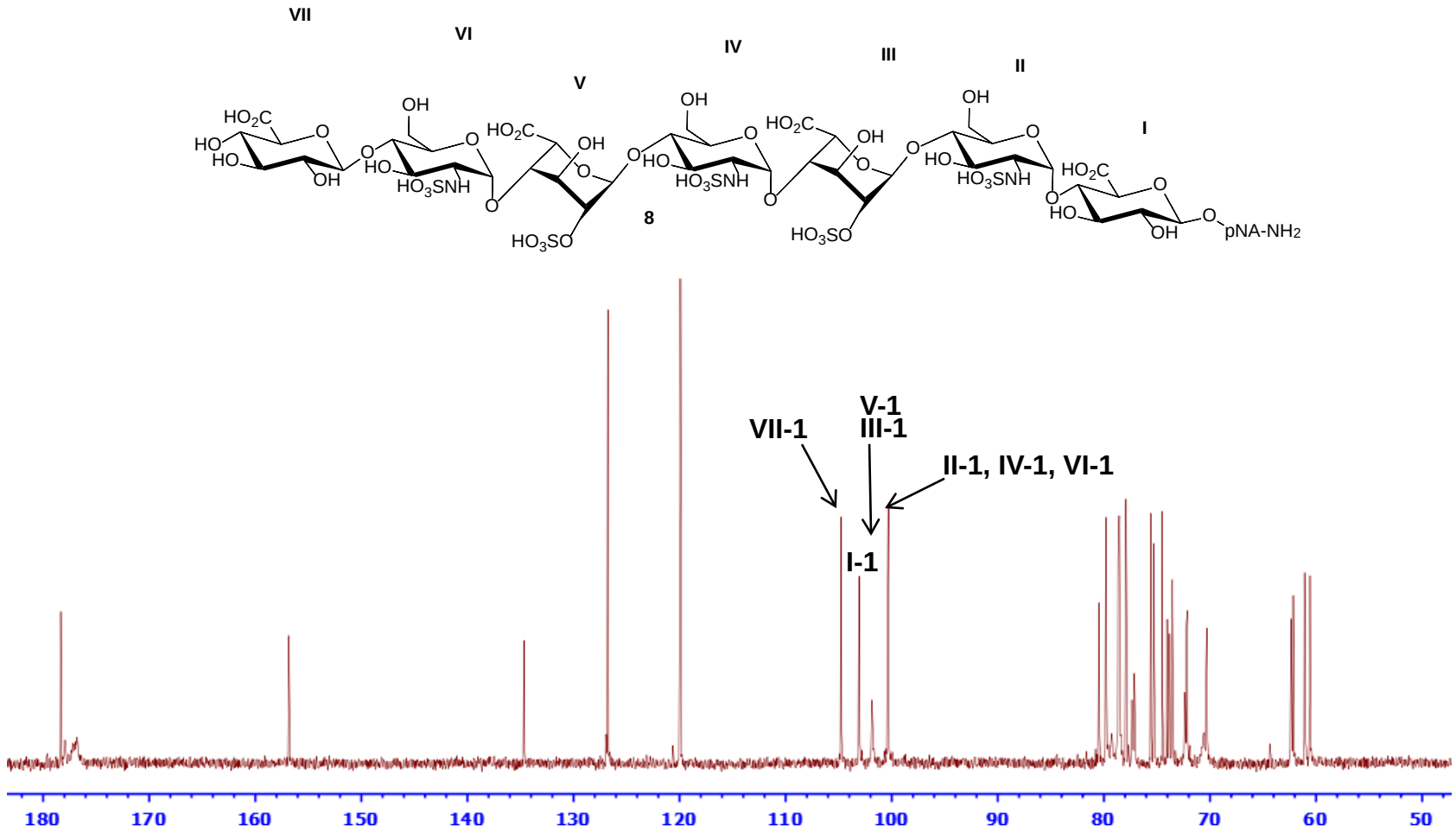


**Supplementary Fig 25**. $^{13}$C-NMR of compound **8** (212.5 MHz, $D_2O$). The signals of anomeric carbons are indicated. The anomeric carbons resonate at δ 104.8, 103.1, 101.9, 101.9, 100.4, 100.3, and 100.3 ppm. Chemical structure of compound **8** is shown on top of figure.

# $^{1}H$-$^{13}C$ HSQC spectrum of compound **8**

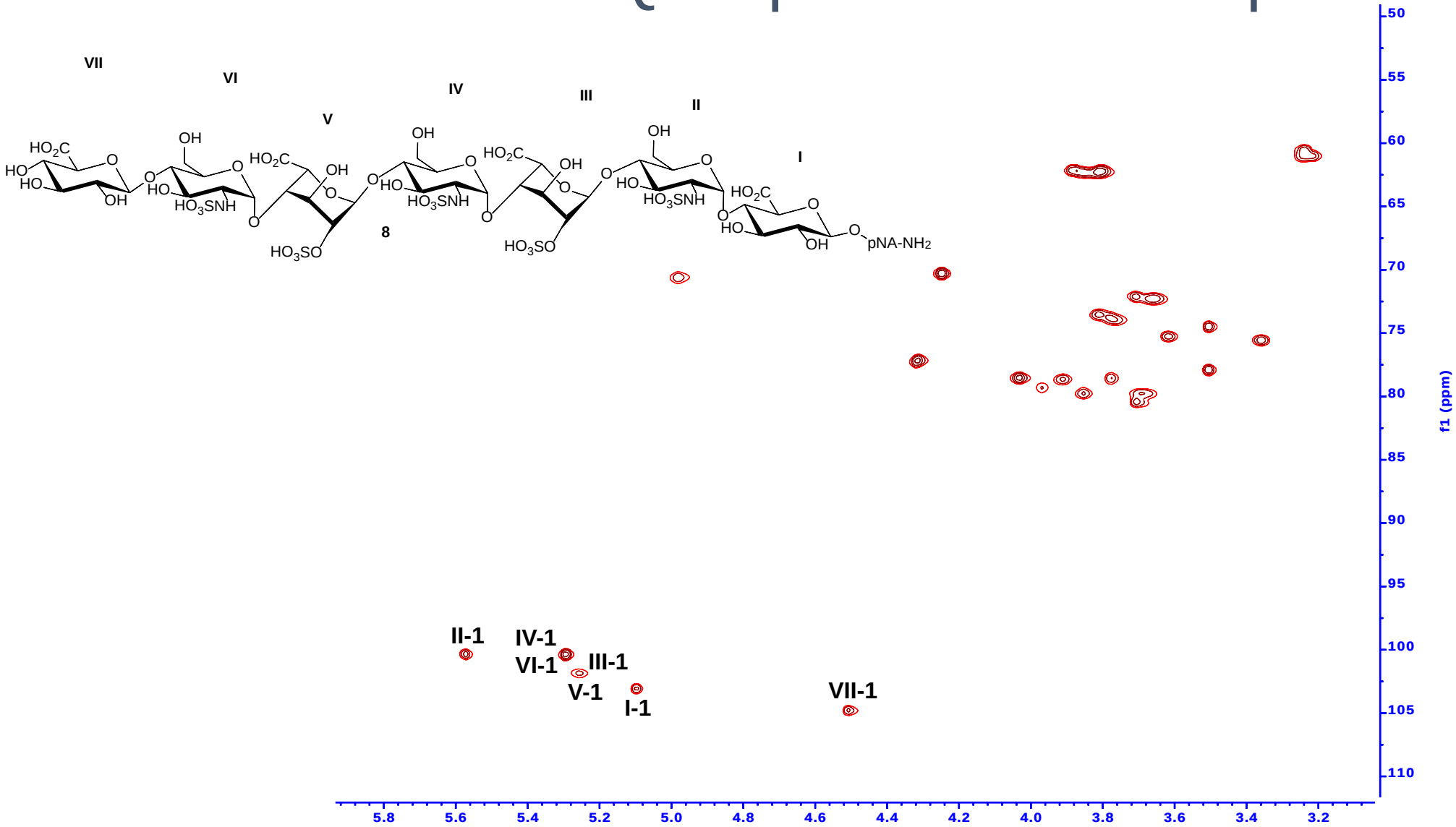


**Supplementary Fig 26**. $^{1}H$-$^{13}C$ HSQC spectrum of compound **8** (850 MHz, $D_2O$). The anomeric signals are indicated. Chemical structure of compound **8** is shown on top of figure.

# $^{1}$H-NMR of compound **9**

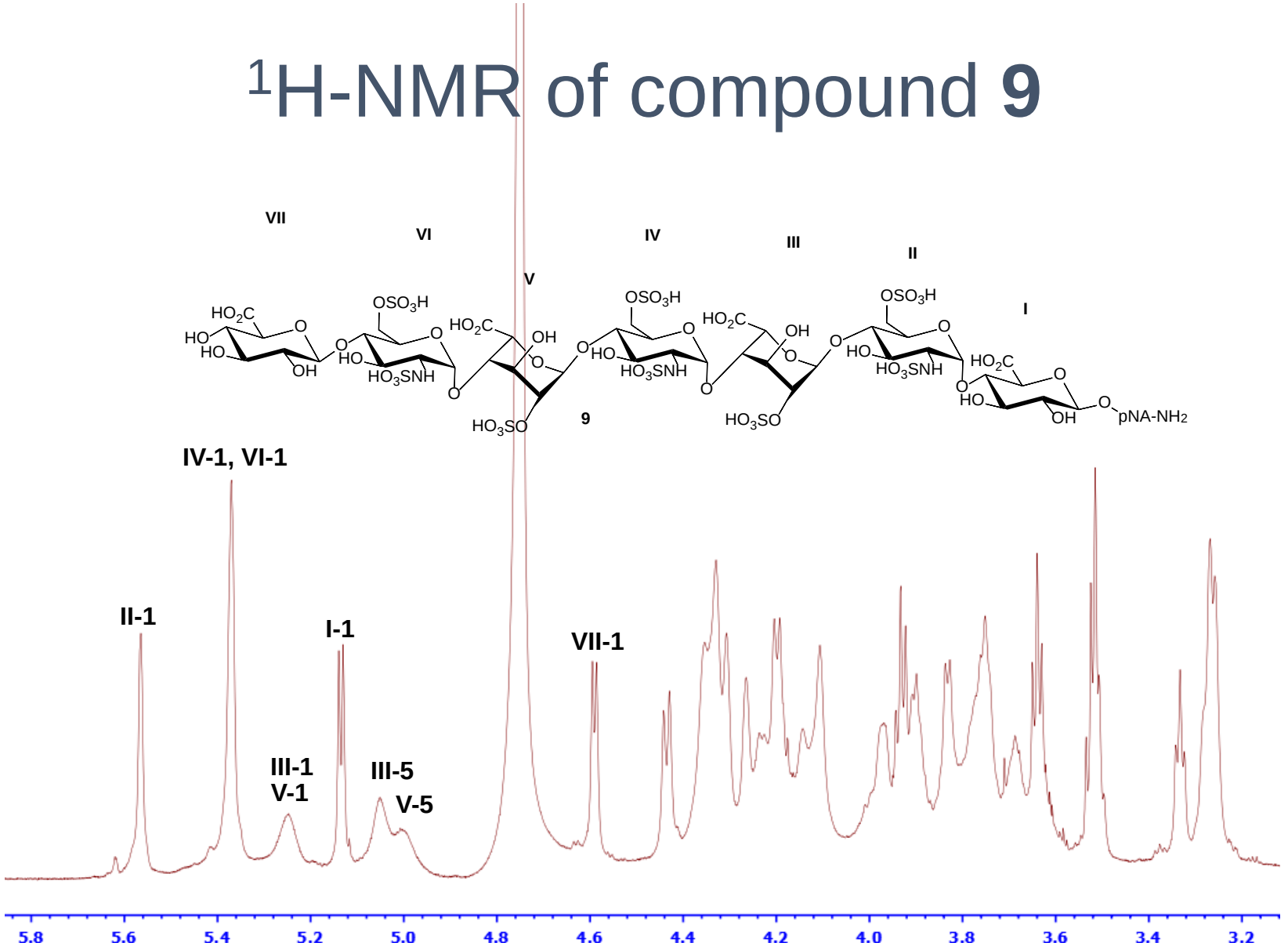


**Supplementary Fig 27**. $^{1}$H-NMR of compound **9** (850 MHz, $D_2O$). The signals of anomeric protons are indicated. The anomeric protons resonate as doublet at δ 5.57, 5.37, 5.37, 5.25, 5.25, 5.14, and 4.59 ppm. Chemical structure of compound **9** is shown on top of figure.

# $^{13}$C-NMR of compound **9**

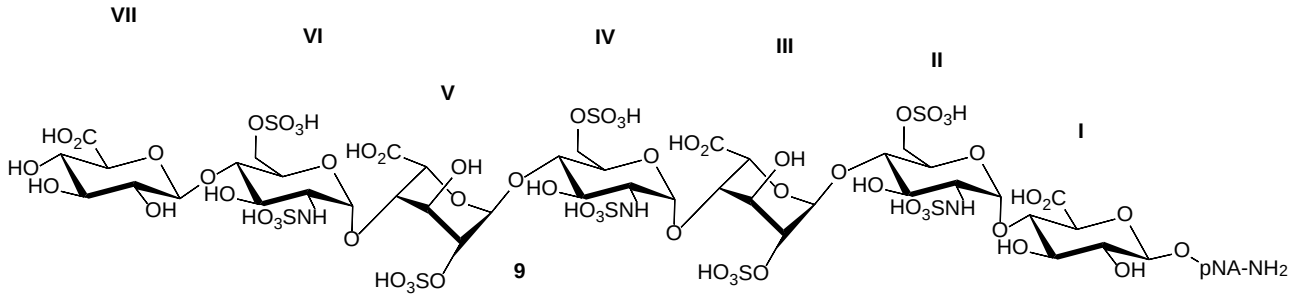


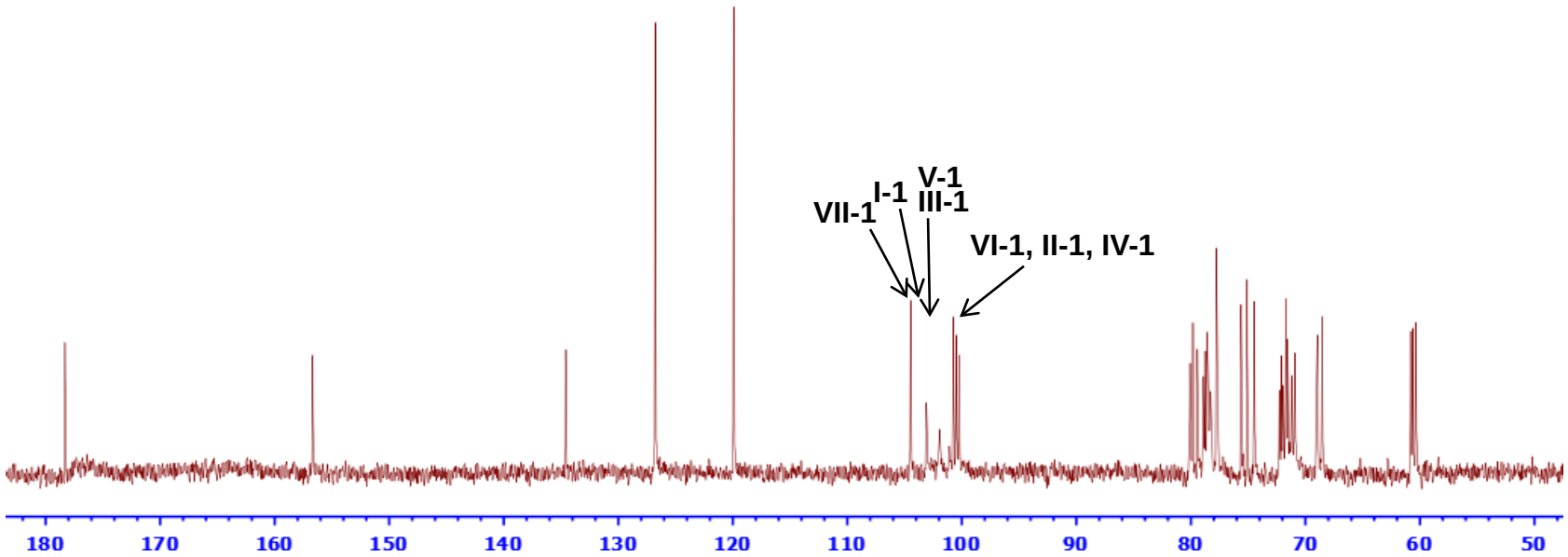


**Supplementary Fig 28**. $^{13}$C-NMR of compound **9** (212.5 MHz, $D_2O$). The signals of anomeric carbons are indicated. The anomeric carbons resonate at δ 104.5, 103.1, 101.9, 101.9, 100.7, 100.5, and 100.2 ppm. Chemical structure of compound **9** is shown on top of figure.

# $^{1}H$-$^{13}C$ HSQC spectrum of compound **9**

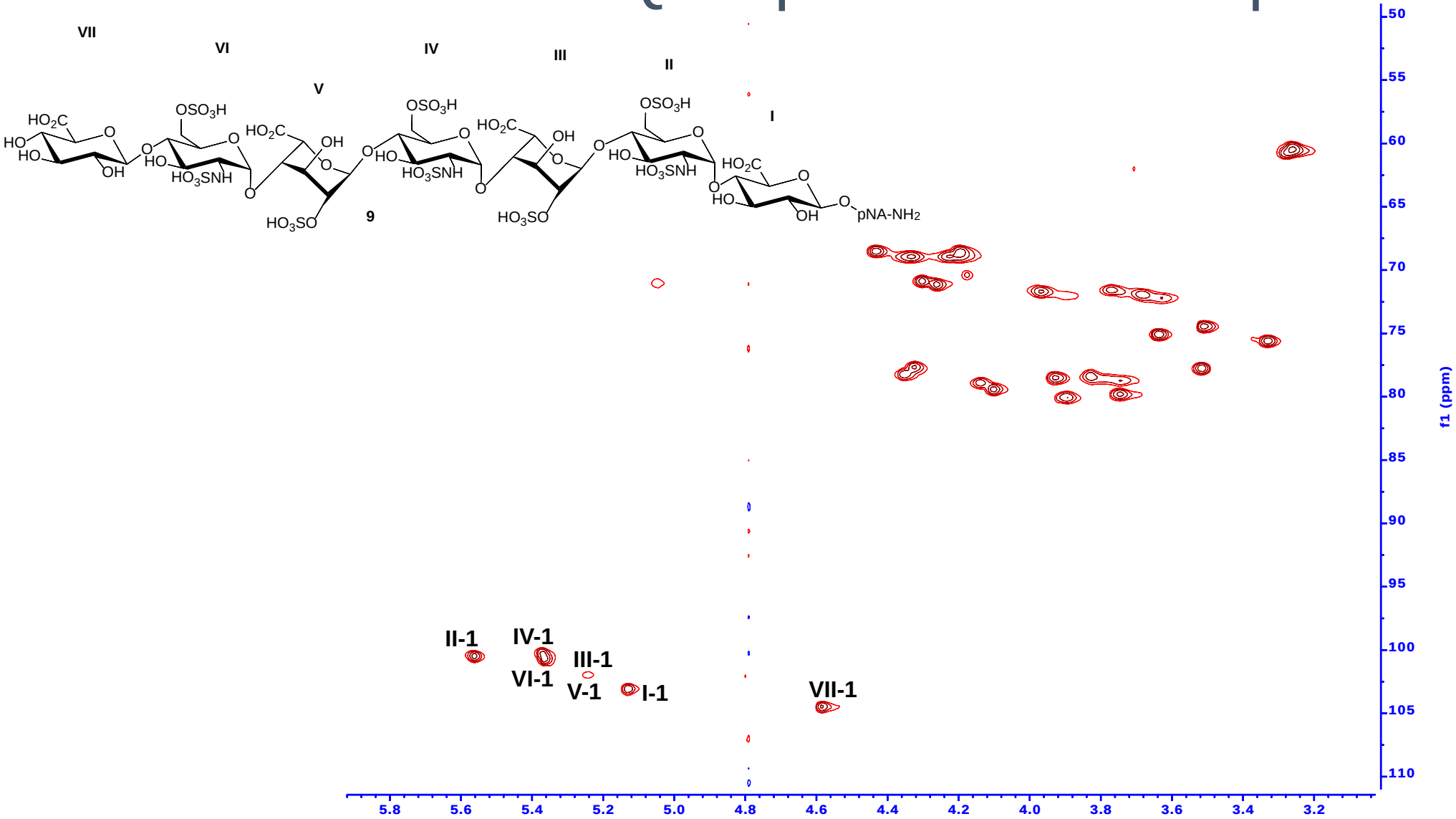


**Supplementary Fig 29**. $^{1}H$-$^{13}C$ HSQC spectrum of compound **9** (850 MHz, $D_2O$). The anomeric signals are indicated. Chemical structure of compound **9** is shown on top of figure.

# $^{1}$H-NMR of compound **10**

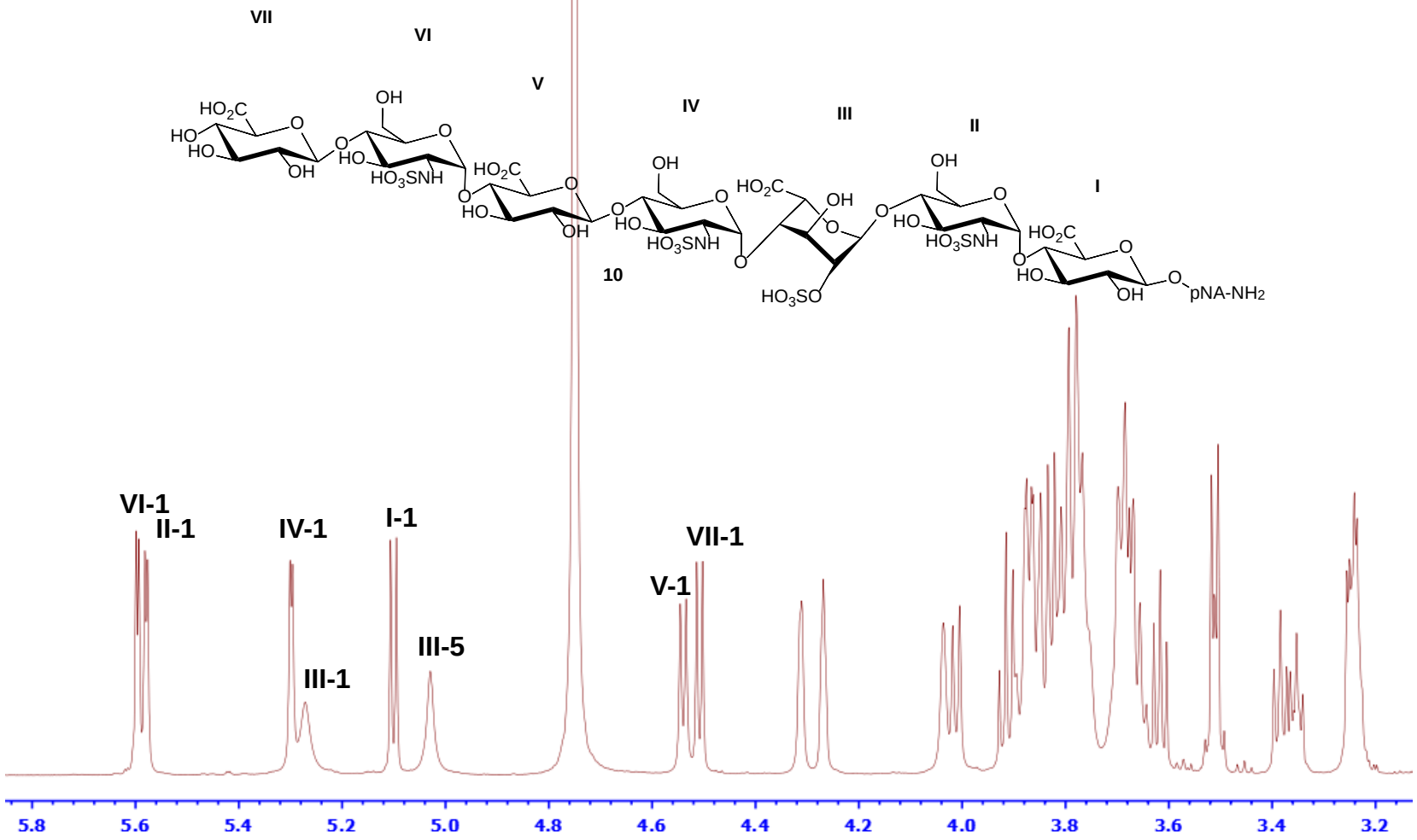


**Supplementary Fig 30**. $^{1}$H-NMR of compound **10** (700 MHz, $D_2O$). The signals of anomeric protons are indicated. The anomeric protons resonate as doublet at δ 5.60, 5.58, 5.30, 5.27, 5.10, 4.54, and 4.51 ppm. Chemical structure of compound **10** is shown on top of figure.

# $^{13}$C-NMR of compound **10**

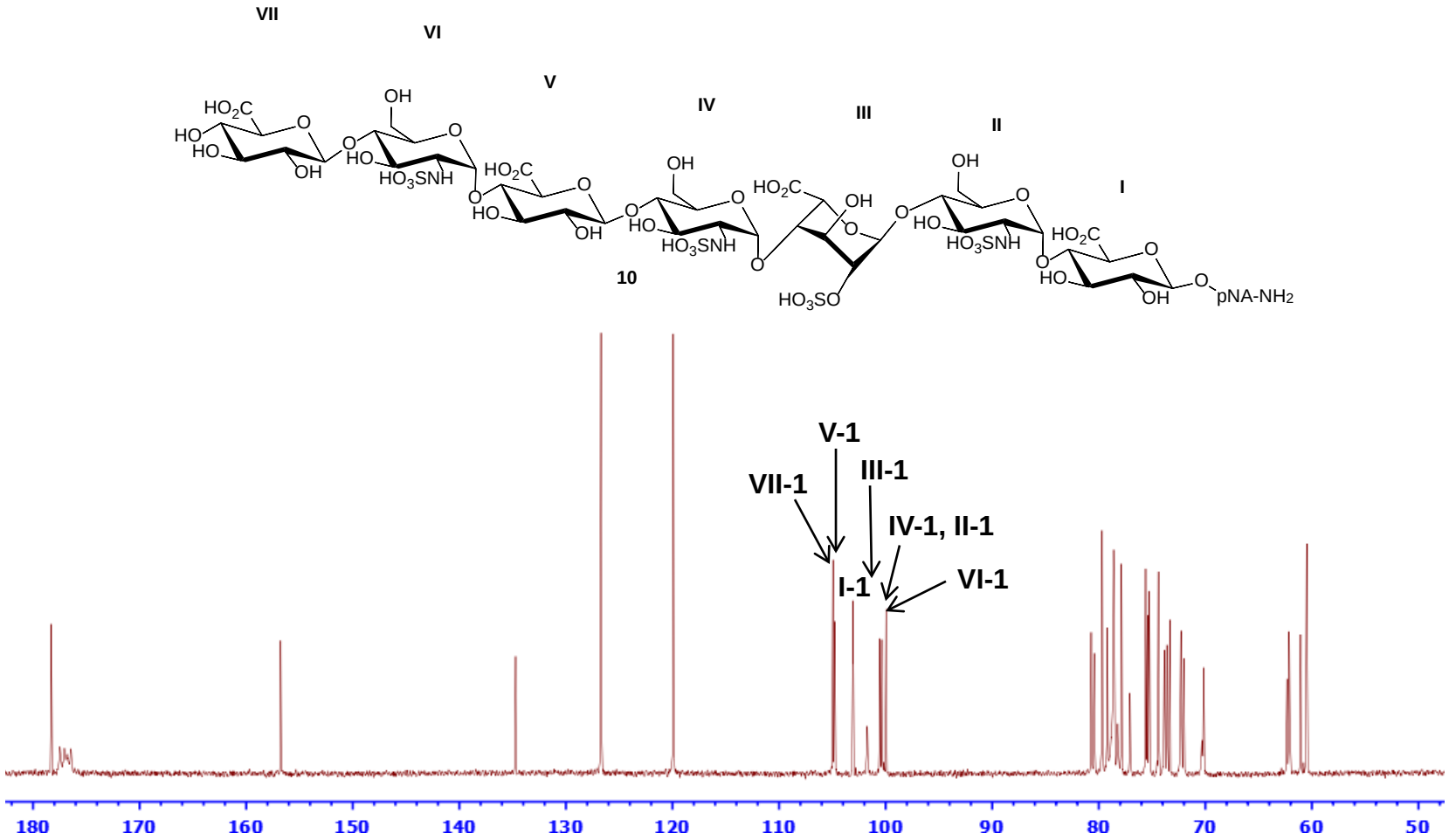


**Supplementary Fig 31**. $^{13}$C-NMR of compound **10** (175 MHz, $D_2O$). The signals of anomeric carbons are indicated. The anomeric carbons resonate at δ 104.9, 104.8, 103.1, 101.7, 100.6, 100.4, and 100.0 ppm. Chemical structure of compound **10** is shown on top of figure.

# $^{1}H$-$^{13}C$ HSQC spectrum of compound **10**

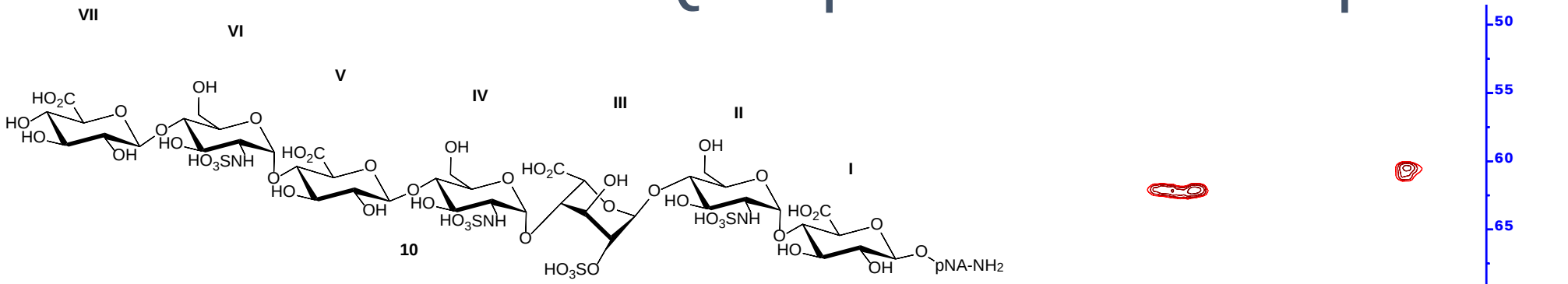





**Supplementary Fig 32**. $^{1}H$-$^{13}C$ HSQC spectrum of compound **10** (700 MHz, $D_2O$). The anomeric signals are indicated. Chemical structure of compound **10** is shown on top of figure.

# $^{1}$H-NMR of compound **11**

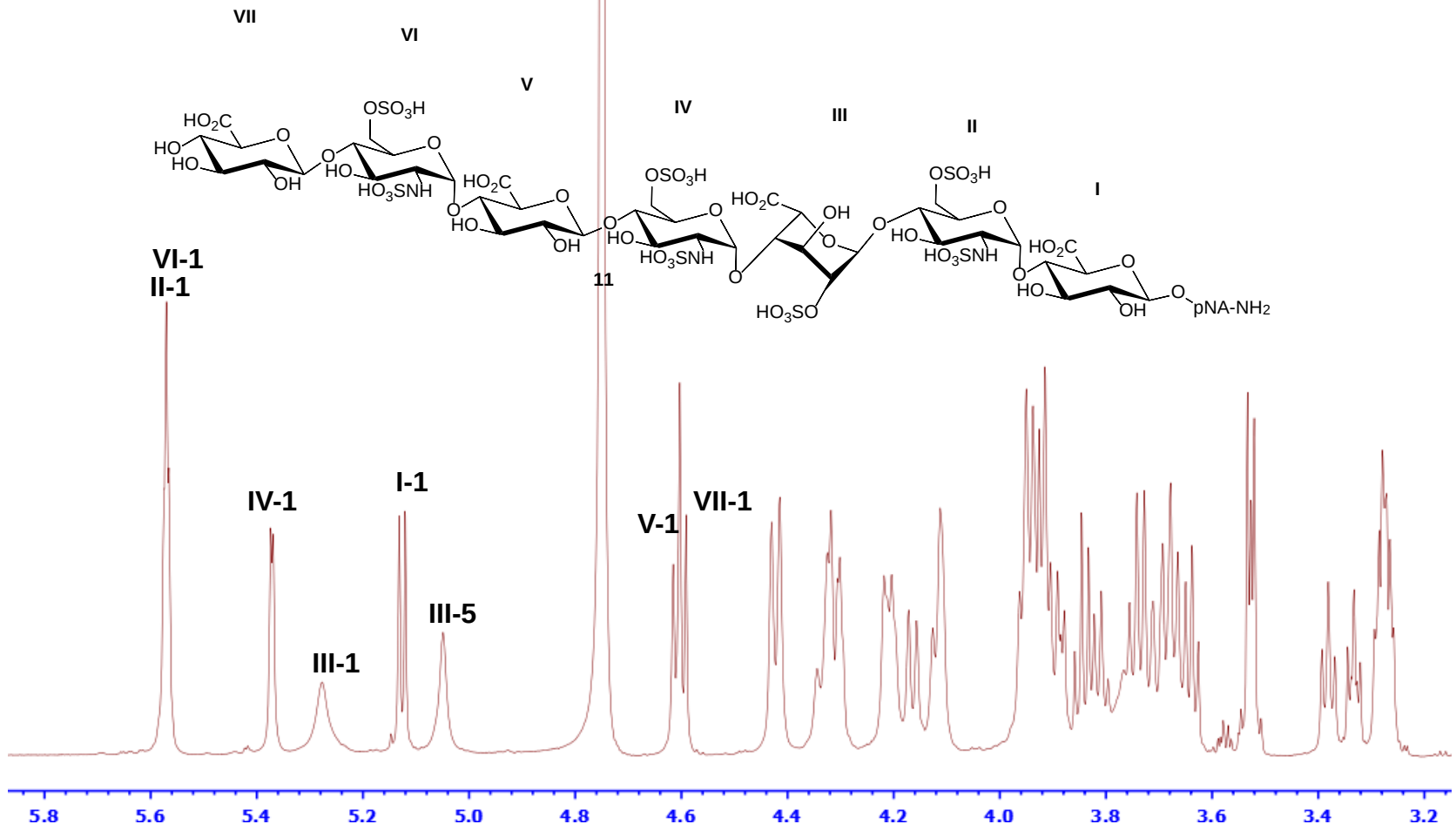


**Supplementary Fig 33**. $^{1}$H-NMR of compound **11** (700 MHz, $D_2O$). The signals of anomeric protons are indicated. The anomeric protons resonate as doublet at δ 5.57, 5.57, 5.37, 5.28, 5.13, 4.61, and 4.60 ppm. Chemical structure of compound **11** is shown on top of figure.

# $^{13}$C-NMR of compound **11**

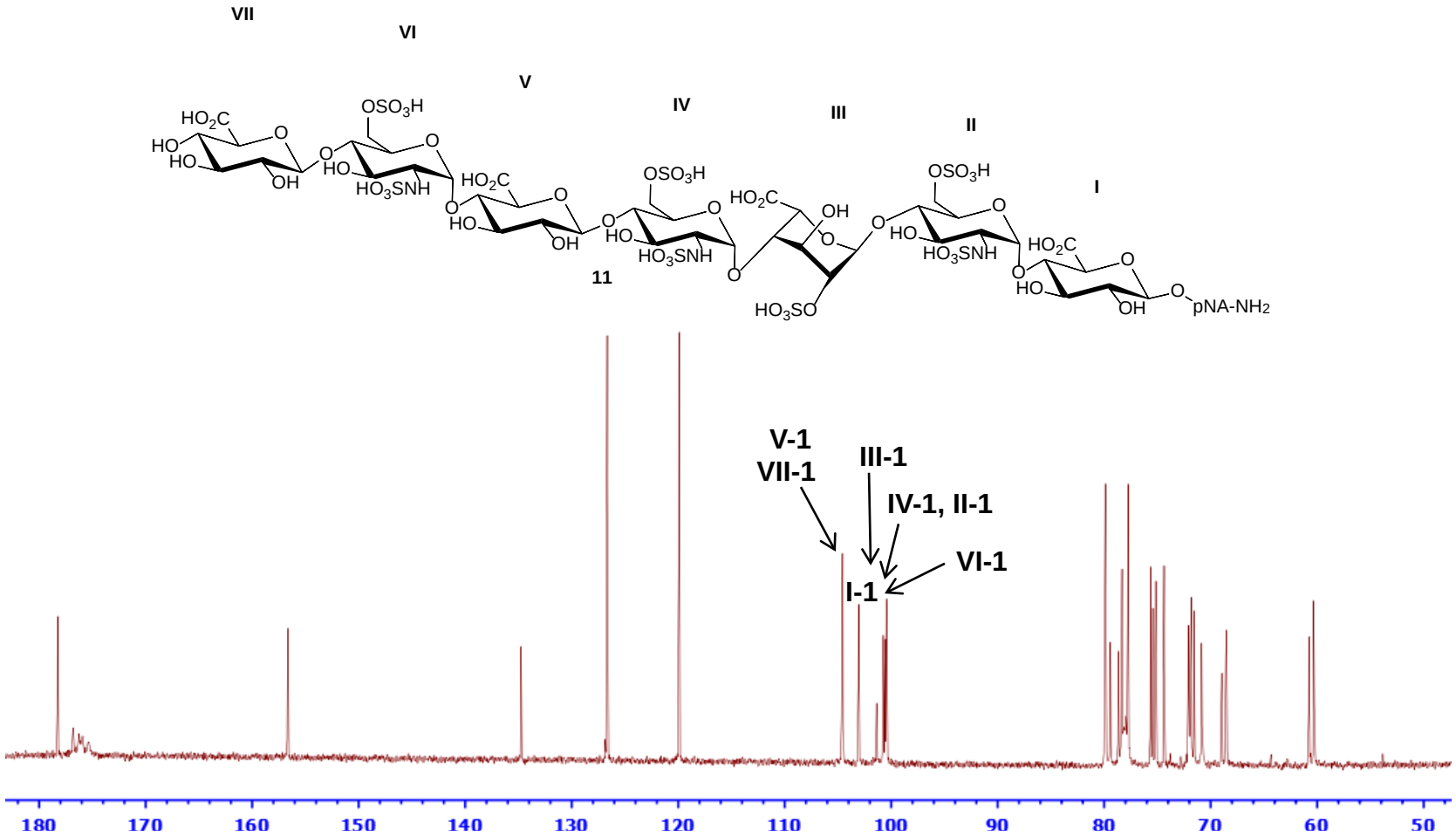


**Supplementary Fig 34**. $^{13}$C-NMR of compound **11** (175 MHz, $D_2O$). The signals of anomeric carbons are indicated. The anomeric carbons resonate at δ 104.6, 104.6, 103.1, 101.4, 100.7, 100.6, and 100.4 ppm. Chemical structure of compound **11** is shown on top of figure.

# $^{1}H$-$^{13}C$ HSQC spectrum of compound **11**

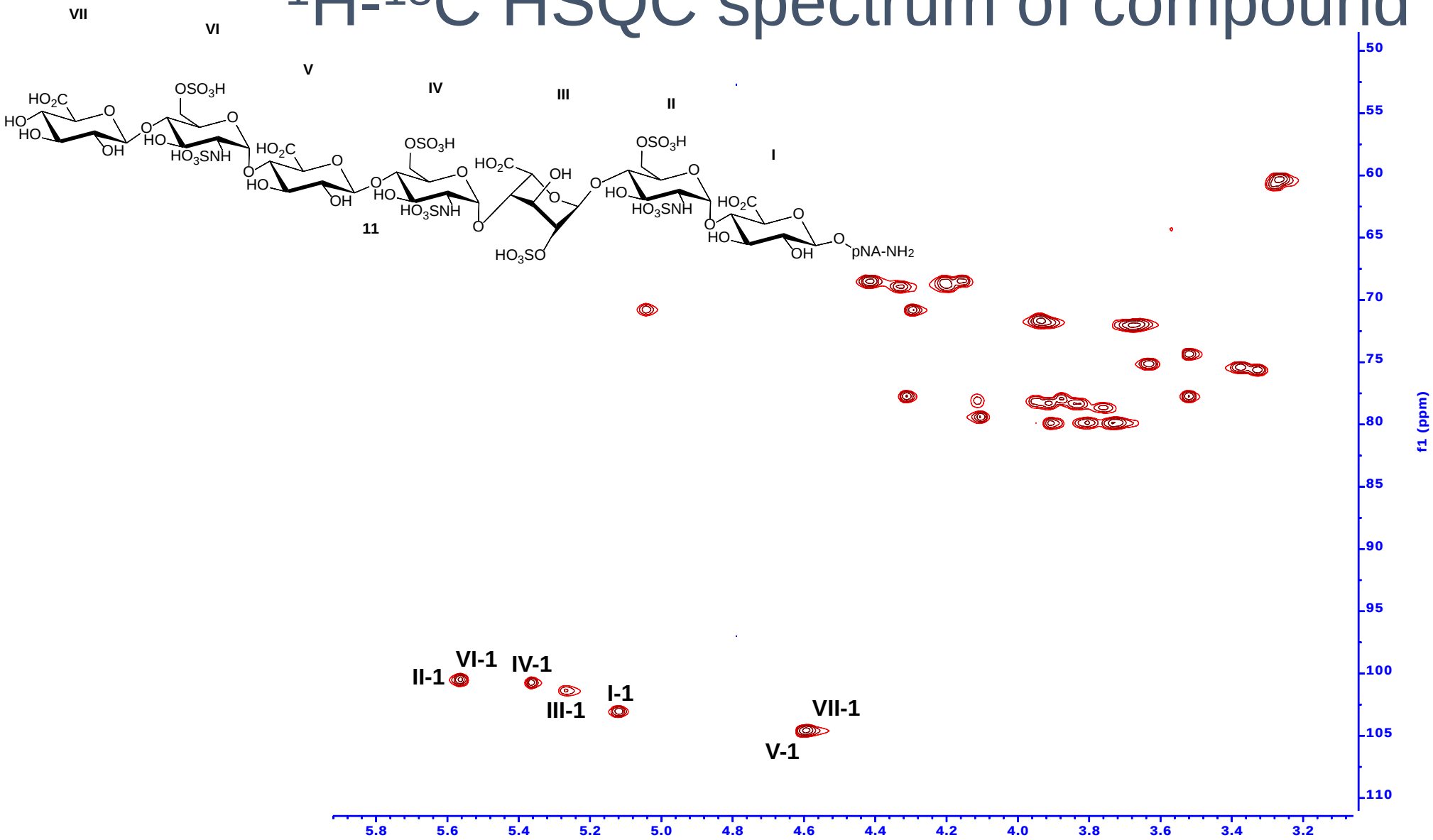


**Supplementary Fig 35**. $^{1}H$-$^{13}C$ HSQC spectrum of compound **11** (700 MHz, $D_2O$). The anomeric signals are indicated. Chemical structure of compound **11** is shown on top of figure.

# $^{1}$H-NMR of compound **12**

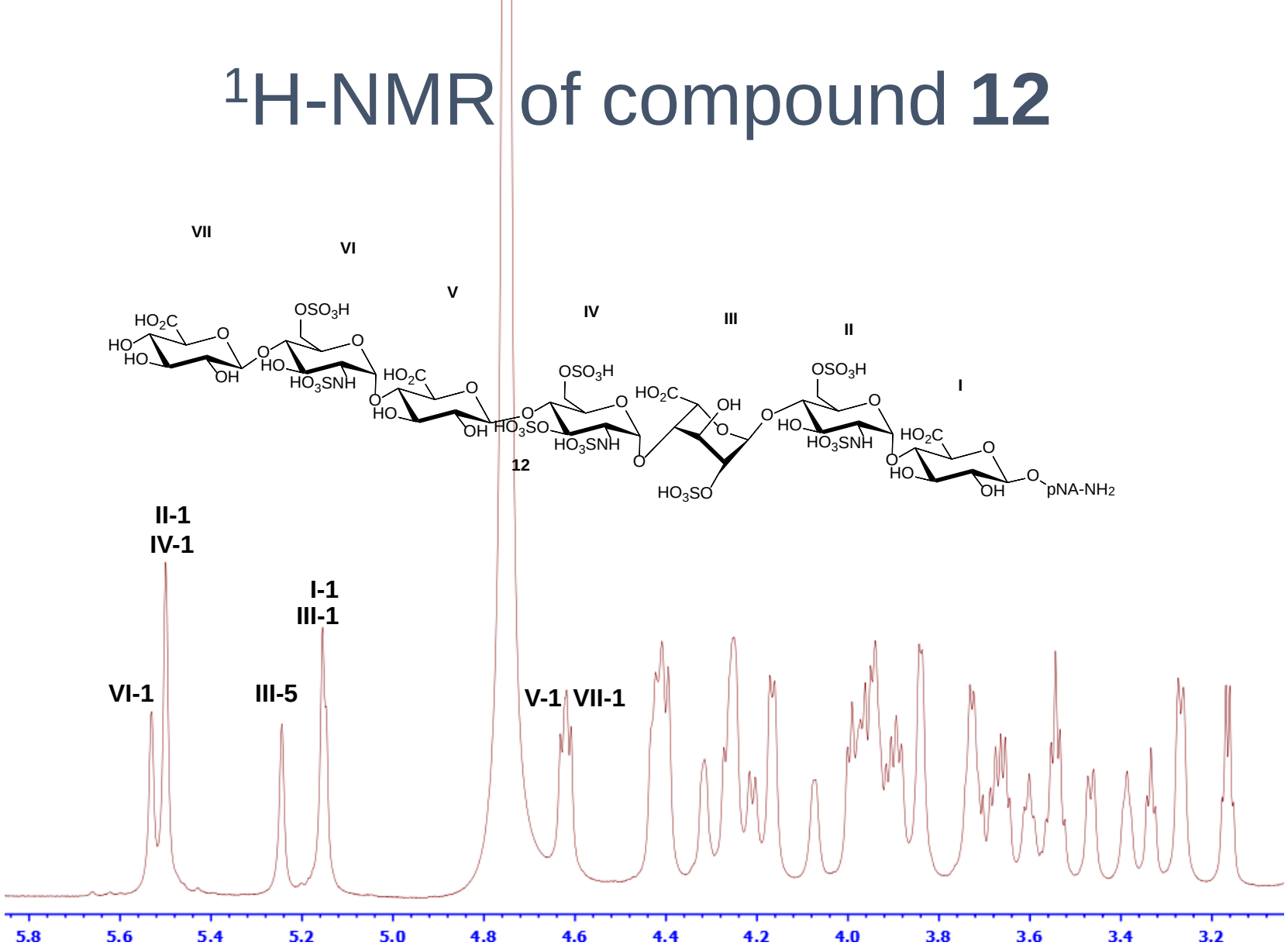


**Supplementary Fig 36**. $^{1}$H-NMR of compound **12** (850 MHz, $D_2O$). The signals of anomeric protons are indicated. The anomeric protons resonate as doublet at δ 5.53, 5.50, 5.50, 5.16, 5.15, 4.63, and 4.61 ppm. Chemical structure of compound **12** is shown on top of figure.

# $^{13}$C-NMR of compound **12**

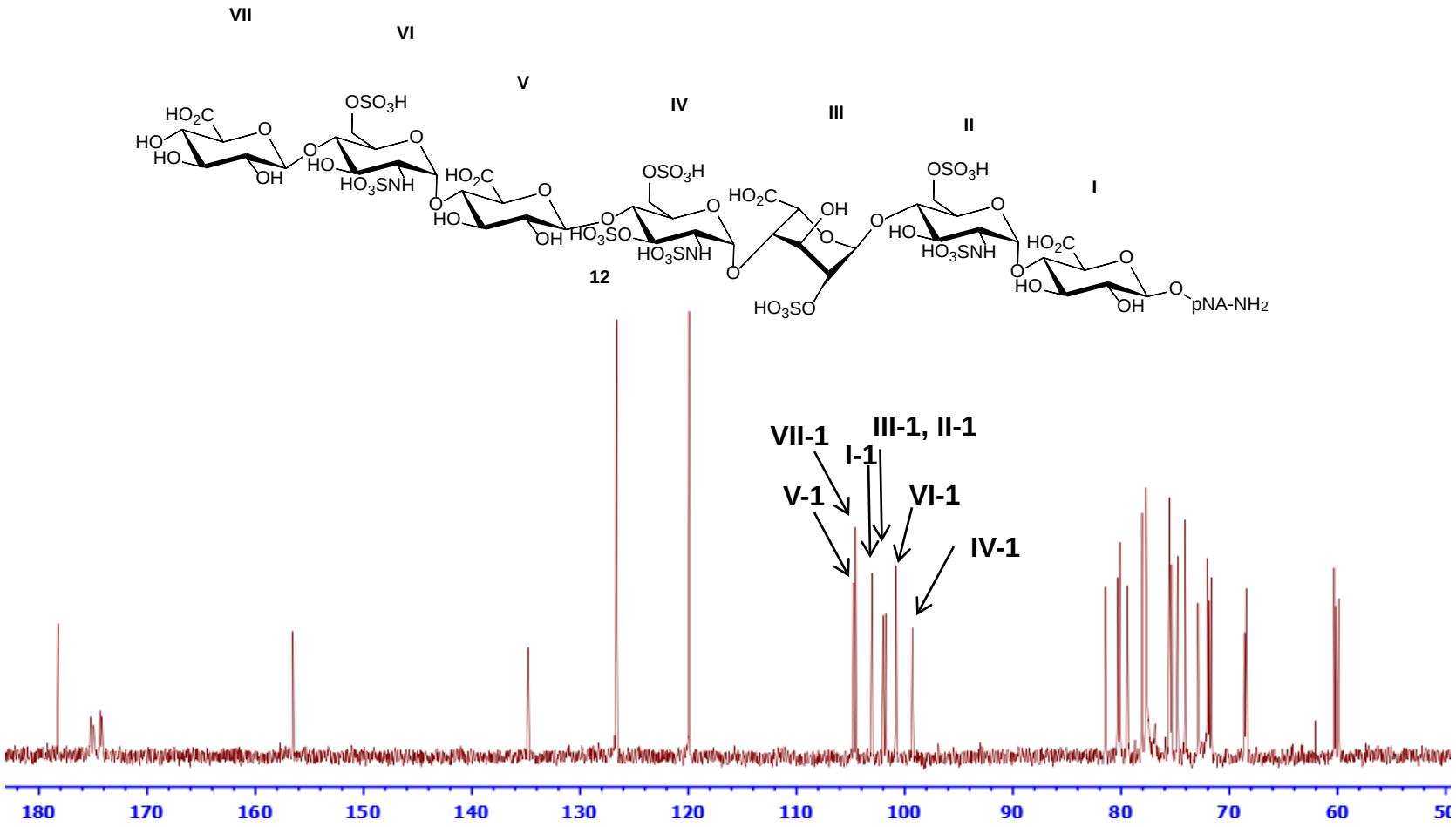


**Supplementary Fig 37**. $^{13}$C-NMR of compound **12** (212.5 MHz, $D_2O$). The signals of anomeric carbons are indicated. The anomeric carbons resonate at δ 104.7, 104.5, 103.0, 102.0, 101.8, 100.8, and 99.3 ppm. Chemical structure of compound **12** is shown on top of figure.

# $^{1}H$-$^{13}C$ HSQC spectrum of compound **12**

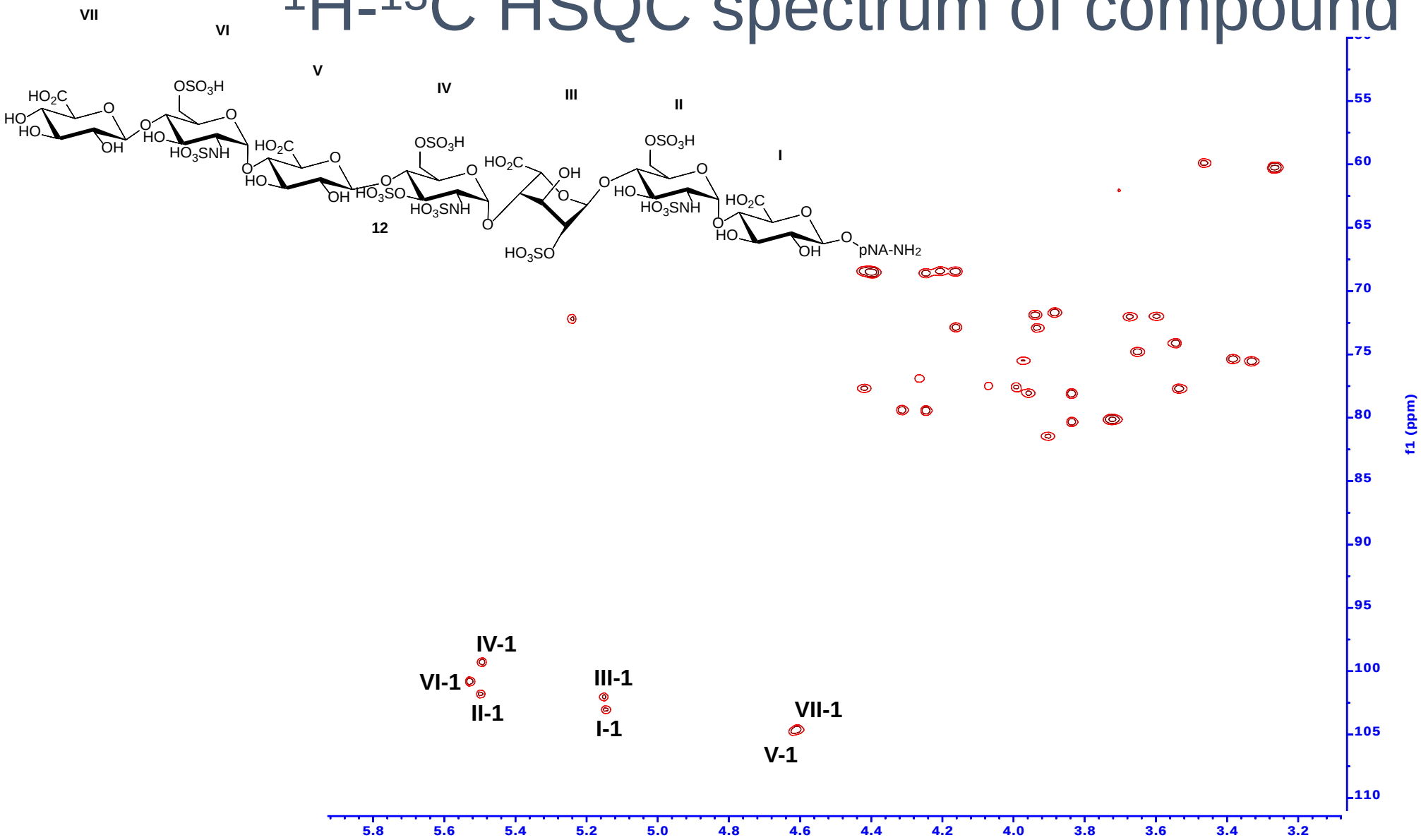


**Supplementary Fig 38**. $^{1}H$-$^{13}C$ HSQC spectrum of compound **12** (850 MHz, $D_2O$). The anomeric signals are indicated. Chemical structure of compound **12** is shown on top of figure.

# $^{1}$H-NMR of compound **13**

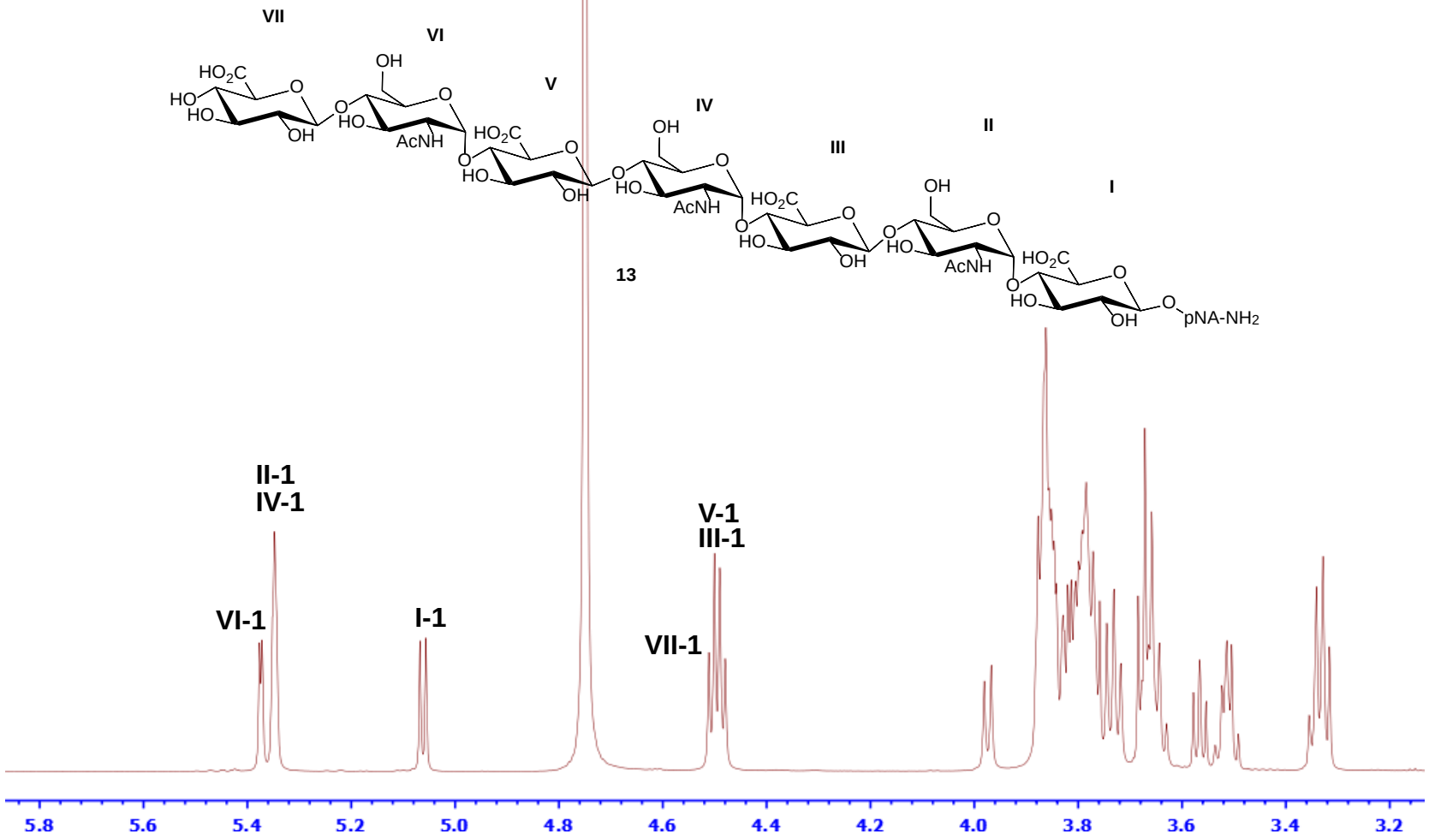


**Supplementary Fig 39**. $^{1}$H-NMR of compound **13** (700 MHz, $D_2O$). The signals of anomeric protons are indicated. The anomeric protons resonate as doublet at δ 5.38, 5.35, 5.35, 5.06, 4.51, 4.50, and 4.49 ppm. Chemical structure of compound **13** is shown on top of figure.

# $^{13}$C-NMR of compound **13**

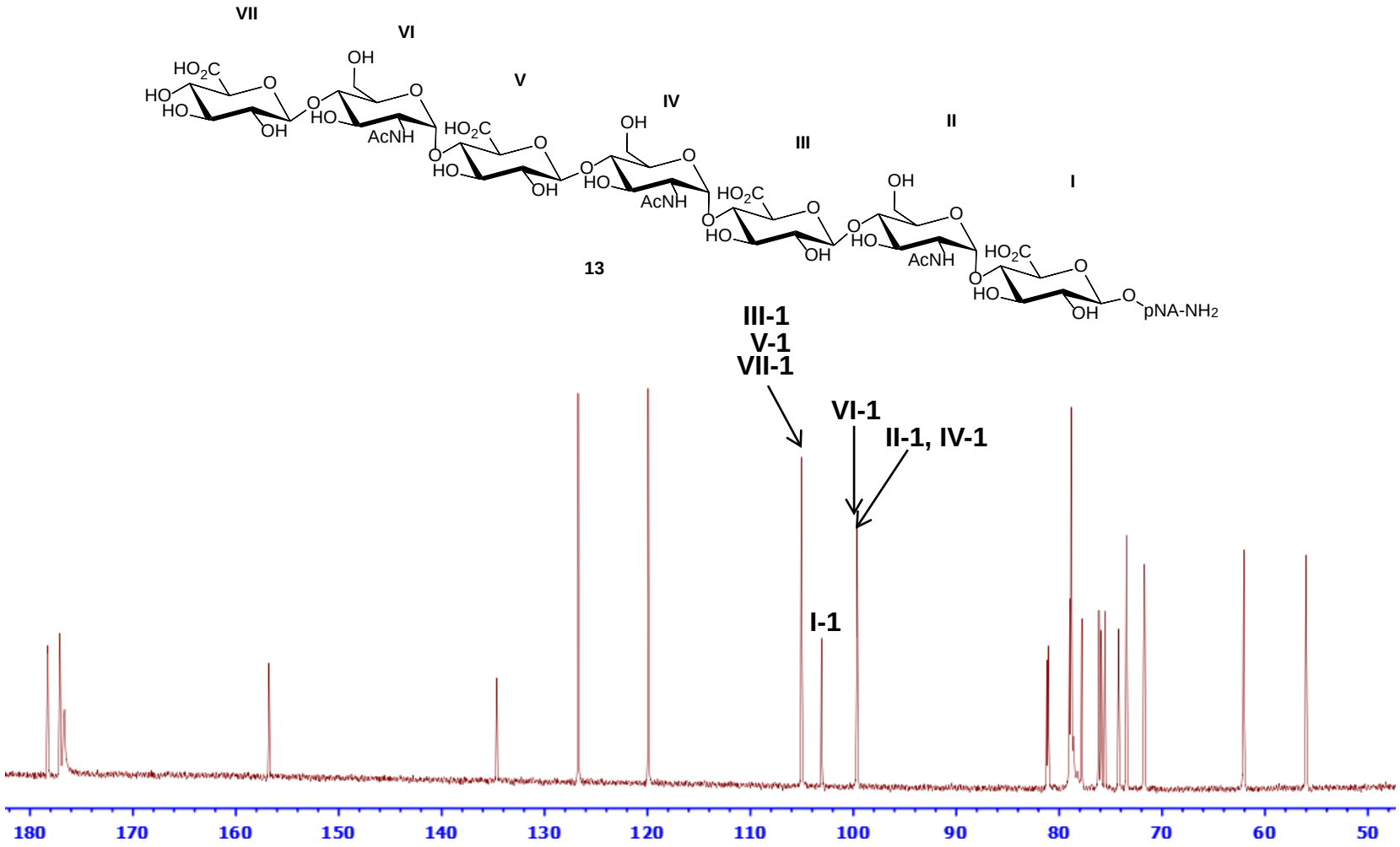


**Supplementary Fig 40**. $^{13}$C-NMR of compound **13** (175 MHz, $D_2O$). The signals of anomeric carbons are indicated. The anomeric carbons resonate at δ 105.0, 105.0, 105.0, 103.1, 99.7, 99.6, and 99.6 ppm. Chemical structure of compound **13** is shown on top of figure.

# $^{1}H$-$^{13}C$ HSQC spectrum of compound **13**

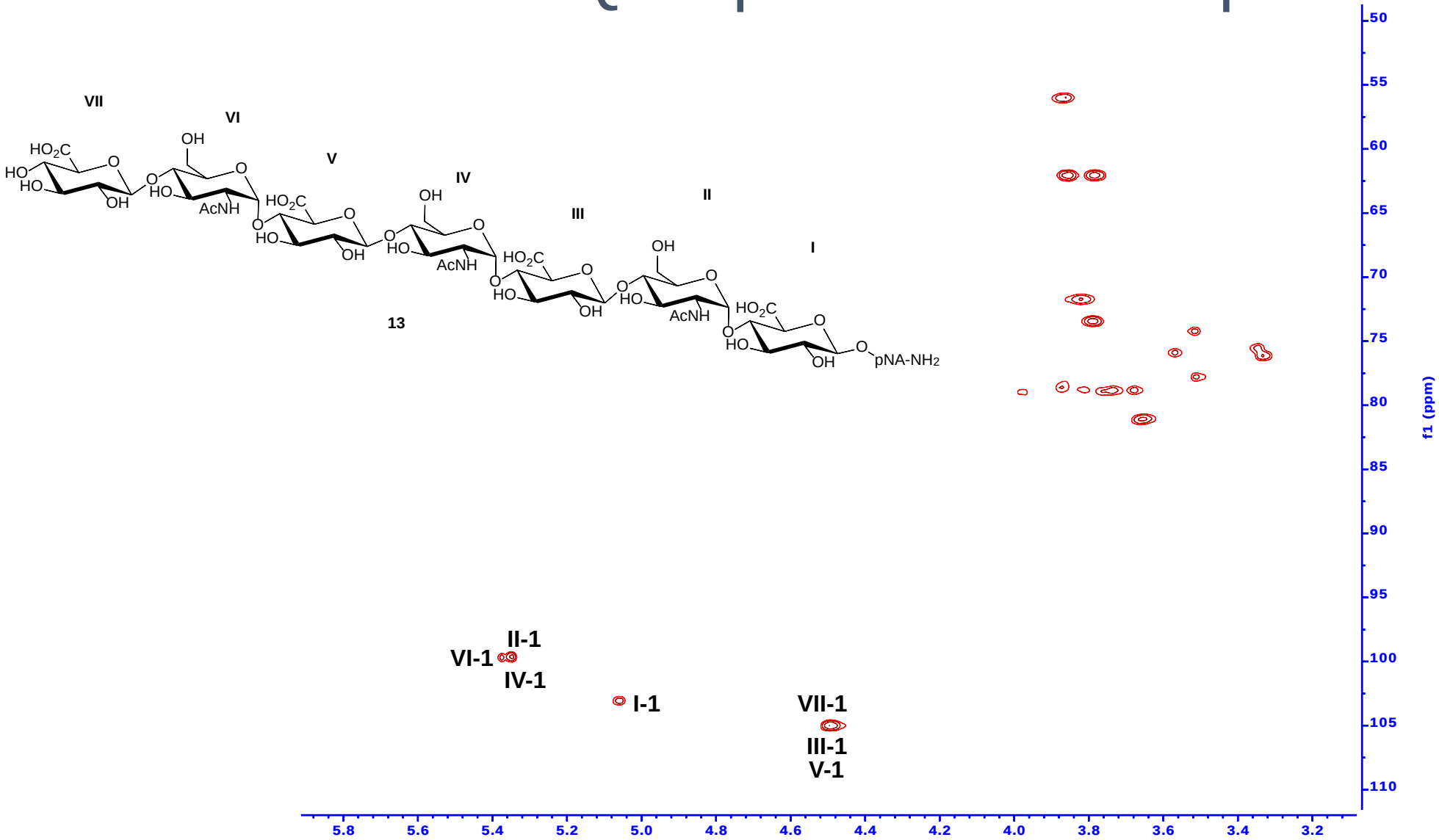


**Supplementary Fig 41**. $^{1}H$-$^{13}C$ HSQC spectrum of compound **13** (700 MHz, $D_2O$). The anomeric signals are indicated. Chemical structure of compound **13** is shown on top of figure.

# $^{1}$H-NMR of compound **14**

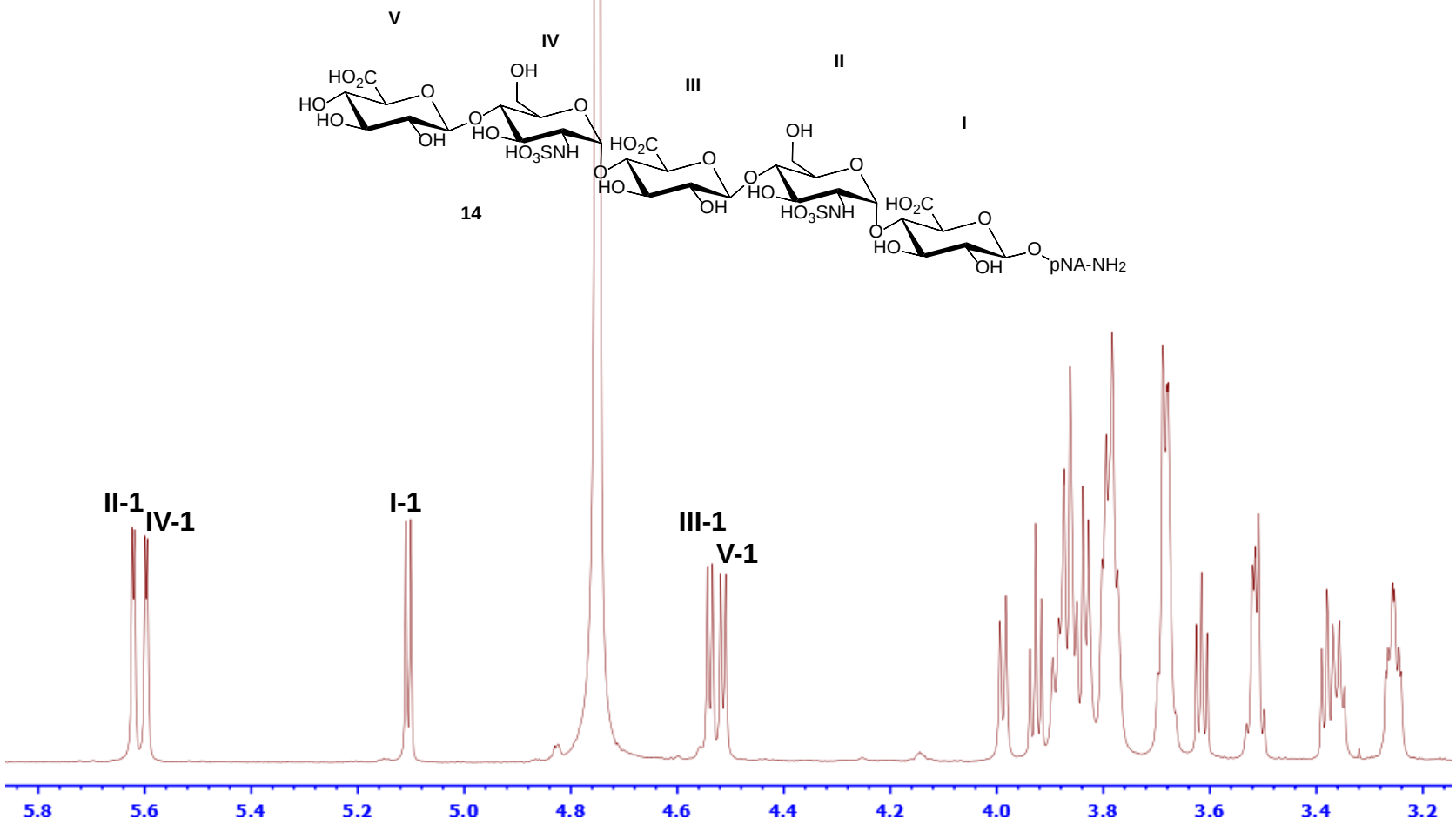


**Supplementary Fig 42**. $^{1}$H-NMR of compound **14** (850 MHz, $D_2O$). The signals of anomeric protons are indicated. The anomeric protons resonate as doublet at δ 5.62, 5.60, 5.11, 4.54, and 4.51 ppm. Chemical structure of compound **14** is shown on top of figure.

# $^{13}$C-NMR of compound **14**

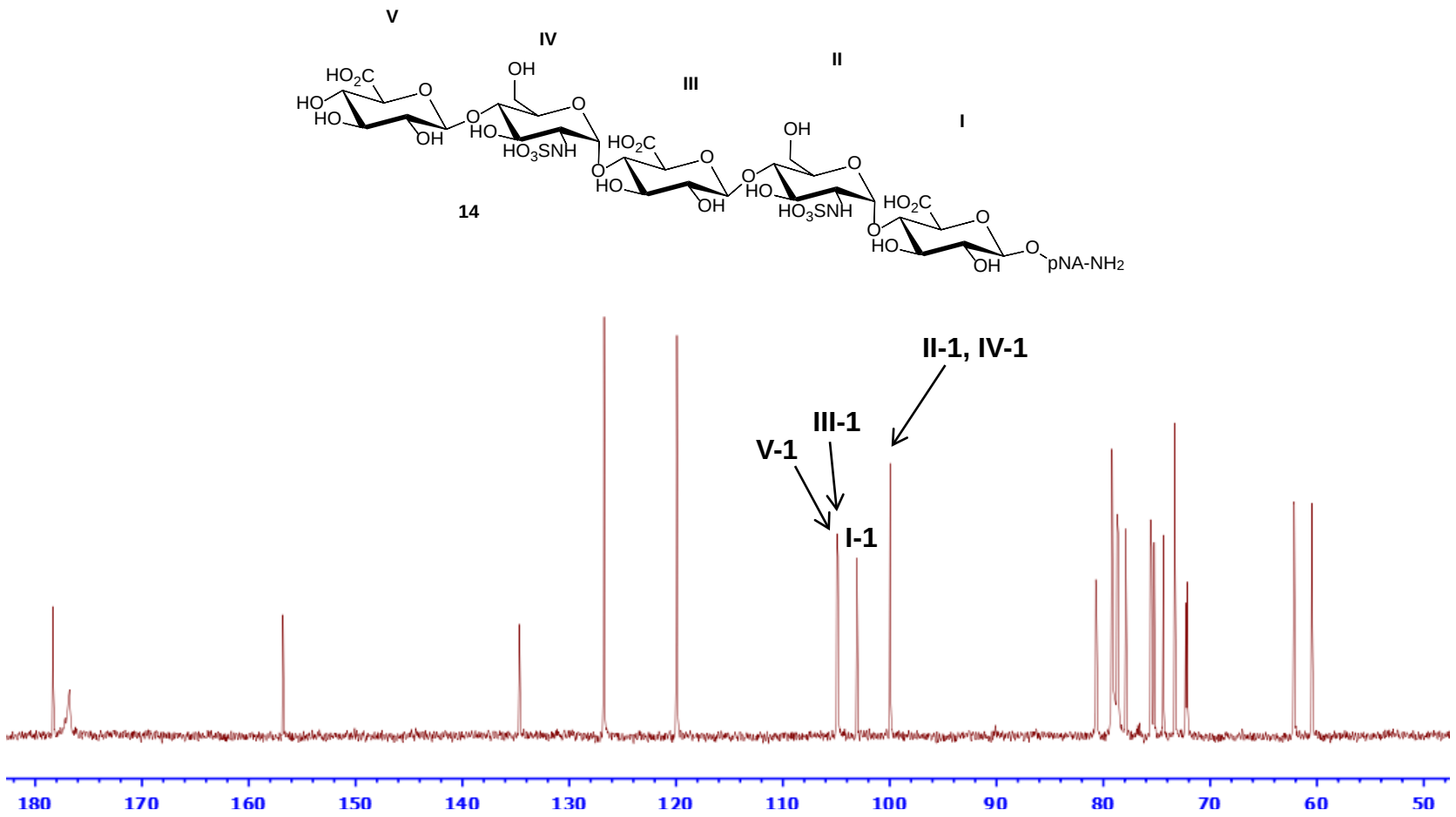


**Supplementary Fig 43**. $^{13}$C-NMR of compound **14** (212.5 MHz, $D_2O$). The signals of anomeric carbons are indicated. The anomeric carbons resonate at δ 104.9, 104.8, 103.1, 100.0, and 100.0 ppm. Chemical structure of compound **14** is shown on top of figure.

# $^{1}H$-$^{13}C$ HSQC spectrum of compound **14**

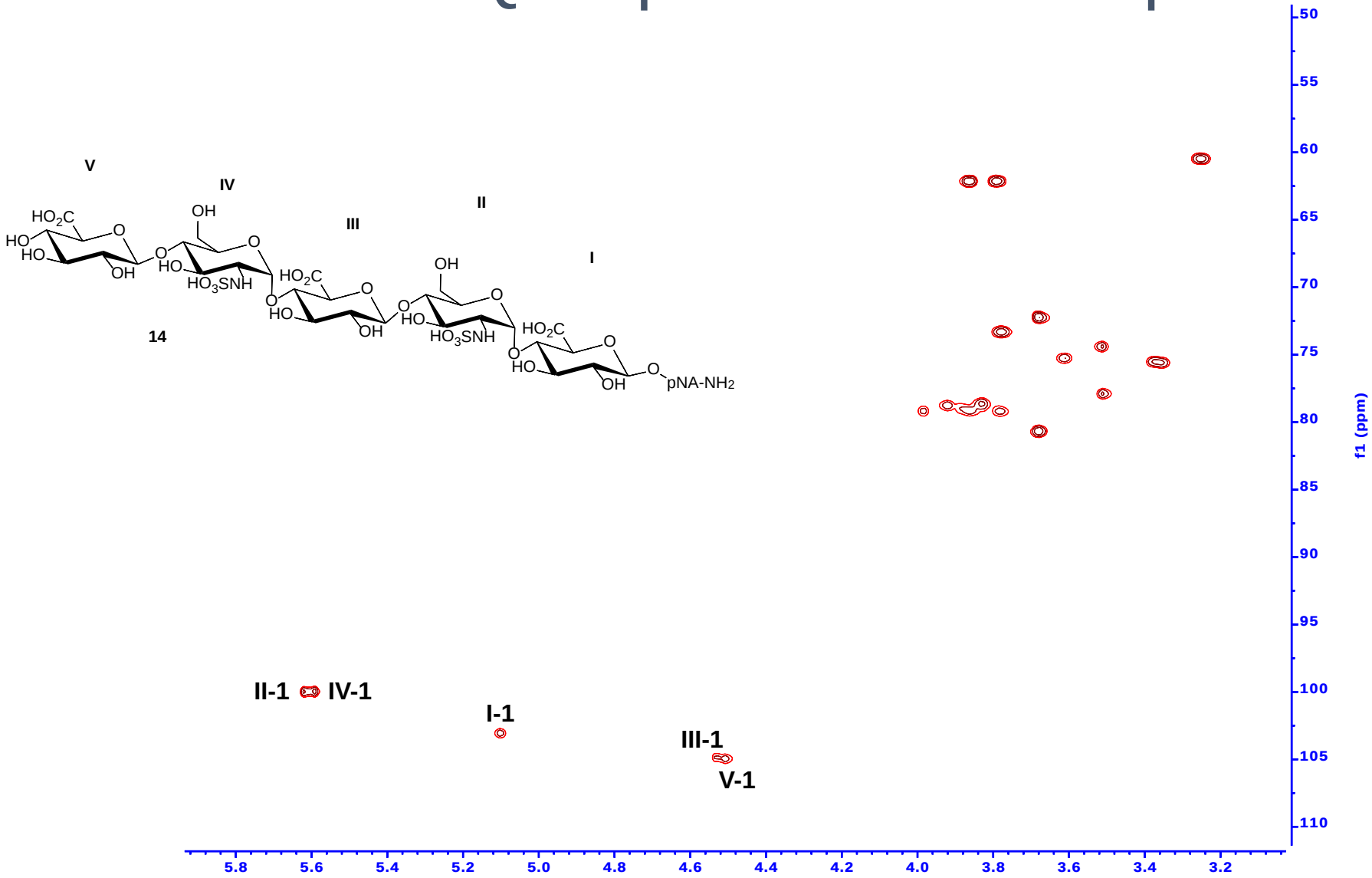


**Supplementary Fig 44**. $^{1}H$-$^{13}C$ HSQC spectrum of compound **14** (850 MHz, $D_2O$). The anomeric signals are indicated. Chemical structure of compound **14** is shown on top of figure.

Images of different concentrations of compound **19** spotted on the chip

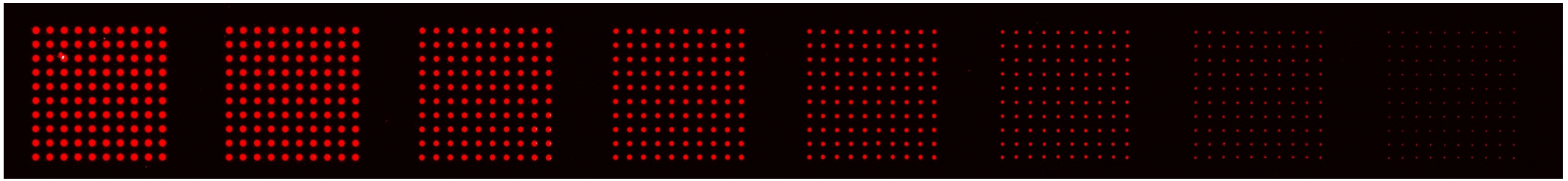


Relationship of fluorescence intensity and spot concentrations

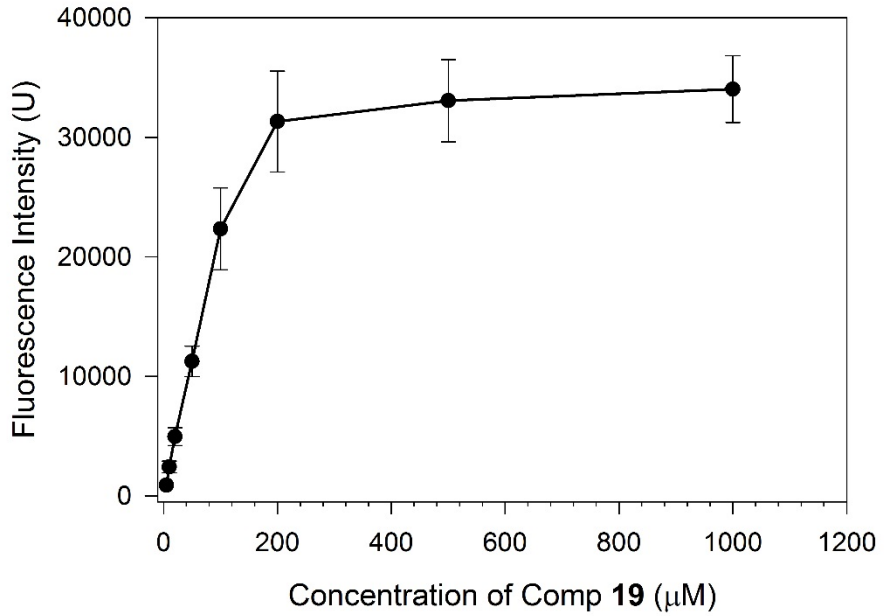


**Supplementary Fig 45**. Top panel shows the image of array slides spotted with different concentrations of compound **19**. Bottom panel shows the fluorescence intensity curve vs the concentration of compound **19** spotted on the array slides.

Images of different concentrations of Comp **16** and **17** spotted on the chip

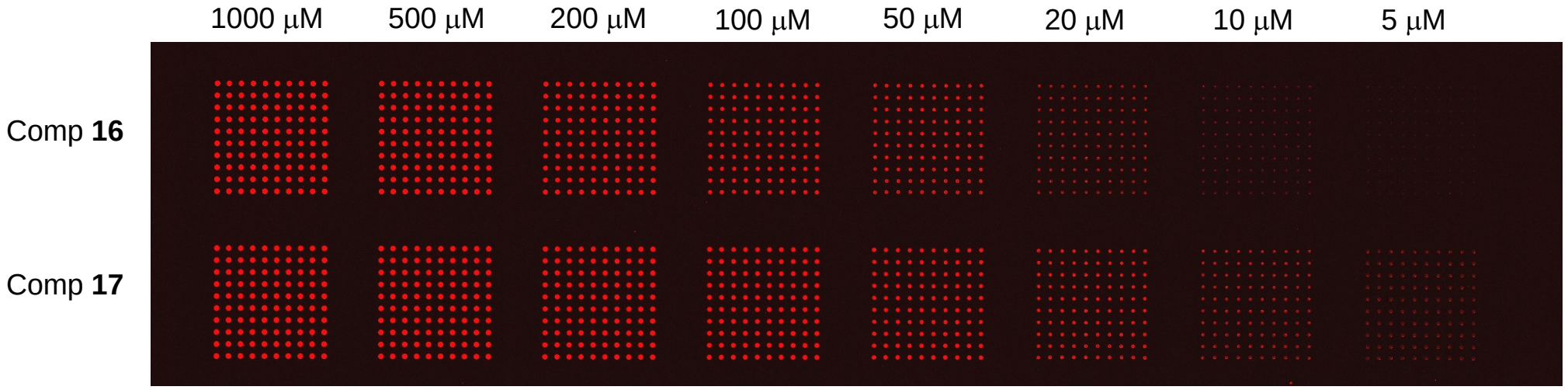


Relationship of fluorescence intensity and spot concentrations

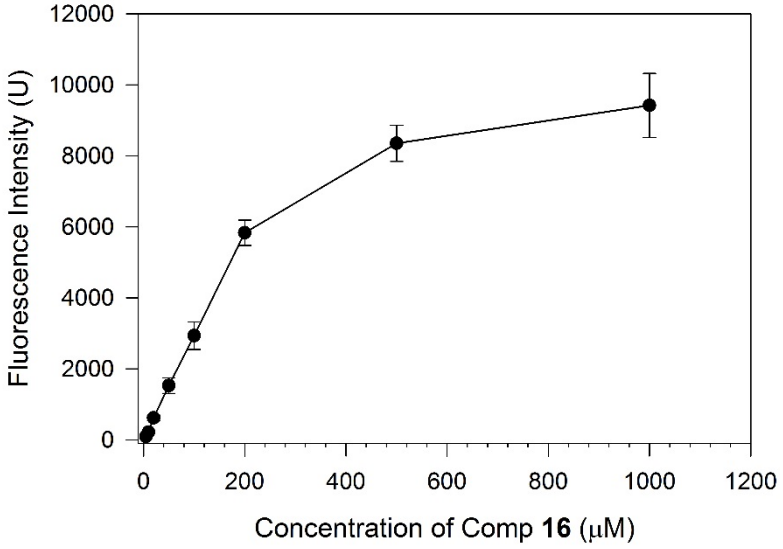


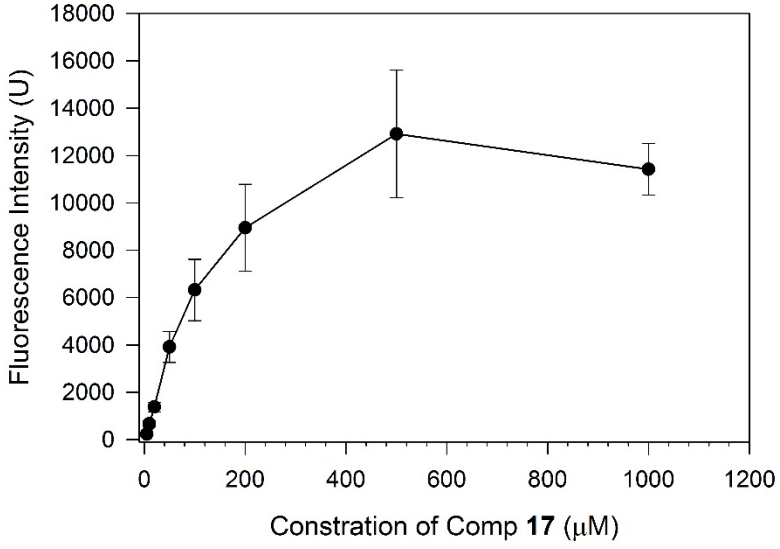


**Supplementary Fig 46**. Top panel shows the images of array slides spotted with different concentrations of Comp **16** and **17**. Bottom panel shows the fluorescence intensity curve vs the concentration of Comp **16** and **17** spotted on the array slides.

Images of different concentrations of compounds **15** and **20** spotted on the chip

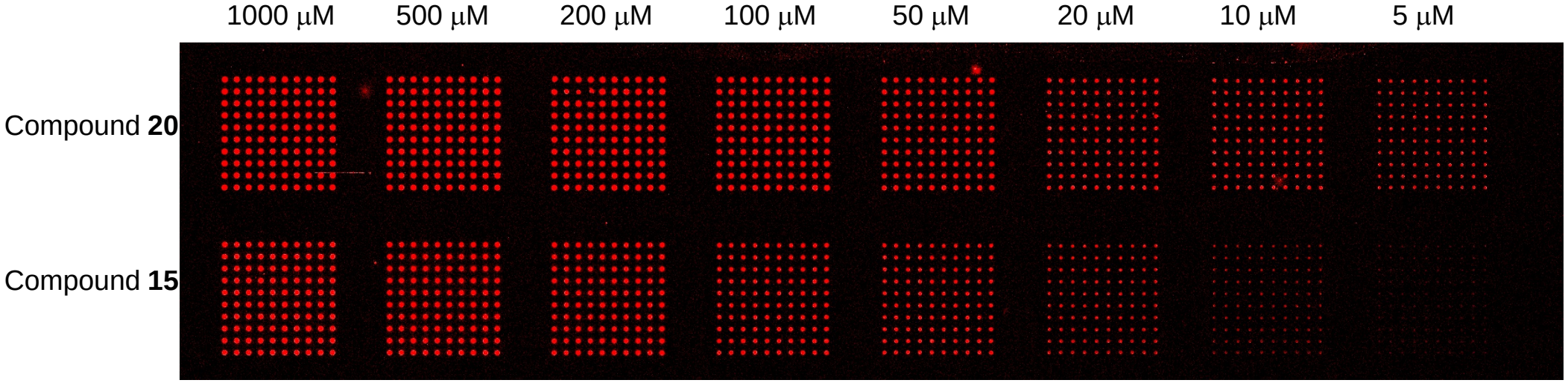


Relationship of fluorescence intensity and oligosaccharide concentrations

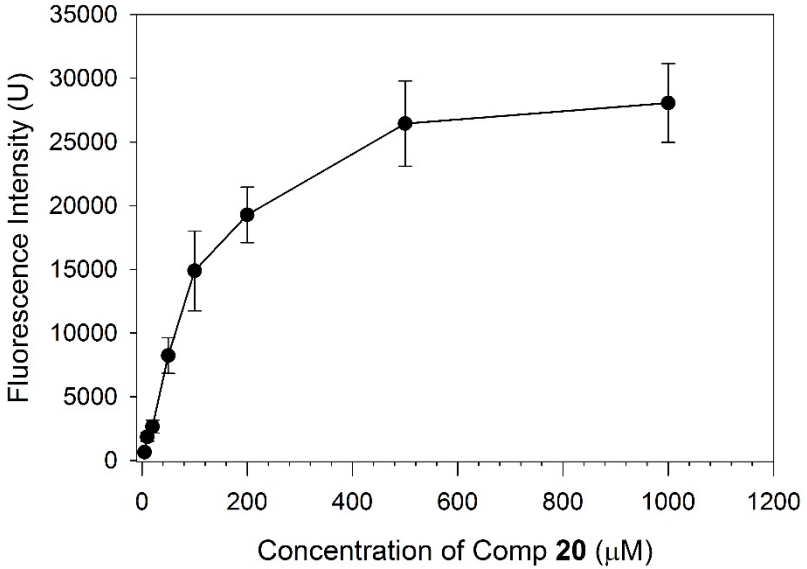


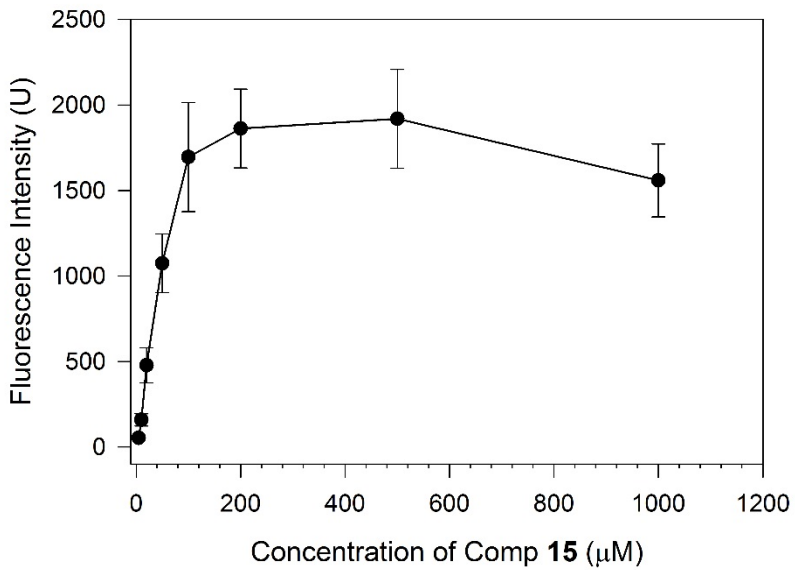


**Supplementary Fig 47**. Top panel shows the images of array slides spotted with different concentrations of compounds **20** and **15**. Bottom panel shows the fluorescence intensity curve vs the concentration of compounds **20** and **15** spotted on the array slides.

A. LC/MS chromatogram of heparin lyase-digested compound **1**

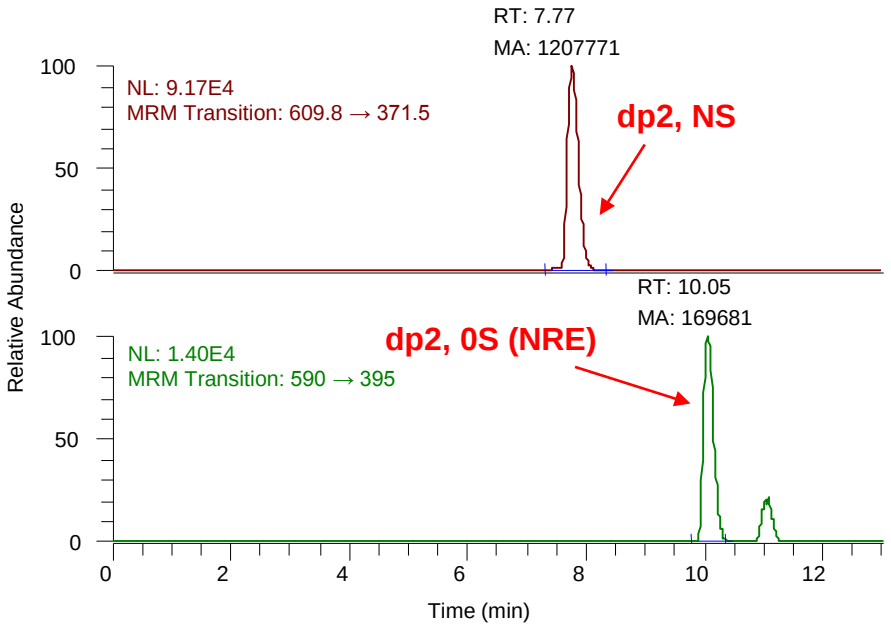


B. LC/MS chromatogram of disaccharides liberated from the slide

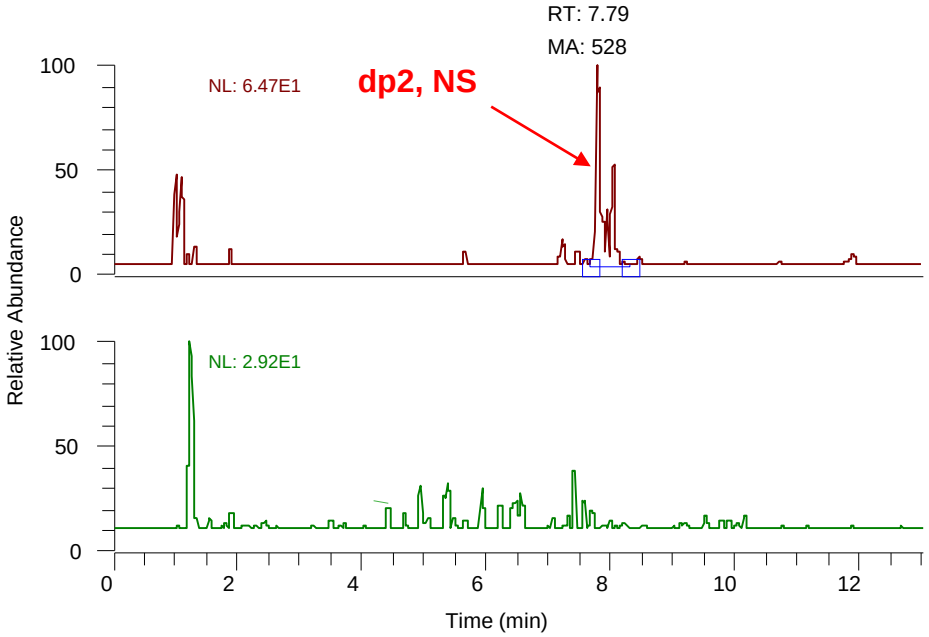


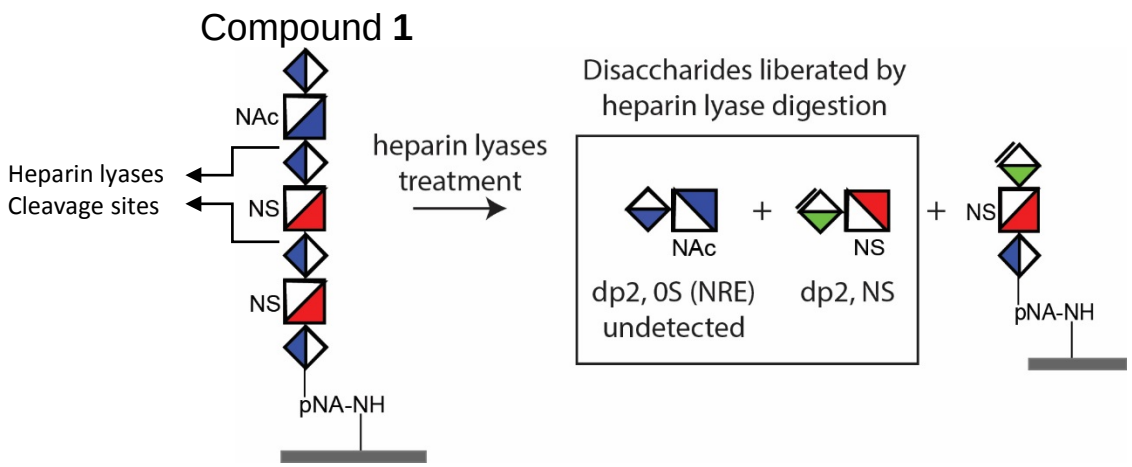

**Supplementary Fig 48**. Disaccharide analysis of heparin lyase-treated array slide that is covered by compound **1**. Panel A shows the MRM-tandem MS chromatograms of the disaccharides resulted from heparin lyase-degraded compound **1**. Panel B shows the LC/MS chromatograms of the disaccharides liberated from the array slide by heparin lyase digestion. GlcA-GlcNAc6S (Dp2 0S from NRE) disaccharide was not detected in disaccharides liberated from the array slide. Bottom shows the reaction involved in the degradation of compound **1** by heparin lyases. The quantitative analysis was conducted by comparing the area of disaccharide signal of ΔUA2S-GlcNS (dp2,2SNS) from MRM analysis between heparin lyase-digested compound **1** and on-site heparin lyase digestion from the array surface covered by compound **1**. From the analysis of digested compound **1** (6.5 μg), the peak area for 2SNS was 1,207,771. From the analysis of on-site digested surface that consisted 830 spots, the peak area for 2SNS was 528. The calculated amount for compound **1** on the surface based on the disaccharide signal of 2SNS was 3.4 pg per spot (= $528 \div 1207771 \times (6.5 \times 10^6) \div 830$).

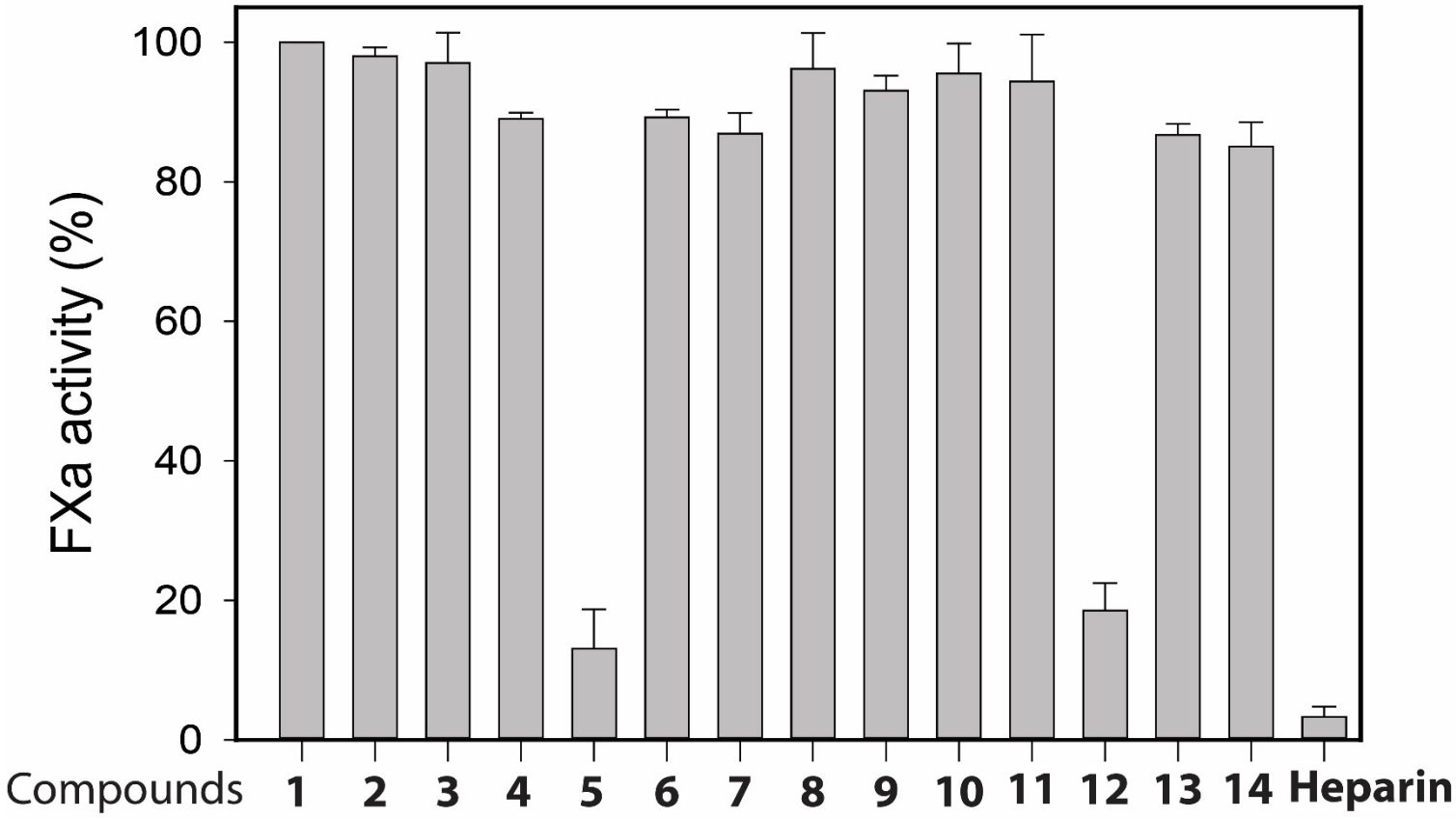


**Supplementary Fig 49**. Anti-FXa effects of compounds **1** to **14**. The inhibition effect of each compound (2.5 μM) on the activity of FXa. The 100% activity of FXa was determined without compound. The inhibition effect of heparin (2.5 $\mu gmL^{-1}$) was also measure, which served as a positive control. The data presented are the average of three independent determinations ± S.D. Conclusion: compound **5** and **12** display anti-FXa activity.